~~Environmental~~

Benthic macrofaunal carbon fluxes and environmental drivers of spatial variability ~~in benthic macrofauna biomass and associated carbon fluxes~~ in a large coastal-plain estuary

Authors: Seyi Ajayi[1*], Raymond Najjar[1], Emily Rivest[2], Ryan Woodland[3], Marjorie A.M. Friedrichs[2], Pierre St-Laurent[2], Spencer Davis[1]

~~[1]Pennsylvania~~[1]The Pennsylvania State University, University Park, PA, USA

[2]Virginia Institute of Marine Science, William & Mary, Gloucester Point, VA, USA

[3]University of Maryland Center for Environmental Sciences, Cambridge, MD, USA

Correspondence to: Seyi Ajayi ~~(oaa5061@psu.edu)~~(oaa5061@psu.edu)

Abstract

~~Extensive datasets document the distribution and composition~~ While the importance of carbon cycling in estuaries is increasingly recognized, the role of benthic macrofauna ~~in some estuaries, yet their impact on carbon cycling~~ remains poorly quantified~~. To address this, we investigated (1) how water chemistry and sediment composition correlate with benthic biomass distribution and (2) the contributions of benthic macrofaunal carbon fluxes~~ due to ~~estuarine carbon budgets.~~limited spatial and temporal resolution in biomass measurements. Here, we ask: (1) To what extent do benthic macrofauna contribute to estuarine carbon cycling via respiration and calcification? and (2) How well can routinely collected environmental variables predict their biomass? We analyzed 8,128 benthic samples collected from the Chesapeake Bay ~~(~~between 1995~~–~~ and 2022~~) and~~ and estimated associated carbon fluxes using empirical relationships. We then used generalized additive models to relate observed and modeled environmental variables to the biomass. ~~We also estimated their associated carbon fluxes (calcification and respiration rates) using empirical relationships. The~~ Biomass was highest ~~biomass was found~~ in the upper main stem of the Bay (Upper Bay) and upper Potomac River Estuary~~ and Upper Bay; moderate dissolved oxygen, low salinity, and high nitrate concentrations were the clearest predictors of these zones (explaining 52% of the deviance in biomass). Low surface NO_3^- concentrations~~

~~within,~~ the ~~estuary coincide with high inputs of allochthonous particulate organic carbon (POC) from riverine sources; this POC be the primary food source supporting high biomass zones.~~largest tidal tributary of the Bay. In the ~~oligohaline~~ Upper Bay, benthic macrofauna ~~respire 17–50% of total organic carbon available in that region, whereas their contribution is lower downstream. Moreover,~~ respired 18–45% of the estimated ~~benthic macrofaunal~~organic carbon supply. Calcification-driven alkalinity reduction reached 6.31 ± 2.84 mol m^{-2} yr^{-1} in the Potomac River Estuary, aligning with prior estimates of alkalinity sinks in the tributary and highlighting the potential importance of calcifying fauna in alkalinity dynamics. Estimated CO_2 production ~~rates~~in the Upper Bay from benthic respiration and calcification ~~rates in the Upper Bay (205±70 g C m^{-2} yr^{-1}) exceeds estimated outgassing (74.5 g C m^{-2} yr^{-1}), suggesting benthic macrofauna contribute significantly to~~(151 g C m^{-2} yr^{-1}) also exceeded observed air~~-~~–sea ~~gas exchange. The explainable spatial distribution of~~ CO_2 fluxes (74.5 g C m^{-2} yr^{-1}). Generalized additive models revealed that low salinity, moderate dissolved oxygen, and elevated nitrate best predicted high-biomass zones, with the three predictors explaining 52% of biomass deviance. These predictive relationships offer a pathway to estimate macrofaunal biomass and ~~major~~associated carbon fluxes in systems where direct biomass measurements are sparse. Our findings demonstrate that benthic macrofauna play a substantial and spatially structured role in estuarine carbon cycling ~~highlight the importance and feasibility of incorporating the impacts of benthic macrofauna~~ . Incorporating their contributions into ~~numerical~~estuarine biogeochemical models~~. Refining these models could~~ will improve predictions of ~~estuarine~~ecosystem responses to ~~natural~~environmental and anthropogenic ~~changes~~change.

1. Introduction

Benthic macrofauna are vitally important to estuarine ecosystems ~~because they can improve~~by improving water quality, ~~produce~~producing and ~~consume~~consuming organic matter, ~~recycle~~recycling nutrients, ~~dilute or cycle~~cycling pollutants, ~~stabilize~~stabilizing and ~~transport~~transporting sediment, and ~~provide~~providing food ~~to~~for both human populations and other estuarine organisms (Schratzberger & Ingels, 2018; Snelgrove, 1997; Wilson & Fleeger, 2023). ~~As adults, benthic~~Benthic macrofauna often have limited mobility and, in some cases, long life spans, making them reliable indicators of local environmental variability caused by natural and anthropogenic stresses. Their relative abundance and diversity are often used as a proxy to describe the condition of estuaries (Dauer, 1993; Pearson & Rosenberg, 1978; Rosenberg, 1995; Weisberg et al., 1997).

~~***1.1 Environmental drivers of***~~ In addition to shaping ecosystem structure and serving as indicators of environmental health, benthic macrofauna play a central role in estuarine carbon cycling. Through~~***distribution***~~

~~Because benthic macrofauna are ecologically significant and sensitive to environmental conditions, numerous studies have examined the key factors influencing their distribution in estuaries. Here, we summarize key studies that have investigated how water quality and sediment composition influence benthic macrofauna distribution in estuaries.~~

~~Dissolved oxygen is one of the primary environmental variables affecting benthic composition; hypoxia (extremely low dissolved oxygen concentration events) significantly degrades the benthic habitat quality (Borja et al., 2008; Diaz et al., 1995; Murphy et al., 2011; Seitz et al., 2009; Woodland & Testa, 2020). Seitz et al., (2009) found that oxygen was the single best predictor of summer benthic biomass by depth in the Chesapeake Bay. In another study of the Chesapeake Bay, dissolved oxygen explains 42% of the variation in the benthic index of~~

biotic integrity (B-IBI), a benthic habitat quality score compiled from multiple factors, including species composition, trophic composition, biomass and abundance, and diversity (Borja et al., 2008). Similarly in the Baltic Sea, near-bottom oxygen content was among the most important environmental variables shaping benthic communities (Rousi et al., 2019). Among aquatic organisms, benthic macrofauna are the most severely affected by low dissolved oxygen events because they are furthest from the atmosphere, immobile, and coastal sediments are often depleted in oxygen relative to the water column (Dauer & Alden, 1995; Vaquer-Sunyer & Duarte, 2008). Even within benthic communities, vulnerability to hypoxia can vary among taxonomic groups (Vaquer-Sunyer & Duarte, 2008). For example, bivalves are more tolerant of short-term hypoxic stress, which could increase their dominance among benthos as hypoxia increases (Seitz et al., 2009; Vaquer-Sunyer & Duarte, 2008; Woodland & Testa, 2020).

Salinity is also a very important control on benthic community structure (Dauer, 1993; Sturdivant et al., 2013) because different species have different physiological tolerances (Holland et al., 1987; Little et al., 2017; Seitz et al., 2009). In the Humber estuary in the United Kingdom, salinity was amongst the most important environmental variables that contributed to 80% of the biomass variation of the two most dominant bivalve species (Fujii & Raffaelli, 2008). In addition, it was predicted that a 0.3 m rise in sea level would result in a 6.9% loss of benthic macrofaunal biomass, partially due to salinity intrusion.

Ocean acidification, the decrease in seawater pH due to the uptake of atmospheric CO_2, has also negatively affected calcifying organisms in coastal systems. Mollusks (predominately bivalves) are the most strongly affected; ocean acidification decreases their ability to calcify and significantly reduces their survival, growth, development, and abundance (Kroeker et al., 2013). The mechanism of calcification in bivalves will make it difficult for them to adapt to ocean

~~acidification in the future. Bivalves are weak acid-base regulators because they have poorly developed ion exchange mechanisms (Jakubowska & Normant-Saremba, 2015; Thomsen et al., 2015). They are also most susceptible to damage from ocean acidification in their early stages (Jansson et al., 2013). Among other benthic groups, there is a broad variation of sensitivity to variations in pH (Birchenough et al., 2015).~~

~~Very fine sediment grain size (i.e., high silt-clay fraction & low sand fraction) is associated with lower benthic biomass (Dauer & Alden, 1995; Seitz et al., 2009). A study off Siberia's coast found that sediment grain size is a key predictor of benthic macrofaunal composition, while organic carbon is a key indicator of benthic biomass (Grebmeier et al., 2015). In Chesapeake Bay, Woodland & Testa, (2020) found a negative correlation between accumulated organic matter and benthic biodiversity and a positive association between sediment sand percentage and benthic biodiversity.~~

~~Food availability has long been known as an important factor influencing benthic biomass (Ehrnsten et al., 2019; Pearson & Rosenberg, 1978). Food availability is driven by primary production in the Bay, which is dominated by phytoplankton in most estuaries (i.e. Chesapeake Bay, Hagy, 2002). A synthesis of shallow, normoxic estuaries worldwide found that as primary production increases, benthic biomass increases (Hagy, 2002; Kemp et al., 2005). However, the timing, size, and location of primary production could lead to hypoxia in the bottom waters, which could have a detrimental effect on the benthos (Dauer et al., 2000; Kemp et al., 2005). In a model of the Baltic Sea, Ehrnsten et al., (2020) predicted that climate change will cause benthic biomass to decrease. However, reduced nutrient loading (due to management efforts) was also predicted to cause the benthic biomass to decrease. Results from the (Ehrnsten et al., 2020) study suggest that the harmful effects of climate change can effectively cancel out~~

~~the partially positive effects of moderate nutrient loading, perhaps due to increased primary production.~~

~~In summary, studies theorize that dissolved oxygen, salinity, pH, sediment composition, and primary production are all significant predictors of benthic macrofauna biomass distribution in estuaries.~~

~~*1.2 Impact of benthic macrofauna on carbon cycling*~~

~~Benthic macrofauna biomass influences estuarine biogeochemical cycling, particularly carbon cycling through three major processes:~~ secondary production, respiration, and calcification~~.~~, they influence carbon transport and the partitioning of carbon between organic and inorganic forms. Secondary production refers to the consumption of organic matter by benthos to produce soft tissue biomass (Diaz & Schaffner, 1990; Dolbeth et al., 2012; Sturdivant et al., 2013). ~~Secondary production is an important pathway for~~ This biomass contributes to trophic transfer, as ~~the benthos~~benthic organisms are ~~eventually~~ consumed by predators or decomposers, with much of the associated organic carbon ~~ultimately~~eventually being removed from the ~~estuarine system~~ estuary through advection ~~into~~to the open ocean or burial in sediment (Diaz & Schaffner, 1990; Wilson & Fleeger, 2023). ~~The direct impact of secondary production on~~ Respiration and calcification influence carbon cycling ~~is more limited, as involves the transformation of organic matter into biomass rather than shifting carbon between organic and inorganic pools. Respiration is the process by which organic matter and oxygen are consumed, and CO_2, water, and energy are released. As a result, dissolved inorganic carbon (DIC) increases in the water column. During calcification, benthic calcifiers~~through their impact on the carbonate system, which describes the partitioning of inorganic carbon among its primary forms and strongly regulates key biogeochemical variables, such as ~~bivalves, uptake bicarbonate and~~ pH,

calcium carbonate saturation state, and the partial pressure of carbon dioxide (pCO_2).~~to produce calcium carbonate shells. CO_2 and water are also released as byproducts. However, calcification decreases DIC because bicarbonate utilization exceeds CO_2 production. The removal of bicarbonate also decreases alkalinity (Waldbusser et al., 2013). Together, these processes play a significant role in the carbon budget, with respiration and calcification notably contributing to CO_2 generation (Chauvaud et al., 2003).~~

~~Studies have quantified the relative contributions of~~ Impacts of respiration and calcification on the carbonate system are best understood via their impacts on two master variables, dissolved inorganic carbon (DIC) and total alkalinity (TA). DIC is a measure of the total concentration of inorganic carbon species in water, including CO_2, bicarbonate ion, and carbonate ion:

$$[\mathrm{DIC}] = [\mathrm{CO_2}] + [\mathrm{HCO_3^-}] + [\mathrm{CO_3^{2-}}]. \quad (1)$$

TA is the excess of proton acceptors over donors and reflects the capacity of a water body to buffer pH changes. For understanding impacts of biogeochemical processes, the form of TA known as the explicit conservative alkalinity (Glud, 2008; Wolf-Gladrow et al., 2007) is useful:

$$[\mathrm{TA}] = [\mathrm{Na^+}] + 2[\mathrm{Mg^{2+}}] + 2[\mathrm{Ca^{2+}}] + [\mathrm{K^+}] + 2[\mathrm{Sr^{2+}}] + \ldots - [\mathrm{Cl^-}] - [\mathrm{Br^-}] - [\mathrm{NO_3^-}] - \ldots - \mathrm{TPO_4} + \mathrm{TNH_3} - 2\mathrm{TSO_4} - \mathrm{THF} - \mathrm{THNO_2}, \quad (2)$$

where the last five terms represent the total forms of phosphate, ammonia, sulfate, fluoride, and nitrite, respectively.

Respiration, unlike secondary production, directly alters the carbonate system. Respiration is the metabolic process by which organisms break down organic matter to release energy. In aerobic respiration, oxygen serves as the terminal electron acceptor, producing carbon dioxide (CO_2), water, and energy:

$$\mathrm{CH_2O} + \mathrm{O_2} \rightarrow \mathrm{CO_2} + \mathrm{H_2O}. \quad (3)$$

When oxygen becomes depleted, anaerobic respiration takes over, relying on alternative electron acceptors such as nitrate, sulfate, or iron oxides. For benthic macrofauna, oxygen is essential for respiration; anaerobic respiration in sediments is primarily mediated by microbes (Glud, 2008). The CO_2 generated during aerobic respiration increases DIC (Equation 1). Though not shown in Equation 3, aerobic respiration also ultimately releases about 16 moles of nitrate (NO_3^-) for every 106 moles of CO_2 produced (Redfield, 1963), which decreases TA (Equation 2). Anaerobic respiration, such as denitrification and sulphate reduction, which consume nitrate and TSO_4, respectively, increase TA (Equation 2).

During calcification, benthic organisms, such as bivalves, take up calcium (Ca^{2+}) and HCO_3^- to form calcium carbonate ($CaCO_3$) shells, releasing CO_2 and water as byproducts:

$$Ca^{2+} + 2HCO_3^- \rightarrow CaCO_3 + CO_2 + H_2O. \quad (4)$$

Although calcification increases CO_2 in the water column, it results in a net decrease in DIC, since two moles of HCO_3^- are removed for every mole of $CaCO_3$ precipitated, while only one mole of CO_2 is returned to the water column (Equation 1). The removal of Ca^{2+} also decreases TA by twice the amount of DIC (Equation 2). Calcification is thermodynamically favored when the calcium carbonate saturation state (Ω) exceeds 1. The saturation state is defined as:

$$\Omega = \frac{[Ca^{2+}][CO_3^{2-}]}{K_{sp}} \quad (5)$$

where K_{sp} is the solubility product, which varies with the form of calcium carbonate (typically aragonite or calcite), temperature, pressure, and salinity. When $\Omega < 1$ (undersaturation), dissolution is favored, leading to the release of Ca^{2+} and CO_3^{2-} back into solution and increasing TA. Saturation state is the primary driver of calcification in bivalves, especially during early life stages when physiological control over acid–base balance is limited. Low Ω impairs shell formation and increases mortality in juveniles, regardless of pH or pCO_2, making bivalve

recruitment particularly vulnerable in coastal systems prone to acidification (Green et al., 2009; Thomsen et al., 2015; Waldbusser et al., 2015).

In addition to altering carbon chemistry through metabolic processes, benthic macrofauna also influence carbon cycling through physical mechanisms such as bioturbation, which is the physical reworking of sediments via burrowing, feeding, and irrigation. In the short term, such activity creates a heterogenous sediment–water interface, characterized by tracks, fecal mounds, burrows, and funnels (Meysman et al., 2006). Over longer timescales, bioturbation acts as an effective mixing mechanism that homogenizes the upper sediment layers. This reworking alters redox gradients, enhances organic matter decomposition, and facilitates solute exchange between porewaters and the overlying water column (Glud, 2008). As a result, bioturbation can increase rates of respiration, promote the release of DIC, and influence carbonate chemistry by exposing calcareous material to undersaturated conditions, thereby enhancing dissolution (Middelburg, 2018). These physical processes play a critical but often underappreciated role in regulating sediment–water carbon dynamics.

Building on these conceptual and mechanistic insights, field and modeling studies have revealed the potentially large influence of benthic macrofauna on estuarine carbon cycling~~.~~, particularly through respiration and calcification. Respiration has been ~~the most~~studied more extensively ~~studied~~than calcification. A compilation of data from 20 ~~different~~ estuaries estimated that benthos (encompassing microbes, meiofauna, and macrofauna) respire approximately 24% of the total input of organic carbon, defined here as the sum of inputs ~~to estuaries are respired by benthos, while plankton respiration is generally much lower~~of autochthonous (from primary production) and allochthonous (e.g., from rivers) organic carbon, (Hopkinson & Smith, 2004). ~~Macrofauna~~ This definition of the total input of organic carbon is used throughout the remainder

of this paper. In a study of coastal seagrass meadows, macrofauna were found to account for 40% of ~~all~~total benthic respiration (Rodil et al., 2022). ~~Given the high rates of benthic respiration~~ In a broader meta-analysis, Glud (2008) compiled oxygen uptake measurements across marine sediments and concluded that fauna-mediated respiration can account for roughly half of total benthic metabolism at upper continental slope depths. The excess of benthic respiration over primary production observed in many estuaries~~, autochthonous primary production alone cannot account for the total organic matter being processed, indicating relatively high~~ implies significant allochthonous inputs (Hopkinson & Smith, 2004; Kemp et al., 1997; Schwinghamer et al., 1986). Bivalves, in particular, substantially contribute to benthic respiration and have been ~~thought~~hypothesized to significantly decrease the phytoplankton and suspended particulate concentrations in estuaries (Galimany et al., 2020; Nakamura & Kerciku, 2000; Newell & Ott, 2011). Cerco & Noel~~,~~ (2010) modeled the effect of bivalve filter feeders in the Chesapeake Bay and found that they removed 14% to 40% of the riverine particulate organic carbon (allochthonous) load. ~~Beyond~~

In contrast to respiration, the impact of benthic calcification on estuarine carbon cycling ~~is~~remains underexplored (Waldbusser et al., 2013). However, recent discoveries of large alkalinity sinks in estuarine tributaries ~~could~~ suggest ~~a large role for~~that calcifying organisms, such as bivalves~~-~~, may play a substantial role (Najjar et al., 2020). The combined CO_2 production ~~of CO_2~~ from respiration and calcification may ~~be~~also constitute a significant ~~contributor to~~ carbon ~~cycling~~flux to the atmosphere. In San Francisco Bay, this production is estimated to be twice the rate of CO_2 consumption by primary production (Chauvaud et al., 2003). A global extrapolation of the CO_2 generated from calcifying benthos in estuaries is comparable to the magnitude of the total CO_2 emissions from the world's lakes or planetary volcanism (Chauvaud

et al., 2003). As previously described, although both respiration and calcification generate CO_2, they have opposite effects on DIC: respiration increases DIC, whereas calcification reduces it. Thus whether calcifying benthos act as a net source or sink of DIC depends on the relative magnitudes of these two processes.

~~The absolute fluxes~~To quantify the magnitude of these benthic contributions to carbon cycling, researchers often estimate rates of secondary production, respiration, and calcification~~,~~ ~~and~~ based on benthic biomass. Because secondary production can ~~also~~ be time-consuming and costly to measure, it is often estimated ~~from biomass. Multiple studies use~~using empirical relationships ~~to~~that relate it to benthic biomass ~~to secondary production based on the biomass,~~, incorporating variables such as taxon, average body mass, and water temperature~~, and other characteristics~~ (Brey, 1990; Chauvaud et al., 2003; Dolbeth et al., 2012; Edgar, 1990; Schwinghamer et al., 1986; Sturdivant et al., 2013; Tumbiolo & Downing, 1994). ~~Secondary production rates are often calculated indirectly because they can be expensive and time-consuming to measure (Sturdivant et al., 2013; Tumbiolo & Downing, 1994).~~ Calcification and respiration rates can be ~~estimated~~inferred from these secondary production estimates using empirical relationships or ~~simple~~ proportional scaling (Chauvaud et al., 2003; Schwinghamer et al., 1986).

Despite their importance to carbon cycling, benthic macrofauna biomass is often sparsely measured across space and time due to the high cost and logistical challenges of benthic sampling (Pearson & Rosenberg, 1978; Snelgrove et al., 2018). In contrast, environmental variables that influence benthic communities are typically collected more frequently and with greater spatial and temporal resolution. To better incorporate benthic macrofaunal processes into

carbon budgets and numerical models, it is useful to assess how well these more readily available environmental variables can serve as predictors of biomass.

There are many environmental influences on the distribution of benthic macrofauna. Hypoxia (dissolved oxygen concentrations ≤2 mg L^{-1}) is a major stressor that reduces biomass, alters community structure, and impairs key functions such as metabolism, bioturbation, and calcification (Borja et al., 2008; Diaz et al., 1995; Diaz & Rosenberg, 2008; Levin et al., 2009; Murphy et al., 2011; Rousi et al., 2019; Seitz et al., 2009; Woodland & Testa, 2020). Benthic macrofauna are particularly vulnerable due to their proximity to the sediment–water interface, immobility, and limited capacity to avoid low-oxygen zones (Dauer & Alden, 1995; Vaquer-Sunyer & Duarte, 2008). Behavioral and physiological responses to hypoxia differ among taxa, with some groups like bivalves showing greater tolerance to short-term events (Seitz et al., 2009; Vaquer-Sunyer & Duarte, 2008; Woodland & Testa, 2020). Salinity also plays a central role in structuring benthic communities, with species distributions reflecting distinct physiological tolerances (Dauer, 1993; Holland et al., 1987; Little et al., 2017; Seitz et al., 2009; Sturdivant et al., 2013). Ocean acidification has been shown to negatively impact calcifying taxa, particularly mollusks, by reducing growth, survival, and development (Birchenough et al., 2015; Jakubowska & Normant-Saremba, 2015; Jansson et al., 2013; Kroeker et al., 2013; Thomsen et al., 2015). Sediment characteristics also influence benthic biomass and diversity. Finer grain sizes and higher organic content tend to be associated with lower biomass and biodiversity, whereas sandy sediments are generally more favorable (Dauer & Alden, 1995; Grebmeier et al., 2015; Seitz et al., 2009; Woodland & Testa, 2020). Finally, food availability, primarily from phytoplankton production, strongly governs benthic biomass (Ehrnsten et al., 2019; Hagy, 2002; Kemp et al., 2005; Pearson & Rosenberg, 1978). However, the relationship is complex, as high primary

production can also lead to oxygen depletion that ultimately suppresses benthic communities (Dauer et al., 2000; Kemp et al., 2005). In summary, dissolved oxygen, salinity, pH, sediment composition, and food availability all serve as important environmental predictors of benthic macrofauna biomass in estuarine ecosystems.

~~*1.3 Focus of this Study*~~

While numerous studies have examined the environmental drivers of benthic biomass in estuaries, most have focused on relatively small spatial ~~and/~~or temporal scales. ~~Benthic biomass~~Biomass, as opposed to other metrics such as diversity and abundance, is particularly important because it is most directly related to estuarine carbon cycling processes (Cerco & Noel, 2010; Snelgrove, 1999). ~~Chesapeake Bay is~~While benthic respiration has been widely quantified, estimates of benthic calcification remain rare (e.g., Chauvaud et al., 2003; Waldbusser et al., 2013), limiting our understanding of benthic contributions to ~~special interest because the~~ carbon and alkalinity dynamics ~~span the range observed~~. The Chesapeake Bay, a large, coastal-plain estuary in ~~estuaries and there is~~the eastern United States (Fig. 1), provides a valuable case study due to its extensive historical monitoring data and diversity of carbon and alkalinity dynamics across its several tidal tributaries (Najjar et al., 2020). ~~To our knowledge, the most recent~~Although prior studies ~~that specifically~~ in the Bay have linked environmental variables ~~with~~to benthic biomass (Seitz et al., 2009; ~~in the Chesapeake Bay were (~~Woodland et al., 2021), these studies either used older datasets or~~, which~~ focused on ~~these relationships through the lens of forage for~~ biomass primarily as a food source for higher trophic levels ~~and Seitz et al., (2009), which investigated benthic data from 1996–2004. Woodland & Testa, (2020) also explored the relationship between environmental variables and benthic species diversity in the Bay. However, benthic biomass and biodiversity are not correlated, so our study's results~~

~~may differ significantly (Alden et al., 2002; Testa et al., 2020). Few studies have also looked at the effect of primary productivity on benthic biomass in the Bay (e.g., Hagy, 2002; Kemp et al., 2005), even though organic matter produced from primary production is considered the main food source for the benthos.~~.

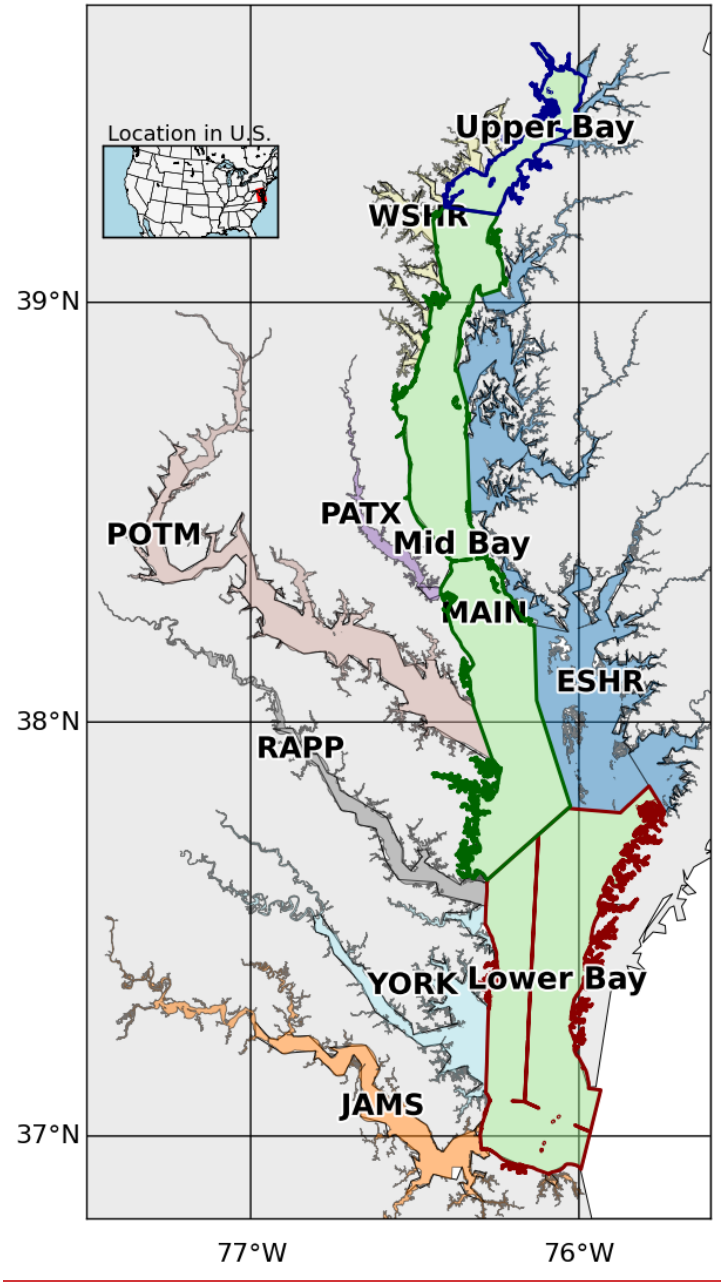

Figure 1: Segmentation of the mainstem of the Chesapeake Bay and its tidal tributaries. The mainstem is divided into three regions, Upper Bay, Mid Bay, and Lower Bay, based on geographic and ecological distinctions. Acronyms denote specific tributaries and sub-estuarine areas: ESHR refers to Eastern Shore tributaries, WSHR to Western Shore tributaries, POTM to the Potomac River, PATX to the Patuxent River, RAPP to the Rappahannock River, YORK to the York River system (including the Mattaponi and Pamunkey Rivers), and JAMS to the James River.

~~The resulting carbon fluxes from benthic macrofauna biomass have large implications for carbon cycling. Although numerous studies have quantified respiration rates in estuaries, very few have provided even rough estimates of calcification (Chauvaud et al., 2003; Waldbusser et al., 2013). Given the potentially important role calcification plays in carbon cycling, addressing this gap is essential for contextualizing the relative contribution of benthic calcification within the broader estuarine carbon budget.~~

In our study, we ~~address the~~ build on this previous work by addressing the following research questions in the context of the Chesapeake Bay:

1) To what extent do benthic macrofauna contribute to estuarine carbon cycling through respiration and calcification, and how might these contributions vary across space?
2) How ~~do water chemistry and sediment composition~~well can environmental variables routinely collected in estuarine monitoring programs predict benthic macrofauna biomass?

~~1)~~ Answering these questions will help clarify the ~~spatial distribution~~role of benthic ~~biomass?~~macrofauna in estuarine carbon cycling and improve the ability of monitoring programs

and numerical models to account for benthic processes using more accessible environmental data.

~~2) What impact do benthic macrofaunal respiration and calcification have on the carbon budget in estuaries?~~

2. Methods

2.1 Overview

We examined historic benthic macrofauna biomass data collected annually by the Chesapeake Bay Long-Term Benthic Monitoring Program (BMP) (Dauer et al., 2000; Llansó & Zaveta, 2017) ~~and time-averaged the data to emphasize the spatial distribution. To contextualize the benthic biomass data, we used~~. We applied empirical relationships linking biomass to secondary production, respiration, and calcification to quantify the impact of benthic macrofauna on carbon cycling in the Bay. To identify environmental predictors of benthic biomass, we compiled measurements of bottom water temperature, salinity, dissolved oxygen, and sediment sand fraction measured by the BMP at the same time and location as the benthic biomass samples. In addition to these measured environmental variables, we utilized ~~biogeochemical model~~ output from ROMS-ECB, which is a ~~fully coupled,~~ three-dimensional~~, hydrodynamic, and~~ estuarine carbon and biogeochemistry (ECB) ~~implementation of~~model embedded into the Regional Ocean Modeling System (ROMS; Shchepetkin & McWilliams, 2005) developed for the Chesapeake Bay (St-Laurent & Friedrichs, 2024b). We identified correlations between these environmental variables (observed and modeled) and benthic macrofauna biomass using generalized additive models (GAMs). ~~We reviewed the literature to identify empirical relationships between benthic biomass and secondary production, respiration, and calcification~~

~~fluxes. We used these empirical relationships to quantify the impact of benthic macrofauna on carbon cycling in the Bay.~~

2.2 Benthic biomass data

Details of the BMP data we used in our study are described elsewhere (Dauer, 1993; Dauer et al., 2000; Dauer & Lane, 2010; Llansó & Scott, 2011; Llansó & Zaveta, 2017) and are summarized here. The program began in 1984, but consistency in sampling started in 1995~~,~~ ~~which is when we began our analysis.~~. The sampling occurs mainly in the summer, between July 15 and September 30, at both fixed and random stations, with the latter changing location every year. The sampling is conducted ~~by~~separately by the states of Maryland (Llansó & Zaveta, 2017) and Virginia (Dauer & Lane, 2010) ~~separately~~, with slightly different protocols used in each state (see below). Our analysis spanned 1995 to 2022, the recent extent of available data, incorporating 28 years of data.

The Maryland monitoring program comprises 27 fixed and 150 random stations in the upper Chesapeake Bay. The Virginia monitoring program comprises 21 fixed and 100 random stations in the lower Chesapeake Bay. In Virginia, random stations were not sampled in 1995, and fixed stations were not sampled in 2017 or 2018. ~~-~~Water depths greater than 12 m in the mainstem part of the Bay in Maryland are not sampled because the bottom waters become anoxic in the summer, resulting in azoic sediments. The tributaries are sampled only in the tidal zone; areas with less than 1 m mean lower low water are considered non-tidal. Some locations, such as oyster reefs and other hard substrates, are also not sampled due to gear unsuitability in such habitats. To avoid seasonal biases, we excluded samples collected outside of the summer sampling window of July 15–September 30, ~~as some~~which occurred earlier ~~years included some sampling outside of this window~~in the study period. This selection resulted in a dataset of 8128

394 samples across both states, or an average of 290 samples per year, slightly less than the
395 maximum of 298.
396 At each sampling station, the uppermost layers of sediment are collected. In Maryland,
397 the sites introduced in 1995 (two fixed sites and all random sites) are sampled with a Young
398 grab, which collects a surface area of 0.0440 m^2 to a depth of 0.10 m. For the other fixed sites in
399 Maryland, nearshore shallow sandy habitats of the mainstem and tributaries are sampled with a
400 modified box corer with a surface area of 0.0250 m^2 to a depth of 0.25 m. Muddy habitats and
401 deep-water habitats in the mainstem and tributaries of Maryland are sampled with a Wildco box
402 corer with a surface area of 0.0225 m^2 to a depth of 0.23 m. The fixed site in the Nanticoke River
403 is sampled with a Petite Ponar grab with a surface area of 0.0250 m^2 to a depth of 0.07 m. In
404 Virginia, fixed sites use a spade-type box-coring device with a surface area of 0.0182 m^2 to a
405 depth of 0.02 m; random sites use a Young grab with a surface area of 0.0400 m^2 to a depth of
406 0.10 m. One limitation of using multiple types of sampling gear is that differences in design,
407 such as penetration depth, sample volume, and sediment disturbance, can introduce variability in
408 estimates of benthic diversity, abundance, and biomass (Eleftheriou & Moore, 2013).
409 For both monitoring programs, the sampling contents are sieved through a 0.5 mm screen
410 to retain only benthic macrofauna. The macrofauna are identified at the lowest taxonomical
411 level. The specimens are dried on a pan for at least 24 hours to a constant weight, then a final
412 weight is measured. The specimens are then placed in a muffle furnace for 4 hours at ~~500°C~~500
413 °C for ashing, and the specimens are weighed again. The ash-free dry weight (AFDW~~)~~),
414 representing only the soft-tissue biomass, is the difference between the dry and ashed weight. We
415 converted the AFDW in g per sample to biomass density *B* in units of g m^{-2} by dividing the
416 AFDW by the area of the sampling device. The data used in our ~~GAMs~~subsequent statistical

analysis include the biomass density of individually selected species and classes and the total biomass density.

Benthic biomass is known to be highly patchy, with large variability even between samples taken in close proximity, hence the common use of replicate sampling in field protocols. To mitigate this noise and extract meaningful large-scale spatial patterns, we averaged across the 28-year time frame. All 8128 biomass samples collected from 1995 to 2022 were averaged onto a uniform grid with cells each measuring 0.04° in longitude and 0.03125° in latitude (~3.5 km per side). 1295 cells had at least one biomass measurement during the 28-year period. Across these cells, the average number of samples was 6.19, the median was 3, and the maximum was 69. Tributaries and the upper Bay were sampled more densely than the mainstem (Appendix A and Fig. A1). This smoothing approach enabled clearer interpretation of spatial gradients in biomass and strengthened the robustness of subsequent statistical analyses aimed at identifying consistent environmental drivers. Some benthic biomass sampling stations fell outside the Chesapeake Bay Program (CBP) water quality segmentation scheme, which was originally developed to support monitoring and management analyses (Chesapeake Bay Program Analytical Segmentation Scheme: Revisions, Decisions and Rationales, 1983–2003, 2004). The CBP segments are defined at a relatively coarse spatial scale and often exclude narrow nearshore environments and small tributary creeks. To maintain consistency with the spatial framework used in coupled hydrodynamic–biogeochemical models, in our case ROMS-ECB, we excluded these points from analysis. This filtering step ensured that all biomass observations were aligned with the modeled domain, avoiding mismatches at the land–water interface. After this step, 1008 grid cells remained, of which 868 contained at least one biomass observation and the remainder were empty cells.

2.3 Carbon flux estimations

To estimate the impact of benthic macrofauna on carbon cycling, we applied empirical equations from the literature to quantify secondary production, calcification, and respiration. These equations were identified through an informal literature review using online tools (e.g., Google Scholar), with emphasis on studies relevant to soft-sediment bivalves, the dominant macrofauna in the Chesapeake Bay. We prioritized relationships applicable to local taxa and easily scalable to our biomass dataset. While multiple sources were available for secondary production, equations for respiration and calcification were more limited; in those cases, we selected models based on representative species that could be scaled from production estimates. We used a range of published values for biomass-to-carbon conversion, secondary production, and species-specific respiration and calcification ratios to estimate upper and lower bounds of carbon fluxes. Additional details on uncertainty calculations are provided in the Appendix B.

2.3.1 Secondary production

We converted biomass to secondary production S (units of g C m^{-2} yr^{-1}). Multiple approaches have been used for this conversion, and we used the average of three approaches to be able to broadly quantify uncertainty in our estimates.

In the first approach, secondary production is given by:

$$S_1 = \alpha B_c \quad (6)$$

where α is the specific growth rate and B_c is carbon-based biomass (units of g C m^{-2}). We found three studies that estimated α for benthic macrofauna. At the low end, a study of benthic macrofauna in the Chesapeake Bay used α = 1.06 yr^{-1} (Wilson & Fleeger, 2023). At the high end, a study of *C. fluminea* used α = 4.45 yr^{-1} (Chauvaud et al., 2003). An intermediate value of α = 2 yr^{-1} was based on monthly observations of benthic macrofauna dominated by the

crustacean *Corophium volutator* and the bivalve *Limecola balthica* at an intertidal site in the upper Bay of Fundy (Schwinghamer et al., 1986). A mean value of 2.50 yr^{-1} was used in Equation 6. B_c ~~To determine the long-term average spatial distribution, biomass densities from all 8128 biomass samples from 1995–2022 were time-averaged onto a grid with cells 0.04° in longitude and 0.03125° in latitude, making the cells nearly square, ~ 3.5 km per side. At least one biomass sample was collected in all 846 cells. Within those cells, the average number of samples per grid cell was 6.62 ± 10.13 (Fig A1). Tributaries and the upper Bay were sampled more densely than the mainstem.~~

~~***2.3 Bottom water quality data***~~

is computed from biomass B (units of g m^{-2}) using:

$$B_c = r_c B \quad (7)$$

where r_c is the ratio of carbon mass to total mass in benthic organic matter. In a study on the bivalve filter feeders *Rangia cuneata* and *Corbicula fluminea*, which dominate in the tidal fresh and oligohaline waters of the Chesapeake Bay, r_c = 0.47 g C g^{-1} was used (Cerco & Noel, 2010). A slightly lower value of 0.41 g C g^{-1} was used in a study of native and introduced bivalves in six North American freshwater systems (Chauvaud et al., 2003). A mean value of r_c = 0.44 g C g^{-1} was used in our calculation.

In the second approach, temperature (T) dependence for bivalve secondary production was added (Sturdivant et al., 2013):

$$S_2 = S_0 \left(\frac{B}{1\ \mathrm{g\ m^{-2}}}\right)^{0.87} \left(\frac{T}{1\ ^{o}\mathrm{C}}\right)^{0.46} \quad (8)$$

where S_0 = 0.40 g C m^{-2} yr^{-1}. Note that the coefficient at the beginning of the equation differs from that of Sturdivant et al. (2013) because of a change in units of B from mg to g m^{-2} and of S

from mg C d^{-1} to g C m^{-2} yr^{-1}. This equation has been shown to agree well with secondary production and biomass measurements (Sturdivant et al., 2013).

Finally, in the third approach (Tumbiolo & Downing, 1994), depth (Z) dependence was added:

$$\log_{10}\left(\frac{S_3}{1\ \mathrm{g\ C\ m^{-2}\ yr^{-1}}}\right) = \beta_0 + b\ \log_{10}\left(\frac{B}{1\ \mathrm{g\ m^{-2}}}\right) - m\log_{10}\left(\frac{M}{1\ \mathrm{mg}}\right) + t\left(\frac{T}{1\ ^{o}\mathrm{C}}\right) - z\ \log_{10}\left(\frac{Z}{1\ \mathrm{m}}+1\right) \quad (9)$$

where $\beta_0 = 0.24, b = 0.96, m = 0.21, t = 0.03, z = 0.16$, and M is the maximum individual body mass. Equation 9 was developed by Tumbiolo & Downing (1994) through multiple regression analysis of 125 benthic invertebrate populations, including data from the Chesapeake Bay. In their model, M refers to the maximum individual mass of the largest size class observed within a population. It was identified as the second most important predictor of secondary production after total biomass. Their analysis showed that species with greater maximum sizes tend to have slower turnover rates and lower production-to-biomass ratios. In our application, we treated M as a constant, based on the maximum individual mass of the bivalve *R. cuneata* collected in a study in the Choptank River in the Chesapeake Bay, which was 5953 mg (Hartwell et al., 1991). *R. cuneata* is among the most abundant and largest benthic macrofaunal species in our study area (Cerco & Noel, 2010; Hartwell et al., 1991).

In Equations 8 and 9, we used the bottom water temperature measured on the same day the benthic samples were collected. This reliance on summer temperature values represents a key limitation of our study, as it likely leads to overestimation of annual secondary production, particularly for Equation 8. For example, Equations 8 and 9 both predict maximum summer secondary production that is about 5 times larger than the minimum winter production, assuming

an annual temperature range of 1 °C to 25 °C. However, we note that the first approach for secondary production (Equation 6) has no temperature dependence. Figures C1–C3 in Appendix C provide a detailed comparison of secondary production across the three models and assess temperature effects on Models 2 and 3.

2.3.2 Calcification

Benthic macrofaunal calcification C (g $CaCO_3$ m^{-2} yr^{-1}) was computed from secondary production following Chauvaud et al. (2003):

$$C = r_s S \quad (10)$$

where r_s is the ratio of shell $CaCO_3$ mass production to tissue organic C mass production, which has units of g $CaCO_3$ (g C)$^{-1}$. Based on samples of the bivalve *Potamocorbula amurensis* in the northern San Francisco Bay, Chauvaud et al. (2003) found r_s to be 10 g $CaCO_3$ (g C)$^{-1}$. They also cited a ratio of 15 g $CaCO_3$ (g C)$^{-1}$ for the bivalve *C. fluminea*, a more relevant species to our study, but the reference is from unpublished data. We used the average of the two values, 12.5 g $CaCO_3$ (g C)$^{-1}$, which corresponds to a molar ratio of 1.5 mol $CaCO_3$ (mol C)$^{-1}$.

2.3.3 Respiration

The ratio of respiration to secondary production, expressed as energy fluxes, was derived from an empirical relationship between benthic macrofauna biomass and respiration in the Bay-of-Fundy study referenced earlier (Schwinghamer et al., 1986):

$$\log_{10}\left(\frac{R}{1\ \text{kcal m}^{-2}\ \text{yr}^{-1}}\right) = \alpha_0 + s\log_{10}\left(\frac{S}{1\ \text{kcal m}^{-2}\ \text{yr}^{-1}}\right) \quad (11)$$

where $s = 0.993$ and $\alpha_0 = 0.367$. Since s is nearly 1, the relationship simplifies to:

$$R = 10^{\alpha_0} S = 2.33S \quad (12)$$

Assuming that the conversion between carbon and energy is the same for S and R, this equation can be directly applied to these processes expressed as carbon fluxes, consistent with our other

carbon flux estimates. Further, combining the relationships of calcification and respiration with secondary production on a molar basis allows a best estimate of the molar ratio of respiration to calcification: 2.33/1.5 = 1.55.

2.3.4 Impact on the carbonate system

From the estimated benthic macrofaunal calcification (*C*) and respiration (*R*), we calculated TA and DIC fluxes (units of mol m^{-2} yr^{-1}):

$$F_{TA} = \frac{-2C}{M_{CaCO_3}} \quad (13)$$

$$F_{DIC} = \frac{R}{M_C} - \frac{C}{M_{CaCO_3}} \quad (14)$$

where M_{CaCO_3} and M_C are the molar masses of $CaCO_3$ and C, respectively, and the sign convention is positive from the benthic fauna to the water column. Both calcification and respiration will lead to increases in the concentration of aqueous CO_2, and so there is a CO_2 flux from benthic fauna that can be decomposed into CO_2 fluxes resulting from these two processes:

$$F_{CO_2} = F_{CO_2}^{TA} + F_{CO_2}^{DIC} \quad (15)$$

It has been estimated, assuming air–sea CO_2 equilibrium, that every mole of $CaCO_3$ precipitated leads to the evasion of 0.6–1 mole of CO_2 to the atmosphere, depending on the temperature, salinity, atmospheric pCO_2, and initial alkalinity (Chauvaud et al., 2003; Frankignoulle et al., 1998; Ware et al., 1992).

In light of strong departures from air–sea CO_2 equilibrium in estuaries, including the Chesapeake Bay (Herrmann et al., 2020), we instead estimate the production rate of CO_2 using buffer factors, ζ_{TA} and ζ_{DIC}, which are defined as the fractional change in [CO_2] divided by the fractional change in [TA] and [DIC], respectively; e.g., $\zeta_{TA} = (\Delta[CO_2]/[CO_2])/(\Delta[TA]/[TA])$. This approach also allows us to estimate the CO_2 flux from respiration. We computed the buffer

factors in three steps. First, we used output from ROMS-ECB (described in more detail later in the Methods Section 2.4) for the years 1995–2022 and calculated long-term averages of bottom [TA], [DIC], temperature, salinity, and pressure (estimated from water depth) at each model grid cell. These values were used as input to PyCO2SYS (Humphreys et al., 2022) to calculate the baseline [CO_2]. Second, we individually perturbed [TA] and [DIC] by 1% ($\Delta[TA]$ and $\Delta[DIC]$) while holding all other variables constant and recalculated [CO_2] to get $\Delta[CO_2]$. Third, we computed ζ_{TA} and ζ_{DIC} using the definition of the buffer factors.

To relate the fluxes to the buffer factors, we use the flux form of the buffer factors:

$$\zeta_{TA} = \frac{F_{CO_2}^{TA}/[CO_2]}{F_{TA}/[TA]} \quad (16)$$

$$\zeta_{DIC} = \frac{F_{CO_2}^{DIC}/[CO_2]}{F_{DIC}/[DIC]} \quad (17)$$

These flux forms take the definitions of the buffer factors and replace ratios of concentration changes (e.g., $\Delta[CO_2]/\Delta[TA]$) with ratios of fluxes (e.g., $F_{CO_2}/F_{CO_2}^{TA}$). Using Equations 16 and 17 in Equation 15 yields an expression for the CO_2 flux from benthic fauna to the water column:

$$F_{CO_2} = [CO_2]\left(\frac{\zeta_{TA}F_{TA}}{[TA]} + \frac{\zeta_{DIC}F_{DIC}}{[DIC]}\right). \quad (18)$$

2.3.5 Spatial analysis and comparison to other carbon fluxes

To place benthic macrofauna contributions to estuarine carbon cycling in a broader spatial context, we averaged fluxes over 10 regions based on aggregated Chesapeake Bay Program segments (Fig. 1): the major tidal tributaries (the Patuxent, Potomac, Rappahannock, York, and James River Estuaries), the Western and Eastern Shores, and the Upper, Mid, and Lower (mainstem) Bay. Additionally, we computed averages over the mainstem Bay and the

whole Bay. For each region, we calculated benthic respiration and bivalve calcification rates based on observed biomass, using the empirically derived equations just described. We then compared these fluxes to other components of the estuarine carbon budget using published values for primary production, allochthonous organic carbon inputs, oyster calcification, and air–sea gas exchange.

First, we assessed the extent to which benthic macrofauna remineralize organic carbon inputs by comparing our calculated respiration rates to net primary production (NPP) and external particulate organic carbon (POC) loads. Primary production and POC values were obtained from prior studies (Herrmann et al., 2015; Kemp et al., 1997; Najjar et al., 2018; Zhang & Blomquist, 2018) and scaled to match the spatial extent of our biomass data. In the Upper Bay, we calculated organic carbon inputs by distributing the Susquehanna River's POC load over the combined surface area of the oligohaline and tidal fresh segments (CB1 and CB2, (Olson, 2012). This approach assumes that the majority of the annual POC load from the Susquehanna River remains concentrated in the Upper Bay and is respired rather than transported downstream, an assumption supported by Canuel & Hardison (2016). For comparison, we also distributed Susquehanna River POC inputs across the entire mainstem. For brevity, we restricted our tributary-level comparison to the Potomac River Estuary, where the full organic carbon load was distributed across the surface area of the entire tidal tributary (Fig. 1).

Second, we compared our soft-sediment bivalve calcification estimates to published oyster calcification rates from (Fulford et al., 2007). Oyster ash-free dry weight was converted to live weight using a 10:1 ratio (Mo & Neilson, 1994), and a calcification rate of 2 mg $CaCO_3$ per g live weight per day was applied (Waldbusser et al., 2013). Because Eastern oyster (*Crassostrea virginica*) populations in the Chesapeake Bay were historically at least two orders of magnitude

higher than current levels (Fulford et al., 2007; Newell, 1988), we also scaled published oyster calcification rates up by a factor of 100 to estimate potential historical contributions. This comparison allowed us to place present-day bivalve calcification into the broader context of ecosystem function.

Third, we evaluated whether riverine calcium supply could limit observed calcification by estimating annual calcium fluxes from the Susquehanna and Potomac Rivers using non-tidal USGS data from 1995 to 2022 and the Weighted Regression on Time, Discharge, and Season (WRTDS) method (Hirsch et al., 2010). Assuming a 1:1 molar ratio between Ca^{2+} and $CaCO_3$ formation, we estimated the maximum potential calcification that could occur if all incoming calcium were used for shell production in adjacent estuarine zones.

Finally, we compared CO_2 generated from respiration and calcification (Equation 18) to published estimates of air–sea CO_2 exchange (Chen et al., 2013; Herrmann et al., 2020).

The estimated carbon fluxes reveal important spatial patterns, but their interpretation should be tempered by uncertainty in several underlying assumptions. While secondary production models are relatively well-calibrated across estuarine systems, the calculations for calcification and respiration are more sparse and less empirically constrained. Our propagated uncertainty in calcification and respiration incorporates variation in biomass-based carbon content, multiple conversion approaches from biomass to secondary production, and calcification parameters derived from two different bivalve species. Although we used different methods to estimate calcification and propagated these uncertainties accordingly, only one approach was available for respiration.

We estimated uncertainties in F_{DIC} and F_{TA}, which represent the propagated uncertainties from respiration and calcification alone, with no additional sources of uncertainty included in

those calculations. However, we did not calculate formal uncertainties in F_{CO_2} due to the complexity involved. Additional uncertainty in F_{CO_2} arises from the use of annually averaged, model-derived values for salinity, temperature, depth, DIC, and TA. Further uncertainty stems from the method used to calculate ζ from TA and DIC perturbations. While these additional sources contribute to the overall uncertainty in F_{CO_2}, the uncertainties in F_{DIC} and F_{TA} are likely to remain the dominant contributors.

The resulting error bars in the various carbon fluxes reflect these methodological uncertainties, offering a plausible range rather than precise values. Thus, the benthic macrofaunal carbon fluxes presented here should be interpreted with some caution, with more confidence given to the broad spatial patterns and less to the absolute values.

2.4 Environmental predictors of benthic biomass

From the BMP, we used bottom temperature, salinity, and dissolved oxygen data, which are measured with a YSI 660 Sonde or Hydrolab DataSonde 4a in Maryland and a YSI 85 Model meter in Virginia ~~one meter~~1 m above the sediment surface. Extreme outliers, defined as data points that fall beyond three times the interquartile range from the first or third quartile, were removed. As a result, one value for dissolved oxygen and one for water temperature were excluded from the analysis. The salinity zones are also characterized at each site as tidal fresh (<0.5 ppt), oligohaline (0.5–5 ppt), low mesohaline (5–12 ppt), high mesohaline (12–18 ppt), and polyhaline (>18 ppt); these zones are relatively geographically fixed (with some changes in 2011 due to Hurricane Irene and Tropical Storm Lee) based on long-term averages of salinity (Llansó, 2002; Llansó & Zaveta, 2017). Sediment sand fraction was measured by first collecting two 120

ml benthic grab sub-samples. Sand particles are separated by wet-sieving through a 63-µm stainless steel sieve. Sand fraction is recorded after drying and weighing the samples. The bottom water quality and sediment composition data were time-averaged using the same scheme described earlier for the benthic biomass data.

~~*2.4 Biogeochemical model output*~~

ROMS-ECB output was used to characterize environmental variables not measured by the BMP that could be relevant to predicting the benthic macrofauna biomass distribution. ROMS-ECB uses 20 terrain-following vertical levels and a uniform horizontal resolution of 600 m (St-Laurent & Friedrichs, 2024b). We compiled daily averaged output at various grid points from 1995 to 2022 corresponding to the locations of each of the 8128 benthic biomass samples. We selected the ROMS output at the nearest ROMS grid point to each BMP sample location for each variable of interest, described below. ~~Some~~Several ROMS-ECB environmental variables are directly linked to primary production~~. Because~~, but the timing of peak primary production ~~peaks~~ does not always ~~coincide~~align with periods of ~~high~~greatest food availability for ~~benthos, annual averages may obscure important seasonal patterns.~~benthic organisms. To ~~better~~ capture ~~these temporal mismatches~~ecologically meaningful variation in benthic–pelagic coupling, we calculated both seasonal and annual averages for each variable. ~~For seasonal averages,~~Seasonal groupings reflect key ecological periods: spring ~~was defined as~~ (March–May~~,~~), which includes the diatom bloom that delivers fresh organic material to the benthos, and summer ~~as~~ (June–August~~, fall as~~), characterized by stratification, hypoxia, and intense remineralization. Fall (September~~–October,~~November) and winter ~~as~~ (December–February~~. The seasonal and annual averages~~) were also included to represent background seasonal variability. We then time-averaged ~~in the same scheme explained~~the seasonal and annual means as described earlier~~,~~

~~resulting in~~. Coverage dropped from 868 to 846 ~~gridded~~ cells after adding ROMS-ECB outputs, largely where the model masks shallow/tributary cells or lacks complete seasonal data.

We used ROMS-ECB output, as opposed to data from the Chesapeake Bay Water Quality Monitoring Program (WQMP~~) data. WQMP~~), which has ~~also~~ measured water quality variables since 1984 at over 100 tidal stations (Chesapeake Bay Program, n.d.). However, the stations are at different locations than the BMP stations, requiring interpolation to correlate these data with benthic biomass. Other studies have opted to use kriging, a method used to spatially interpolate surface water quality data, to increase the spatial resolution. ~~It~~Kriging has been found to outperform the standard inverse distance weighting tools typically used in the Chesapeake Bay (Murphy et al., 2015). One study evaluated the kriging of surface WQMP data for July 2007 using 117–123 data points (Murphy et al., 2015). In cross-validation, one measured sample is removed, and the interpolation is then performed at that location; the interpolated value is then compared to the observed value. Cross-validation of temperature, salinity, and dissolved oxygen yielded root-mean-square errors (RMSE) of 0.75 °C, 1.1 ppt, and 1.2 mg L^{-1}, respectively. In contrast, ROMS-ECB output was evaluated with over 500,000 WQMP data points at multiple depths and locations from 1985 to 2021 (St-Laurent & Friedrichs, 2024a). The RMSEs for temperature, salinity, and dissolved oxygen were 1 °C, 1.9 psu, and 1.5 mg L^{-1}, respectively. Although these RMSEs are slightly higher than those from kriging, the evaluation was much more robust, and the long time series evaluation is more relevant to our time-averaging technique over 28 years. In addition, we wanted to utilize bottom water quality data, as these variables are measured closer to the location of benthic macrofauna. However, cross-validation for kriging was only performed at the surface~~, presumably~~ (Murphy et al., 2015), possibly due to the

challenges of accounting for bottom topography in spatial interpolation~~. For these reasons, ROMS-ECB output was used instead of interpolated WQMP data~~.

ROMS-ECB simulates many variables, and we considered the subset that might be good predictors of benthic biomass: bottom ~~particulate organic carbon (~~POC~~) concentration~~, bottom total suspended solids (TSS), and surface ~~nitrate (~~NO_3^-~~).~~ $^-$. POC was considered because a large fraction of POC represents food for benthic macrofauna. TSS was considered a metric of suspended inorganic material, which can inhibit filter-feeding organisms (Grant & Thorpe, 1991). Photosynthesis is largely limited by ~~nitrate~~NO_3^- in the Chesapeake Bay (Zhang et al., 2021); because phytoplankton productivity and the subsequent sinking of POC is an important source of organic matter to the benthos, ~~nitrate~~NO_3^- could be a predictor of benthic biomass. ROMS-ECB output was evaluated for robustness with WQMP data using Spearman's rank correlation coefficient, ~~r_s~~R_S, which measures the strength of the association between two variables (Hauke & Kossowski, 2011). In our analysis of benthic biomass predictors, we included only variables with ~~r_s~~R_S above 0.7, which generally indicates a strong association (Akoglu, 2018). NO_3^- was used as it had ~~r_s~~R_S = 0.77, whereas POC and TSS were not as they had ~~r_s~~R_S = 0.26 and 0.24, respectively (St-Laurent & Friedrichs, 2024a).

We also considered potentially good predictors that could be computed from ROMS-ECB output: surface oxygen supersaturation (ΔO_2) and bottom aragonite saturation state (Ω_{arag}). ΔO_2 can be used as a tracer for net ecosystem production (Herrmann et al., 2020) and hence may indicate organic matter availability to the benthos. $\Delta[O_2]$ is equal to O_2 minus the saturation concentration, which was computed from temperature and salinity (Garcia & Gordon, 1992). Positive ΔO_2 values are favored during net autotrophy (photosynthesis exceeds respiration), while negative values are favored during net heterotrophy (respiration exceeds photosynthesis);

temperature change and transport can also create non-zero ΔO_2. Ω_{arag} could predict benthic biomass because bivalve calcification is expected to depend on this metric (Thomsen et al., 2015). ~~$\Delta[O_2]$ is equal to O_2 minus the saturation concentration, which was computed (as in ROMS-ECB), from temperature and salinity (Garcia & Gordon, 1992). Ω_{arag} is the product of calcium ion concentration and the carbonate ion concentration divided by the solubility product for aragonite, which is a function of temperature, salinity, and pressure.~~Ω_{arag} is given by Equation 5, with K_{sp} corresponding to aragonite. PyCO2SYS (Humphreys et al., 2022) was used to derive the solubility product and carbonate ion concentration from alkalinity, DIC, temperature, salinity, and water depth. We ~~retained~~examined ΔO_2 and Ω_{arag} in the subsequent statistical analysis because the ROMS-ECB output variables used to compute them ~~can be evaluated with observation (temperature, salinity, DO, alkalinity, and DIC)~~ all had ~~$r_s >$~~ $R_S > 0.7$~~). Calcium.~~ Although calcium measurements were not available for model evaluation, ~~but calcium~~it is highly correlated to salinity, though deviations may occur at low salinity (Beckwith et al., 2019).

2.5 Statistical modeling of benthic biomass

We used GAMs to evaluate how ~~the~~ bottom water quality ~~data~~ and biogeochemical model ~~output~~outputs predict the spatial distribution of benthic ~~macrofauna~~macrofaunal biomass. GAMs ~~have been used extensively in ecological research since the late 1960s in coastal ecosystems (Guisan et al., 2002; Smith et al., 2023). GAMs have been shown to perform as well or better than other predictor models based on environmental conditions (Drexler & Ainsworth, 2013). They~~ are data-driven statistical models that have been widely applied in coastal ecology since the late 20th century (Guisan et al., 2002; Smith et al., 2023). They model additive, smoothed relationships between predictor and response variables, making them well-suited for capturing the non-linear, non-monotonic patterns often observed in ecological datasets~~find the~~

~~response to a suite of predictor variables~~ (Grüss et al., 2014; Guisan et al., 2002; Hastie & Tibshirani, 1987; Wood, 2017). ~~They examine how well the predictor (or explanatory) variables explain the ecological response,~~GAMs also quantify the strength ~~of the association,~~ and ~~the~~ relative contribution of ~~the different predictors~~ each predictor (Guisan et al., 2002)~~. GAMs assume that the multiple functions describing the association between the predictor and response variables are additive~~ and ~~can be smoothed (Guisan et al., 2002). The GAMs~~ have demonstrated predictive performance comparable to or exceeding other modeling approaches (Drexler & Ainsworth, 2013). We used the mgcv package ~~used here — the mgcv library~~ in R ~~with the~~and applied restricted maximum likelihood (REML) ~~optimization method~~to optimize smoothness (Wood, 2011; Wood, 2017)~~ — automates the polynomial order used to fit the smooth function for each predictor variable. An intercept term and an error term are added to the associated smoothed functions for each predictor variable. Model diagnostics include the percentage of deviance explained, signifying how much of the variance in the response variable can be explained by the additive effects of all the smoothed functions associated with the predictor variables. We used GAMs because they are uniquely suited to model the non-linear and non-monotonic relationships between response and predictor variables in our dataset. GAMs require a relatively large amount of data, and with our extensive dataset, they can estimate~ . This approach is particularly effective with large datasets like ours, enabling robust estimation of spatial patterns in biomass across a broad geographic region (Grüss et al., 2014; Wood, 2011).

~~To ensure predictor variables in the GAMs analysis were not strongly correlated~~ Although GAMs can handle non-normal distributions of the response variable (Guisan et al., 2002), we ~~used six~~found the best model fit by applying a natural logarithmic transformation to

the biomass. A small constant (0.0001 g m^{-2}) was added to the biomass values before applying the natural logarithmic transformation to account for zeros in the data.

As described earlier, we initially identified eight environmental variables ~~in the GAMs analysis:~~: O_2, salinity, total depth, ~~sand fraction, bottom~~ water temperature, ~~bottom salinity, bottom dissolved oxygen, and surface~~ sand fraction, NO_3^- ~~(Table 1). If predictor variables are highly correlated, they distort the GAMs~~, Ω_{arag}, and $\Delta[O_2]$. To avoid multicollinearity, which can distort GAM results (Grüss et al., 2014; Grüss et al., 2018; Guisan et al., 2002)~~. We~~, we used Pearson's correlation coefficients~~, a common approach for evaluating cross-correlation in GAMs,~~ (r) to evaluate the linear correlation between the predictor variables. ~~If~~When two ~~predictor~~ variables ~~have correlations greater than~~were highly correlated ($r >$ 0.7~~, one of the variables was discarded~~) (Dormann et al., 2013)~~. As an alternate means of evaluating multicollinearity, concurvity~~, we retained the variable that was ~~also analyzed after the smooth functions were applied~~ more directly measurable and broadly understood across estuarine systems. Based on this assessment, we excluded Ω_{arag} and $\Delta[O_2]$ due to ~~the predictor variables. High concurvity values (>0.8) indicated that the model might struggle to distinguish between the individual contributions of correlated smooth terms (Wood, 2017). However, applying the Pearson's correlation coefficient cut-off also eliminated high concurvity values (St-Laurent & Friedrichs, 2024a). Ω_{arag} and $\Delta[O_2]$ were not used as predictor variables because of~~ their ~~high~~strong correlation with other ~~predictor variables.~~ variables and retained the remaining six variables for GAM analysis. While necessary for model stability, this approach may limit the explanatory power of the GAM by excluding ecologically meaningful predictors. The full list of candidate variables and their inclusion status is provided in Table 1.

Table 1: Predictor variables from the Chesapeake Bay Benthic Monitoring Program and ROMS-ECB~~. Information collected~~ compiled from 1995–~~2022 with~~2002. For ROMS-ECB output, daily values were used to calculate annual averages ~~giving every daily average value for the entire period. Seasonal~~and seasonal averages ~~were taken~~ for spring (March–April), summer (July–August), fall (September–November), and winter (December–February)

Dataset	Location	Variable	Units	Processing~~?~~	Used in GAMs?
BMP	Bottom	~~DO~~O_2	mmol m^{-3}	Removed extreme outliers	Yes
BMP	Bottom	Salinity	ppt	None	Yes
BMP	Bottom	Total depth	m	None	Yes
BMP	Bottom	Water temperature	°C	Removed extreme outliers	Yes
BMP	Bottom	Sand fraction	%	None	Yes
ROMS-ECB	Surface	NO_3	mmol m^{-3}	Annually and seasonally averaged	Yes
ROMS-ECB	Bottom	POC	mmol m^{-3}	Annually and seasonally averaged	No, model ~~data validation~~ evaluation gave poor results

ROMS-ECB	Bottom	TSS	mg L^{-1}	Annually and seasonally averaged	No, model ~~data validation~~ evaluation gave poor results
ROMS-ECB	Bottom	Ω_{arag}		Calculated from alkalinity, DIC, temperature, water depth, and salinity using PyCO2SYS. Annually and seasonally averaged	No, highly correlated with salinity
ROMS-ECB	Surface	$\Delta[O_2]$	mmol m^{-3}	Calculated from oxygen, salinity and temperature using Gracia & Gordon (1991, 1992). Annually and seasonally averaged	No, highly correlated with salinity and NO_3

We used Akaike's Information Criterion (AIC), a statistical measure that has been increasingly used in ecology, to evaluate which combination of parameters results in the best model fit (Symonds & Moussalli, 2011).~~)~~ AIC is calculated using the number of fitted parameters in the model, the maximum likelihood estimate, and the residual sum of squares (Symonds & Moussalli, 2011). Among the candidate models, the one~~). The model~~ with the

lowest AIC value ~~indicates the most parsimonious model with the minimum number of~~ offers the best balance between explanatory power and simplicity, requiring the fewest necessary parameters. We chose the assemblage of predictor variables in our model ~~by minimizing~~that minimized AIC. We generally used annually averaged predictor variables from the ROMS-ECB output because using seasonal averages had a negligible difference on the AIC. To assess the relative influence of each predictor variable, we used Akaike weights, which indicate the probability that a given model is the best among those considered. We ranked models by AIC and summed the Akaike weights for all models containing each predictor variable. Higher Akaike weights indicate stronger support for a variable's inclusion in the best-fitting models. Interaction terms between predictor variables were examined, but their inclusion did not significantly improve the AIC values.

~~We also evaluated the model fit by looking at the distribution of the residuals and a scatter plot of observed vs model response values. A good model would have relatively normally distributed residuals as well and a near 1:1 line in the observed vs model response values. Although GAMs can handle non-normal distributions of the response variable (Guisan et al., 2002), we found the best model fit by applying a natural logarithmic transformation to the biomass. A small constant (0.0001 g m^{-2}) was added to the biomass values before applying the natural logarithmic transformation to account for zeros in the data. The resulting biomass was normally distributed after applying the natural logarithm function, so the GAMs model was fitted with a Gaussian distribution with an identity link function.~~

~~2.6 Carbon Flux Estimations~~

~~To estimate the relative impact of benthic macrofauna on carbon cycling, we used empirical equations to quantify carbon fluxes, including secondary production, calcification, and respiration.~~

~~The first step involved converting biomass~~ ~~(units of g m^{-2}) to a carbon-based biomass~~ ~~(units of g C m^{-2}) using:~~

~~where~~ ~~is the ratio of carbon mass to total mass in benthic organic matter. In a study on the bivalve filter feeders *Rangia cuneata* and *Corbicula fluminea* that dominate in the tidal fresh and oligohaline waters of the Chesapeake Bay,~~ ~~= 0.47 g C g^{-1} was used (Cerco & Noel, 2010). A slightly lower value of 0.41 g C g^{-1} was used in a study of native and introduced bivalves in six North American freshwater systems (Chauvaud et al., 2003). Uncertainties for~~ ~~is derived from the two different~~ ~~values:~~

~~=0.03 g C g^{-1}, half the range of possible~~ ~~values.~~

~~We then converted biomass to secondary production rates~~ ~~(units of g C m^{-2} yr^{-1}).~~ ~~Multiple approaches have been used for this conversion, and we used several to be able to broadly quantify uncertainty in our estimates. Some studies assume~~ ~~is proportional to~~ ~~:~~

~~where the constant of proportionality~~ ~~is the specific growth rate. We found three studies that estimated~~ ~~for benthic macrofauna. At the low end, a study of benthic macrofauna in the Chesapeake Bay used~~ ~~= 1.06 yr^{-1} (Wilson & Fleeger, 2023). At the high end, a study of *C. fluminea* used~~ ~~= 4.45 yr^{-1} (Chauvaud et al., 2003). An intermediate value of~~ ~~= 2 yr^{-1} was based on monthly observations of benthic macrofauna dominated by the crustacean *Corophium*~~

~~*volutator* and the bivalve *Limecola balthica* at an intertidal site in the upper Bay of Fundy (Schwinghamer et al., 1986). A mean value of 2.50 yr^{-1} was used in Eq. 3. The uncertainty for is derived from and :~~

~~ is half the range of possible values and equals 1.695 yr^{-1}. Temperature dependence for bivalve secondary production was included by Edgar (1990):~~

~~where = 0.40 g m^{-2} yr^{-1}. Note that the coefficient at the beginning of the equation differs from that of Edgar (1990) because of a change in units of from mg to g m^{-2} and of from mg C d^{-1} to g C m^{-2} yr^{-1}. This equation has been shown to agree well with direct secondary production and biomass measurements (Sturdivant et al., 2013). Tumbiolo & Downing (1994) developed Eq. 6, and the model was also validated with direct calculations of production in the Chesapeake Bay:~~

~~where In this calculation, we used the AFDW of biomass for . The bottom water temperature (T) was measured only in the summer on the same day the benthic samples were collected. This reliance on summer bottom water temperatures may be slightly inaccurate, as it reflects summer production scaled up to annual values. For max individual body mass (M), we used the maximum weight of the bivalve *R. cuneata* collected in a study in the Choptank River in the Chesapeake Bay, which was 5953 mg (Hartwell et al., 1991). Z corresponds to the water depth. The Edgar (1990) and Tumbiolo & Downing (1994) secondary production equations do not include explicit sources of uncertainty. The mean value was calculated from the three different secondary production equations (Eqs.~~

3, 5, and 6) and uncertainty arises from the multiple equations used:

$$[\quad]$$

where w corresponds to the weights associated with the uncertainty for each secondary production calculation. The subscripts in [ ] correspond to the secondary production equations (Eqs. 3,5, and 6), with values of 0.1 for w_3, 0.45 for w_5, and 0.45 for w_6. Higher weights were assigned to w_5 and w_6 since the associated secondary production equations have been more extensively validated. Since there is no well-defined source of uncertainty in these two equations, a small error term [ ] of 0.001 was included.

We then calculated calcification rates from secondary production rates. We relied on a study by Chauvaud et al. 2003, which calculates the ratio of shell production ($g\ CaCO_3\ m^{-2}\ yr^{-1}$) to tissue production ($g\ C\ m^{-2}\ yr^{-1}$):

$$[\quad]$$

where [ ] is the ratio of shell production to tissue production. The study samples the bivalve *Potamocorbula amurensis* in the northern San Francisco Bay. The ratio of shell production to tissue production was 10. There was also a ratio of 15 cited for the bivalve *C. fluminea*, a more relevant species to our study, but the reference is from unpublished data. Calcification C (units of $g\ C\ m^{-2}\ yr^{-1}$) is in terms of CO_2 produced as calcification shifts seawater equilibrium and produces dissolved CO_2. [ ] corresponds to the ratio of the mass of CO_2 produced divided by the mass of calcium carbonate produced. Chauvaud et al., (2003) gives a ratio of 0.12 for the bivalve *C. fluminea* and 0.09 for the bivalve *P. amurensis*. For the two bivalve species, the product of the ratio of shell production to tissue production ([ ] and the ratio of mass of CO_2 produced divided by calcium carbonate produced ([ ] gives an average value of 1.35; this value was used in Eq. 8. Calcification uncertainty is derived from [ ], [ ], and [ ]:

where k is the product of and , with one value for *C. fluminea* and one for *P. amurensis*.

 and is half the range of possible values.

We also calculated respiration rates from secondary production. A ratio of respiration rates to secondary production rates was derived from an empirical relationship between benthic macrofauna biomass and respiration rates in the Bay of Fundy study referenced earlier:

where and . Kcal were converted to grams of carbon, using the ratio 1 g C=11.4 kcal (Chauvaud et al., 2003). The estimations for calcification and respiration rates have less data validation than secondary production. However, we are confident they can approximate the relative carbon flux impact of the benthic macrofauna. The uncertainty in respiration rates is derived solely from :

Eq. 12 shows that the total CO_2 generated, TC, is the sum of the CO_2 generated from respiration and calcification (units of g C m^{-2} yr^{-1}) (Chauvaud et al., 2003).

The uncertainties in TC are derived from and :

We grouped the biomass measurements and associated carbon fluxes into 12 regions to highlight broader spatial differences. These regions were created by combining the 92 segments delineated by the Chesapeake Bay Program (CBP; 2004). The 12 regions were the Patuxent River, the Potomac River, the Rappahannock River, the York River, the James River, the Western Shore (the small western tributaries in Maryland), the Eastern Shore (all tributaries east

~~of the mainstem), the Upper Bay (mainstem oligohaline zone and tidal fresh zones or CB1 and CB2), the Mid Bay (mainstem mesohaline zones or CB3, CB4, and CB5), and the Lower Bay (mainstem polyhaline zones or CB6, CB7, and CB8). Biomass density values were calculated for each region.~~

3. Results

3.1 Spatial distribution of benthic macrofauna biomass

~~Benthic~~The time-averaged (1995–2022) summer benthic macrofauna biomass exhibits strong spatial variability across the Chesapeake Bay, with higher concentrations in the tidal fresh and oligohaline zones, and lower concentrations in the Mid Bay and lower sections of many tributaries~~.~~ (Figure ~~1 shows the spatial distribution of the time-averaged (1995–2022) summer benthic macrofauna biomass.~~2, 3a). The arithmetic mean of all biomass measurements ~~(~~based on the full data set, $N = 8128$~~)~~ is 7.93 g m^{-2}~~,~~ (median = 0.98 g m^{-2}), whereas the spatial mean ~~is 6.31 g m^{-2}~~across all grid cells with at least one biomass measurement ($N =$ ~~846).~~1295) is 7.16 g m^{-2} (median = 1.39 g m^{-2}). The sampling scheme oversamples the tidal tributaries (Fig. A1~~)~~), where ~~more~~ biomass density is ~~concentrated~~higher, inflating the arithmetic mean. The standard deviation of the full dataset is 28.~~70~~7 g m^{-2}, indicating that the distribution is heavily skewed to the right, with the highest sample reaching up to 722 g m^{-2}. The standard deviation of the time-averaged data is ~~17.02~~18.0 g m^{-2}, considerably smaller than the full data set since it does not include temporal variability, but is nevertheless still skewed to the right, with the highest gridded value of 220~~.18~~ g m^{-2}. Most of the high~~-~~biomass density zones (>30 g m^{-2}) are concentrated in the tidal fresh and oligohaline sections of the mainstem and Potomac River Estuary. The other tributaries have higher biomass in the tidal fresh and oligohaline and zones compared to the other salinity zones. In the Mid Bay and lower sections of many tributaries, biomass is very low.

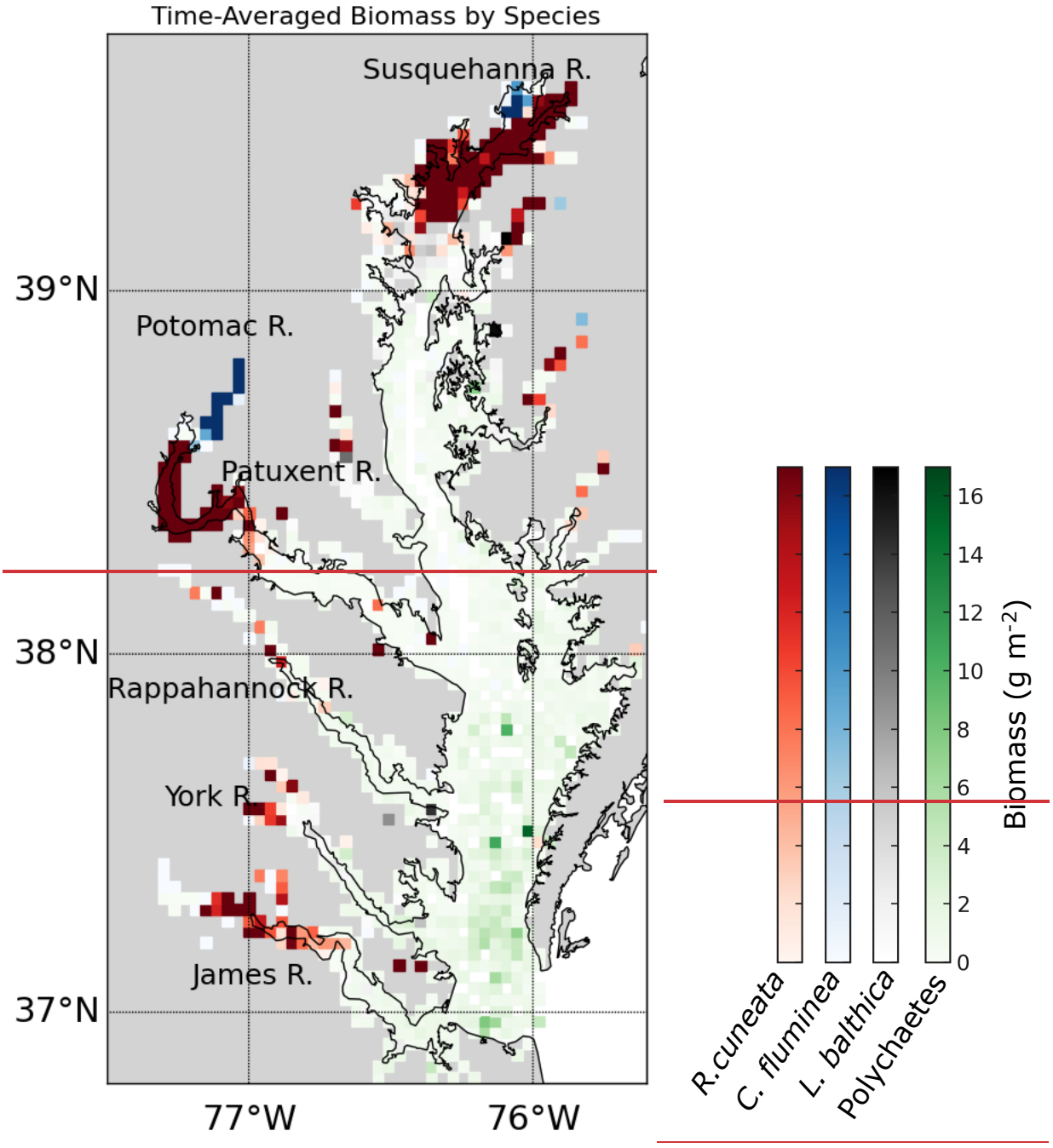
Time-Averaged Biomass by Species
Susquehanna R.
Potomac R.
Patuxent R.
Rappahannock R.
York R.
James R.
39°N
38°N
37°N
77°W
76°W
Biomass (g m-2)
0
2
4
6
8
10
12
14
16
R.cuneata
C. fluminea
L. balthica
Polychaetes

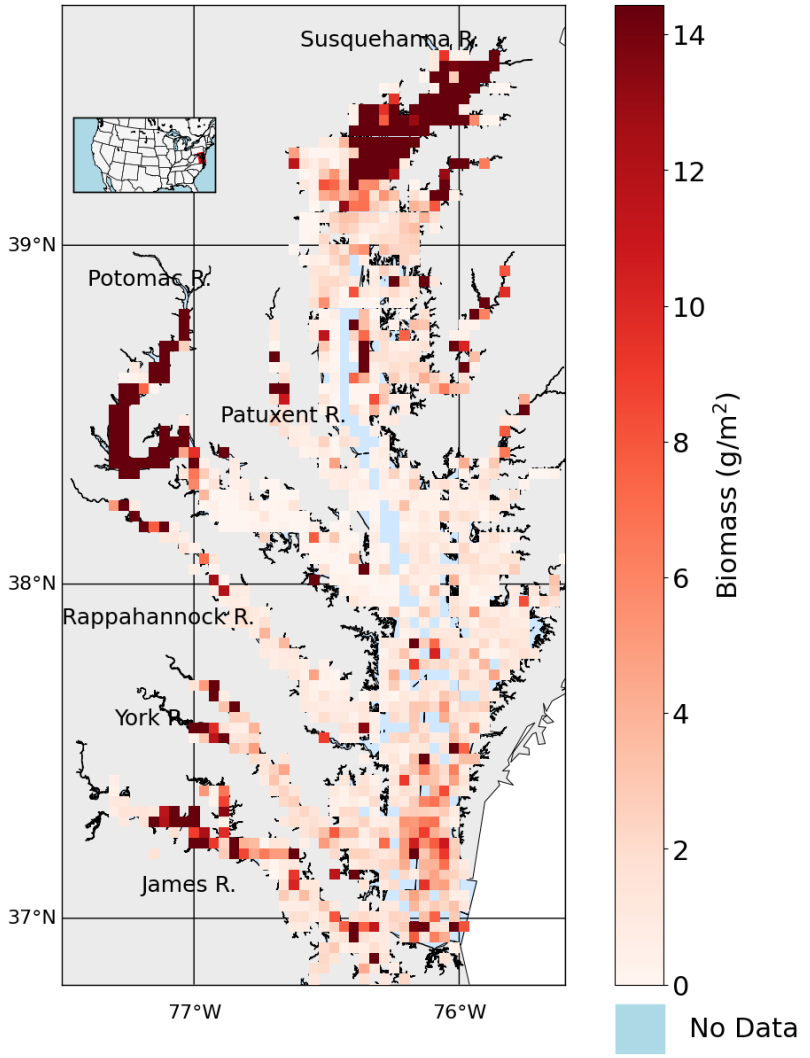

Figure ~~1~~2: Average summer biomass density from 1995 to 2022 from the ~~Maryland and Virginia~~Chesapeake Bay Benthic Monitoring Program. ~~Each~~Biomass values are shown using a red color ~~corresponds to a specific bivalve species (*M. balthica, C. fluminea, or R. cuneata*) or polychaetes. The color shown on the map is the species~~scale, white represents 0 g m^{-2}, light blue indicates open water grid cells with ~~the highest time-averaged biomass in that grid cell~~no data, and gray represents land areas with no data.

~~In the high-biomass tidal fresh and oligohaline zones, bivalves dominate; whereas polychaetes are more prevalent in the lower-biomass mesohaline and polyhaline zones.~~ The distribution of ~~benthic~~the biomass ~~density~~ into salinity zones for multiple taxonomic groups and species is shown in Fig. ~~2.~~3b–f. Bivalves dominate biomass in all salinity zones, except the polyhaline, where they are comparable to polychaetes. Bivalves comprise 88.0% of the benthic biomass, and polychaetes comprise 7.3%. At a taxonomic species level, the bivalve *R. cuneata* comprises 66.1% of the biomass, followed by the ~~bivalve~~bivalves *C. fluminea* (8.0%) and ~~the bivalve~~ *L. balthica* (7.5%). Appendix D provides a more detailed spatial analysis of species distribution. The high-~~-~~biomass zones in the Upper Bay, Potomac River Estuary, and James River Estuary are dominated by *R. cuneata*, mostly in the oligohaline zone (~~Fig. 2~~Figs. 3c & D1). *C. fluminea* also dominates in relatively higher quantities in the tidal fresh zone of the Potomac River Estuary and the tidal fresh zone of the Upper Bay (~~Fig. 2~~Figs. 3d & D1). In general, *R. cuneata* has a higher biomass density in the tidal fresh than *C. fluminea* because *R. cuneata* is present in all tidal fresh zones. *L. balthica* is distributed in multiple salinity zones; it is highest in the lower mesohaline and is the dominant species in the lower mesohaline zone of the Upper Bay and Patuxent River~~.~~ Estuary (Figs. 3e & D1). The biomass density of *L. balthica* in the lower mesohaline (<2 g m^{-2}) is significantly lower than that of *C. fluminea* and *R. cuneata* in the tidal fresh and oligohaline zones. Polychaetes are the species that dominate over the largest geographic area, throughout the polyhaline and part of the higher mesohaline (~~Fig. 1 &~~Figs. 2, 3f, & D1). However, their biomass density is low relative to bivalves (<2 g~~/m²~~ m^{-2}). Bivalves are sparse throughout the higher mesohaline and polyhaline zones.

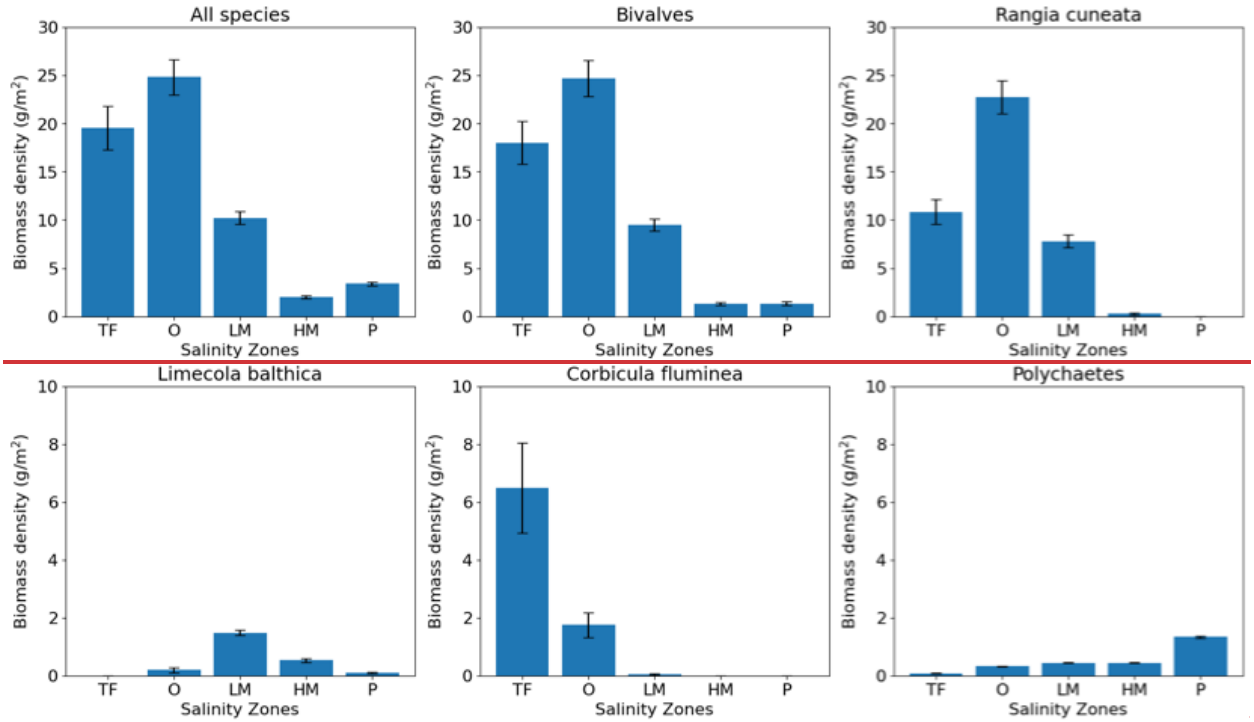
All species
Bivalves
Rangia cuneata
Limecola balthica
Corbicula fluminea
Polychaetes
Biomass density (g/m²)
Salinity Zones
TF
O
LM
HM
P

948

949

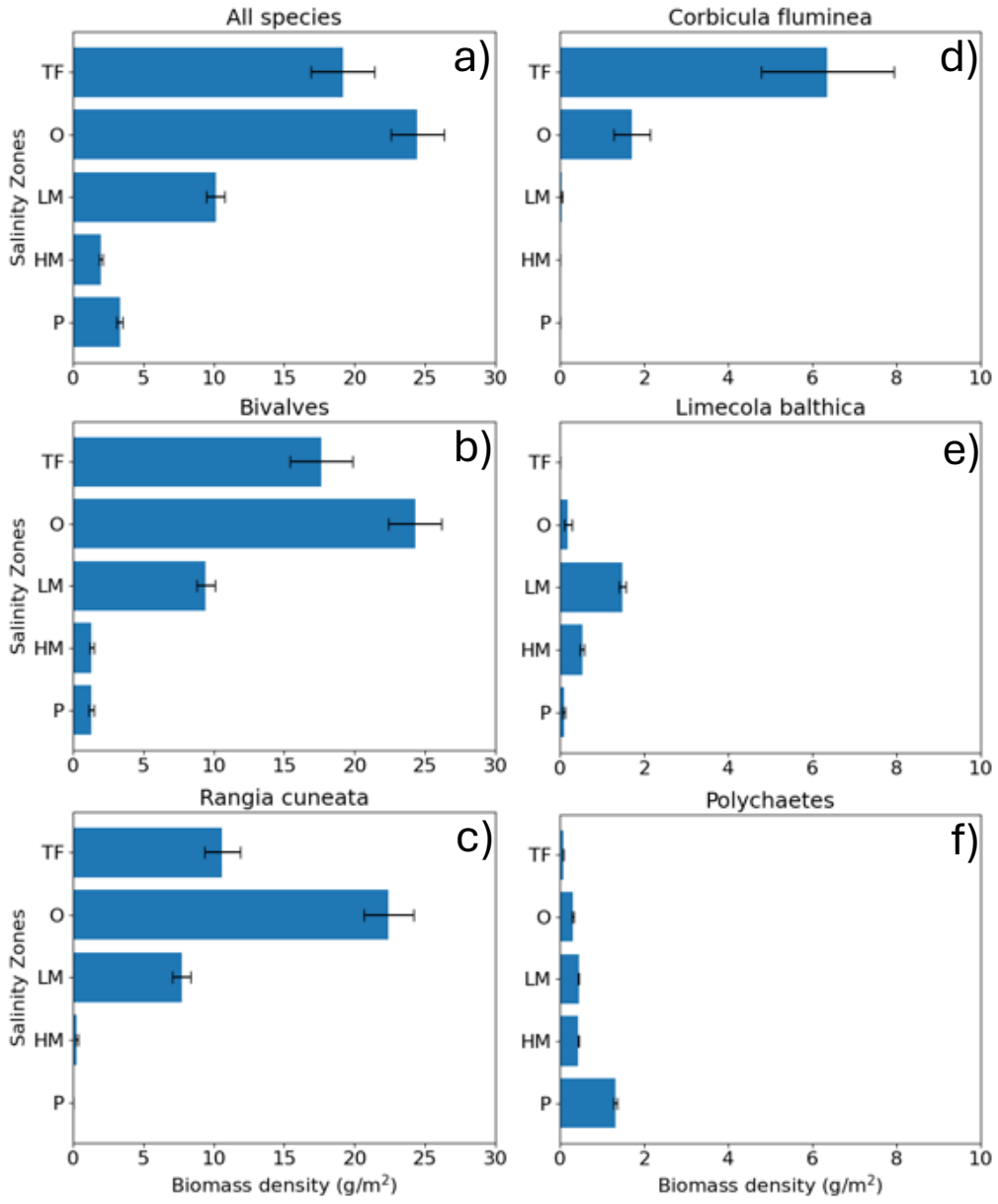

Figure 23: Average summer benthic biomass density of multiple classes and species in each salinity zone from 1995 to 2022. The salinity zones are determined by the BMP program based on the long-term average of salinity in each geographic zone: TF (– Tidal Freshwater) (0–0.5 ppt, OH (), O – Oligohaline) (0.5–5 ppt,), LM (– Low Mesohaline) (5–12 ppt,), HM (– High Mesohaline) (12–18 ppt,), and P – Polyhaline (PO) ≥ (≥18 ppt.). Averages and standard errors

(bars) are computed using the full data set, not the gridded values. Note the difference in ~~vertical~~horizontal scale between ~~upper row~~the left and ~~lower row~~right columns.

3.2 Carbon flux estimates

Average benthic macrofaunal carbon and alkalinity fluxes vary across the 10 regions of the Bay (Fig. 4). Among the different fluxes, which are all presented on a molar basis in Figure 4, F_{TA} has the largest magnitude, followed, in decreasing order, by F_{CO_2}, respiration (R/M_C), calcification (C/M_{CaCO3}), and F_{DIC}. We first discuss calcification, respiration, F_{TA}, and F_{DIC}. Calcification is 1.55 times respiration (best estimate), as a result of the molar ratio of these processes (Section 2.3.3). F_{TA} is always negative, as expected because calcification is an alkalinity sink, and twice the magnitude of calcification (Equation 13). The best estimate of F_{DIC} was mostly positive, though it could be positive or negative because calcification is a DIC sink and respiration is a DIC source (Equation 14). The best estimate of F_{DIC} ends up being positive because respiration exceeds calcification. Using the best estimate of the molar respiration:calcification ratio (1.55) and Equations 13 and 14, it can be shown that $-F_{TA}/F_{DIC}$ = 3.6, consistent with the results in Fig. 4. Estimated uncertainties (Appendix B) were approximately 45% for calcification, 40% for respiration, 135% for F_{DIC}, and 45% for F_{TA}. The uncertainty for F_{DIC} being greater than 100% admits the possibility of negative DIC fluxes.

F_{CO_2} is always positive because benthic macrofauna remove TA from and add DIC to the water column. The magnitude of F_{CO_2} can be understood by first noting that it is proportional to F_{TA} and F_{DIC}, with proportionality constants of $[CO_2]\zeta_{TA}/[TA]$ and $[CO_2]\zeta_{DIC}/[DIC]$, respectively (Equation 18; note that $F_{TA} < 0$ and $\zeta_{TA} < 0$, leading to $F_{CO_2} > 0$). In the open ocean, using mean conditions of pCO_2 = 400 µatm, [TA] = 2300 µmol kg^{-1}, temperature = 15 °C, and salinity = 35, we can use carbonate system equilibria to estimate $[CO_2]$ ~ 15 µmol kg^{-1}, $[DIC]$ ~

2100 µmol kg^{-1}, and $-\zeta_{TA} \sim \zeta_{DIC} = 11$, which leads to F_{CO_2} about 7–8% of $-F_{TA}$ and F_{DIC}. Here, we are seeing F_{CO_2} comparable in magnitude to F_{TA} and F_{DIC} because Bay waters tend to have higher $[CO_2]$ and ζ_{DIC} and lower $[TA]$ and $[DIC]$ than what is observed in open-ocean waters, as we show in Appendix E and Fig. E1. We observe much larger F_{CO_2} in tidal fresh (6–18 mol m^{-2} yr^{-1}) compared to oligohaline (3–7 mol m^{-2} yr^{-1}) waters (Fig. 4), despite comparable values of F_{DIC} and F_{TA}. These differences in F_{CO_2} between tidal zones are primarily driven by $[CO_2]$, which is much higher in the tidal fresh due to a lower TA:DIC ratio (Fig. E1l). The magnitudes of the buffer factors are also greater in lower salinity waters (Figs. E1g & E1h), decreasing slightly in the polyhaline. Polyhaline values (13–16) are comparable to oceanic estimates of 9–15 (Egleston et al., 2010).

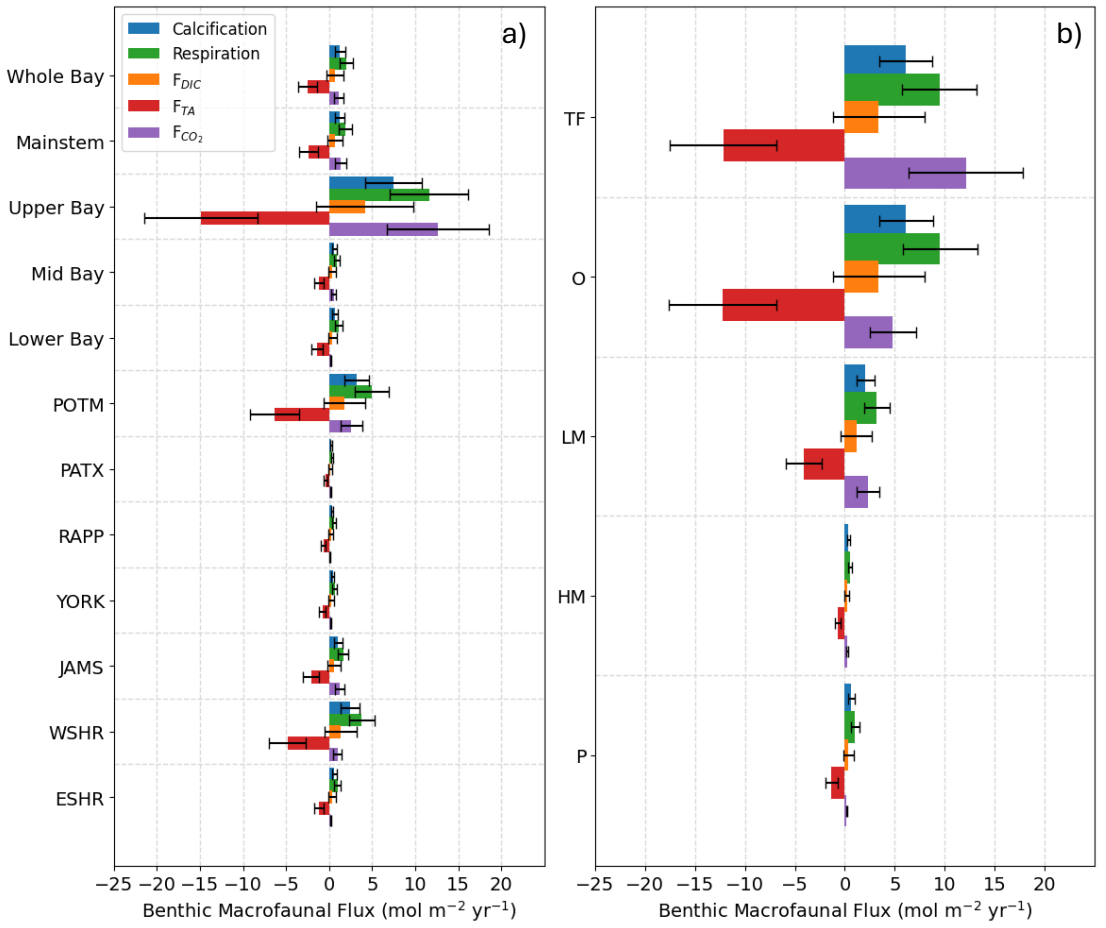

Figure 4: Average benthic macrofaunal fluxes by (a) Bay region and (b) salinity zone. Tributary and sub-estuarine acronyms: ESHR – Eastern Shore tributaries; WSHR – Western Shore tributaries; POTM – Potomac River; PATX – Patuxent River; RAPP – Rappahannock River; YORK – York River system (including Mattaponi and Pamunkey Rivers); JAMS – James River. Salinity zone abbreviations: TF – Tidal Freshwater (0–0.5 ppt), O – Oligohaline (0.5–5 ppt), LM – Low Mesohaline (5–12 ppt), HM – High Mesohaline (12–18 ppt), P – Polyhaline (≥18 ppt). Error bars represent uncertainty ranges (Appendix B).

In multiple segments of the Bay, benthic macrofaunal respiration rates (R) are comparable to the total available organic carbon supply, defined here as the sum of net primary production (NPP) and riverine POC loads (Table 2). In the Upper Bay, benthic macrofaunal respiration rates are within the range of NPP alone. When combined with POC loads, our estimates suggest that benthic macrofauna respire approximately f = 18–45% of the total available organic carbon, where:

$$f = \frac{R}{NPP + POC} \tag{19}$$

$$\frac{\Delta f}{f} = \sqrt{\left(\frac{\Delta R}{R}\right)^2 + \left(\frac{\Delta NPP}{NPP}\right)^2} \tag{20}$$

Here, ΔR and ΔNPP are the standard errors of R and NPP, respectively. This formulation is consistent with the uncertainty propagation approach described in Appendix B.

In the Potomac River Estuary, respiration rates exceed external organic carbon loads, although NPP estimates for this region were unavailable. By contrast, in the mainstem and across the Bay as a whole, benthic respiration rates are much smaller than NPP, accounting for only 3–

8% of the total inputs of organic carbon to the mainstem. These percentages were calculated using the same approach as in Equations 19–20, but substituting mainstem benthic macrofaunal respiration, NPP, and POC inputs.

Table 2: Riverine POC load, net primary production (NPP), and benthic respiration compiled from the listed studies compared with benthic macrofaunal respiration from our study. POC load estimates from Zhang & Blomquist (2018) were based on USGS river monitoring data combined with flow-weighted sediment and organic carbon concentrations. For POC loads we specifically used values from Table S5 of Zhang & Blomquist (2018), which reports long-term average true-condition annual loads. Susquehanna loads were distributed across the mainstem and Upper Bay, Potomac River loads were distributed across the Potomac, and total watershed load was distributed across the whole Bay. These loads were divided by the surface area of the corresponding segment area (Chesapeake Bay Program, 2004) NPP values from Harding et al. (2002) were derived from depth-integrated in situ ^{14}C-uptake incubations across multiple cruises, scaled using statistical models. Benthic respiration values from Kemp et al. (1997) were estimated by combining seasonal in situ measurements of sediment oxygen consumption with sulfate reduction rates, together accounting for microbial and macrofaunal respiration.

Region	Carbon Flux	Value (g C m^{-2} yr^{-1})	Reference
Whole Bay	Riverine POC load	12.0	Zhang & Blomquist (2018)
	Benthic macrofaunal respiration	24 ± 9	This study
Mainstem	Riverine POC load	18.8	Zhang & Blomquist (2018)
	NPP	385 ± 17	Harding et al. (2002)
	Benthic respiration	163.1	Kemp et al. (1997)
	Benthic macrofaunal respiration	22 ± 9	This study
Upper Bay	Riverine POC load	257.7	Zhang & Blomquist (2018)
	NPP	182 ± 27	Harding et al. (2002)

	Benthic respiration	44.3	Kemp et al. (1997)
	Benthic macrofaunal respiration	139 ± 55	This study
Potomac	Riverine POC load	31.9	Zhang & Blomquist (2018)
	Benthic macrofaunal respiration	59 ± 24	This study

Benthic macrofauna also contribute substantially to the calcium budget of the Bay. We estimate that calcification by benthic macrofauna monitored in the BMP is slightly lower than historical (pre-decline) estimates of the Eastern oyster (*Crassostrea virginica*) calcification in the mainstem Bay but exceeds post-decline estimates by about 7 to 19 times in the Upper Bay (Table 3). This range was calculated by taking the upper and lower bounds of our measured calcification rates (mean ± uncertainty) and dividing each by the post-decline oyster calcification rate. Evaluating the role of bivalve calcification in utilizing calcium further underscores its biogeochemical significance. Relative to annual riverine calcium fluxes, benthic macrofauna would use ~22–58% of the available calcium in the Upper Bay and nearly all in the Potomac River. These percentages were likewise calculated by taking the lower and upper bounds of our measured calcification rates (mean ± uncertainty) and dividing each by the corresponding maximum potential riverine calcium input, which was treated as fixed.

Table 3: Historic oyster calcification rates and estimated maximum potential calcification based on riverine calcium input, compared with calcification rates from this study. Riverine calcium load from the Susquehanna River was distributed across the Upper Bay and across the mainstem, calcium load from the Potomac River was distributed within the Potomac segment, and the sum of all riverine calcium inputs was distributed across the Whole Bay.

Region	**Calcification Rate**	**Value (g $CaCO_3$ m^{-2} yr^{-1})**	**Reference**
Whole Bay	Riverine Ca load	135	USGS
	Benthic macrofauna	142 ± 62	This study
Mainstem	Riverine Ca load	213	USGS

	Oysters	139	Fulford et al. (2007); Waldbusser et al. (2013)
	Benthic macrofauna	120 ± 54	This study
Upper Bay	Riverine Ca load	1861	USGS
	Oysters	57	Fulford et al. (2007); Waldbusser et al. (2013)
	Benthic macrofauna	747 ± 329	This study
Potomac	Riverine Ca load	262	USGS
	Benthic macrofauna	316 ± 142	This study

The role of benthic macrofaunal metabolic processes in the carbon budget is particularly pronounced when the effects of calcification and respiration are combined to estimate CO_2 production. This CO_2 flux exceeds the amount of outgassing estimated in the Upper Bay and the mainstem overall (Table 4).

Table 4: Air–sea gas exchange from the listed studies compared with total benthic macrofaunal CO_2 flux calculated in our study.

Region	**CO_2 Flux**	**Value (g C m^{-2} yr^{-1})**	**Reference**
Whole Bay	Benthic macrofauna	13 ± 10	This study
Mainstem	Air–sea exchange	14.5 (outgassing)	Herrmann et al. (2020)
	Benthic macrofauna	16 ± 13	This study
Upper Bay (CB1–CB3)[a]	Air–sea exchange	74.5 (outgassing)	Herrmann et al. (2020)
(CB1 & CB2)[a]	Benthic macrofauna	151 ± 121	This study

[a] CB1–CB3 refer to Chesapeake Bay Program segmentation units (Chesapeake Bay Program, 2004): CB1 = tidal fresh, CB2 = oligohaline; CB3 = mesohaline.

3.3 Correlation of environmental variables with biomass

The GAMs analysis, based on gridded, time-averaged biomass data, revealed key drivers of benthic biomass both at the community level (all taxa combined) and for specific taxonomic groups and species. The results for total benthic biomass (all taxa), polychaetes, and the bivalve species *R. cuneata*, *C. fluminea*, and *L. balthica* are shown in Table ~~2~~5. The bivalve group was

excluded from the table because its results were nearly identical to total benthic biomass results. For total benthic biomass, the predictor variables (O_2, salinity, total depth, water temperature, sand fraction, and NO_3^-) explain 54.9% of the deviance in biomass. For individual taxa, the predictive capability of GAMs increases, with 73.7% of *R. cuneata* biomass deviance explained by the predictor variables. For total benthic biomass, dissolved oxygen ~~was~~emerged as the ~~most influential~~strongest predictor ~~variable ((~~with the highest summed Akaike weight), followed by total depth, salinity, and ~~NO_3^-~~ NO_3^-. Although~~,~~ water temperature and sand fraction were included in the model, they had relatively little influence. For individual taxa, dissolved oxygen became less influential, especially for *R. cuneata* and *C. fluminea*. Salinity generally increased in influence as a predictor variable for species-specific models, most notably for *C. fluminea*. NO_3^- also generally increased in influence as a predictor variable for species-specific models, with very high influence as a predictor of *C. fluminea* biomass.

Table ~~2: This table presents the~~5: The best-fitting generalized additive model (GAM) for each taxa assemblage, determined by minimizing Akaike's Information Criterion (AIC). $N = 846$ (number of grid boxes with data) for all models. Summed Akaike weights indicate the relative importance of each predictor variable across all models considered, with higher values suggesting stronger support for a variable's inclusion in the best-fitting models. "N/A" indicates that the variable was not included in the best model. Some variables may have high summed Akaike weights even if they are not in the best-fitting model. For example, in the *R. cuneata* model, ~~DO~~O_2 has a summed Akaike weight of 0.571, while water temperature has 0.032. In the *C. fluminea* model, ~~DO~~O_2 has 0.384, and total depth has 0.24.

Taxa	~~N~~	Deviance Explained	Summed Akaike Weight

			O_2 ~~DO~~	Salinity	Total Depth	Water temperature	Sand fraction	NO_3^-
All taxa	~~846~~	54.9%	0.536	0.032	0.400	0.000	0.000	0.031
Polychaetes	~~846~~	50.0%	0.457	0.173	0.266	N/A	0.000	0.104
R. cuneata	~~846~~	73.7%	N/A	0.161	0.183	N/A	0.024	0.059
C. fluminea	~~846~~	65.9%	N/A	0.212	N/A	0.122	0.078	0.132
L. balthica	~~846~~	58.4%	0.888	0.000	0.112	N/A	0.000	0.000

The relative effects of ~~DO~~O_2, salinity, NO_3^- ~~-~~ and total depth on benthic biomass varied considerably~~. Figure 3 shows~~, as shown in the partial plots of ~~the relative effect of these four significant predictor variables on total benthic biomass~~Figure 5. Macrofauna biomass reaches its lowest values at low dissolved oxygen, the only section of all the partial plots that reach 0 g m^{-2}. Biomass is generally higher at shallower depths, although the effect is small. Biomass is highest at both low and high salinities and high surface NO_3^-. In summary, biomass is highest at moderate dissolved oxygen, shallow depths, low or high salinities, and high NO_3^-.

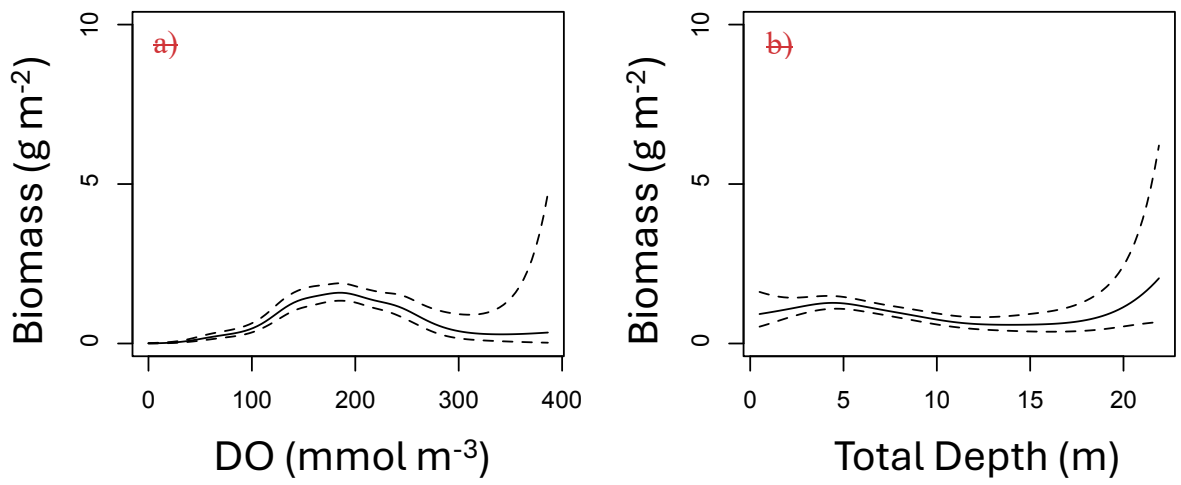
a)
b)
Biomass (g m-2)
DO (mmol m-3)
Total Depth (m)

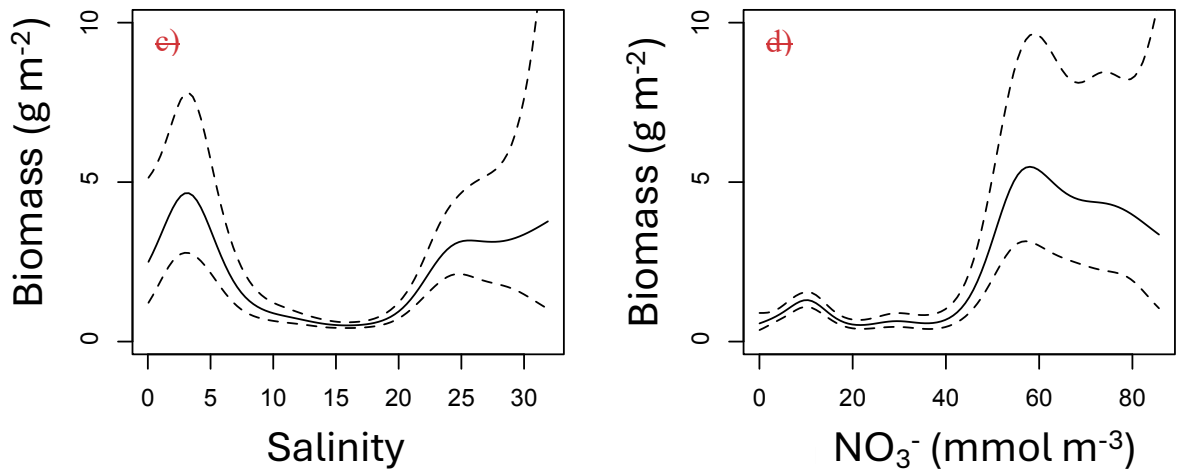
c)
d)
Biomass (g m-2)
Salinity
NO3- (mmol m-3)

1085

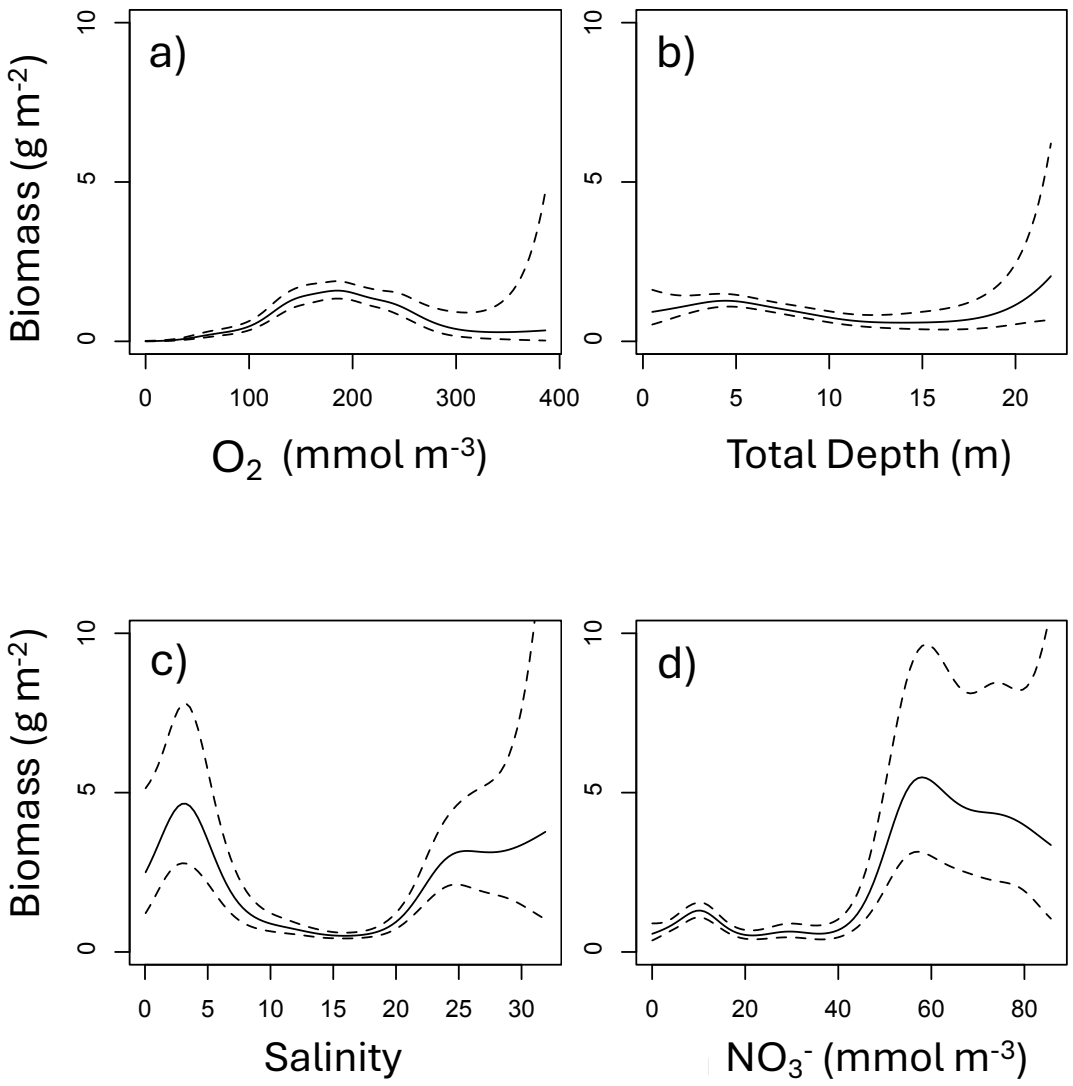

Figure ~~3~~5: Partial plots of the effect of significant predictor variables on ~~all species~~total biomass: (a) bottom dissolved oxygen, (b) total depth, (c) bottom salinity, and (d) surface nitrate. Water temperature and sand fraction were included in the model but omitted from display as they ~~since they~~ did not significantly improve the model fit. The solid black line shows the response ~~with~~and the dashed lines ~~showing~~show the 95% confidence interval. The natural log transformation was removed from biomass to enhance viewing of the partial plots. The x-axis was cut~~-~~ off at the upper quartile plus three interquartile ranges in order to remove extreme outliers from the plots.

The model fit evaluation, presented in Appendix F and Fig. F1, reveals some systemic biases ~~examined in Fig. A2.~~. The residuals (observed values minus model-fitted values) are slightly skewed to the left (Fig. ~~A2b~~F1b), meaning the model is more likely to overestimate biomass. The response vs. fitted value scatter plot shows a nearly linear relationship (Fig. ~~A2a~~F1a). The map of residuals (Fig. ~~A2c~~F1c) shows that ~~the regions where the model is most likely to overestimate the biomass response are at the lowest biomass zones in the Mid Bay and the lower Potomac River. In these sections, the biomass is nearly zero. There~~there is also an underestimation in the model fit at the high biomass zones, especially in the Upper Bay.

~~***3.3 Carbon flux estimates***~~

~~The biomass density and associated carbon fluxes vary across watershed regions, as shown in Fig. A3. The associated carbon fluxes scale proportionally to the biomass with large uncertainty. To evaluate our secondary production calculations, we examined the ratio of secondary production to biomass. The ratio of the secondary production (in g C m^{-2} yr^{-1}) to biomass (in g m^{-2} yr^{-1}) for the whole Bay was 1.6, with ratios ranging from 1.4 to 1.9 for the different regions. Secondary production calculations from the two observationally validated models, Dauer (1993), Edgar (1990), and Sturdivant et al., (2013) also found magnitudes within that range.~~

~~In multiple segments of the Bay, respiration fluxes are comparable to the available organic carbon supply. To assess the relative contribution of macrofaunal respiration, we compared estimated respiration rates from benthic biomass to previously reported values for primary production and other organic carbon inputs (Table 3). To estimate total organic carbon (TOC) and particulate organic carbon (POC) fluxes in the Upper Bay, we calculated the areal flux by distributing the total organic carbon load over the surface area of the tidal fresh and~~

~~oligohaline zones of the mainstem, represented by the CBP segments CB1 and CB2. This approach assumes that the majority of the annual TOC load from the Susquehanna River remains concentrated in the Upper Bay and is respired rather than transported downstream, an assumption supported by Canuel & Hardison, (2016). In the Upper Bay, benthic macrofaunal respiration fluxes are within the range of gross primary production (GPP). To estimate the fraction of organic carbon load respired, we took the extreme ends of the uncertainty ranges of our respiration rates and divided them by the sum of the estimates of GPP and POC in the Upper Bay. The results suggest that 17 to 50% of available carbon in the Upper Bay is respired by benthic macrofauna. Potomac River respiration rates exceed organic carbon production from GPP. However, in the mainstem and the Bay as a whole, respiration fluxes are much lower than GPP. Our estimates suggest that benthic macrofauna respire between 1.8 and 5.0% of the available organic carbon in the mainstem.~~

~~Table 3: Primary production organic carbon, and respiration compiled from the listed studies compared with respiration from our study. All units were converted to g C m^{-2} yr^{-1}. The watershed region areas were determined by summing the areas of the Chesapeake Bay Program segments within each watershed. The Susquehanna River estimates assumed the entire load was concentrated in the Upper Bay.~~

~~**Region**~~	~~**Carbon Flux**~~	~~**Value**~~	~~**Study**~~	~~**Region (our study)**~~	~~**Carbon Flux (our study)**~~	~~**Value (our study)**~~

Eastern North America	Estuarine GPP	309 g C m^{-2} yr^{-1}	Najjar et al., (2018)	Whole Bay	Respiration	25±12 g C m^{-2} yr^{-1}
Mid Atlantic Blight	TOC from tidal wetlands	6.8 g C m^{-2} yr^{-1}	Herrmann et al., 2015			
Mid Atlantic Blight	TOC from streamflow	14.4 g C m^{-2} yr^{-1}	Herrmann et al, 2015			
Mainstem	GPP	657.4 g C m^{-2} yr^{-1}	Kemp et al., 1997	Mainstem	Respiration	23±11 g C m^{-2} yr^{-1}
	Benthic Respiration	163.1 g C m^{-2} yr^{-1}	Kemp et al., 1997			
All Inputs	TOC	90 g C m^{-2} yr^{-1}	Kemp et al., 1997			
	POC	15.6 g C m^{-2} yr^{-1}	Zhang & Blomquist (2018)			
Upper Bay	GPP	123.4 g C m^{-2} yr^{-1}	Kemp et al., 1997	Upper Bay	Respiration	

	Benthic Respiration	44.3 g C m^{-2} yr^{-1}	Kemp et al., 1997			
Susquehanna River	TOC	354 g C m^{-2} yr^{-1}	Kemp et al., 1997			128±63 g C m^{-2} yr^{-1}
	POC	257.7 g C m^{-2} yr^{-1}	Zhang & Blomquist (2018)			
Potomac River	POC	31.7 g C m^{-2} yr^{-1}	Zhang & Blomquist (2018)	Potomac	Respiration	57±29 g C m^{-2} yr^{-1}

Benthic macrofaunal calcification also represents a major flux within the Bay. Our study shows that calcification rates by benthic macrofauna analyzed in the BMP program far exceeds estimates of the Eastern oyster (*Crassostrea virginica*) calcification rates (Table 4). To calculate oyster calcification rates, we used Fulford et al., (2007) model estimates of oyster biomass in different CBP segments and we related the ash-free dry weight of oyster biomass to the live weight using a ratio of 10:1 (Mo & Neilson, 1994). We then calculated calcification rates using a ratio of 2 mg $CaCO_3$ per gram live mass per day of oyster (Waldbusser et al., 2013). To maintain consistency with our results, which frame fluxes in the context of carbon, we converted calcification rates to the equivalent amount of CO_2 generated. While this is a non-standard way of presenting calcification rates, it allows for direct comparison with other carbon fluxes and better integration into our broader analysis of estuarine carbon cycling. We estimated CO_2

generated (in g m^{-2} yr^{-1}) is about 12% of the $CaCO_3$ production (in g m^{-2} yr^{-1}) (Chauvaud et al., 2003). Using these values and CBP segment areas, we derived oyster calcification fluxes for the mainstem and Upper Bay. Remarkably, bivalve calcification rates from our study exceeds oyster calcification rates by over 80 times in the mainstem and by over 1000 times in the Upper Bay.

Table 4: Oyster calcification and riverine calcium input compiled from the listed studies compared with calcification from our study. Calcification calculated from the yearly Ca flux and oyster calcification from the listed studies. All units were converted to g C m^{-2} yr^{-1} with information about how the calculations were made in the text. The watershed region areas were determined by summing the areas of the Chesapeake Bay Program segments within each watershed. The Upper Bay calcification from yearly Ca flux assumed that the entire load from the Susquehanna River was concentrated in the Upper Bay.

Region	**Carbon Flux**	**Value**	**Study**	**Region (our study)**	**Carbon Flux (our study)**	**Value (our study)**
Mainstem	Oyster Calcification	0.17 g C m^{-2} yr^{-1}	Fulford et al., 2007/ Waldbusser et al., 2013	Mainstem	Calcification	14±5 g C m^{-2} yr^{-1}
Upper Bay	Calcification from Yearly Ca Flux	557.6 g C m^{-2} yr^{-1}	USGS	Upper Bay	Calcification	

	Oyster Calcification	0.07 g C m^{-2} yr^{-1}	Fulford et al., 2007/ Waldbusser et al., 2013			78±31 g C m^{-2} yr^{-1}
Potomac River	Calcification from Yearly Ca Flux	77.9 g C m^{-2} yr^{-1}	USGS	Potomac	Calcification	35± 14 g C m^{-2} yr^{-1}

Evaluating the role of bivalve calcification in utilizing calcium further underscores its biogeochemical significance. If all the calcium used in bivalve calcification were sourced from rivers, bivalves would consume a significant fraction of the available calcium (Table 4). To quantify riverine calcium input, we used data from non-tidal USGS stations in the Susquehanna and Potomac Rivers from 1995 to 2022. Annual calcium fluxes were calculated using Weighted Regression on Time, Discharge, and Season (WRTDS; Hirsch et al., 2010). In calcification, one mole of $CaCO_3$ is produced for every mole of Ca consumed. To keep units consistent, we again estimated the CO_2 produced (in g m^{-2} yr^{-1}) from 12% of the $CaCO_3$ production (in g m^{-2} yr^{-1}). The Upper Bay calculation assesses how much CO_2 bivalves would generate if all the Susquehanna calcium input was used in calcification within the Upper Bay. Similarly, the Potomac River calculation estimates the rates of calcification that would occur if all of the calcium input into the Potomac River was utilized for calcification within the Potomac River. Relative to annual riverine calcium fluxes, benthic macrofauna would use ~14% of the available calcium in the Upper Bay and 45% in the Potomac River.

~~The role of benthic macrofaunal metabolic processes in the carbon budget is particularly pronounced when the effects of calcification and respiration are combined. Our estimates indicate that calcification contributes 38% of the total CO_2 flux while respiration accounts for 62% (Table 5). This combined CO_2 flux exceeds the amount of outgassing estimated in the Upper Bay and the mainstem overall (Table 5). Compared to other estuaries worldwide, the Chesapeake Bay exhibits relatively modest levels of CO_2 outgassing (Table 5). In estuaries with greater outgassing rates, the proportional contribution of calcification and respiration to total CO_2 exchange might be lower, but would still be substantial.~~

~~Table 5: Air/sea gas exchange from the listed studies compared with total benthic CO2 flux in our study, calculated as the sum of respiration and calcification fluxes. All units were converted to g C m^{-2} yr^{-1}.~~

~~Region~~	~~Carbon Flux~~	~~Value~~	~~Study~~	~~Region (our study)~~	~~Carbon Flux (our study)~~	~~Value (our study)~~
~~Upper Bay (CB1, CB2, & CB3)~~	~~Air/Sea CO_2 exchange~~	~~74.5 g C m^{-2} yr^{-1} (outgassing)~~	~~Herrmann et al., 2020~~	~~Upper Bay (CB1 & CB2)~~	~~Total CO_2 Flux~~	~~205±70 g C m^{-2} yr^{-1}~~

Mainstem	Air/Sea CO_2 exchange	14.5 g C m^{-2} yr^{-1} (outgassing)	Herrmann et al., 2020	Mainstem	Total CO_2 Flux	36±12 g C m^{-2} yr^{-1}
Global Estuaries	Air/Sea CO_2 exchange	92.5 g C m^{-2} yr^{-1} (outgassing)	Chen et al., 2013	Whole Bay	Total CO_2 Flux	40±14 g C m^{-2} yr^{-1}
Eastern North America	Air/Sea CO_2 exchange	108.1 g C m^{-2} yr^{-1} (outgassing)	Chen et al., 2013	Whole Bay		

4. Discussion

4.1.4.1. Benthic macrofaunal contributions to the Chesapeake Bay carbon budget

The higher benthic biomass in less saline waters of the Chesapeake Bay suggests a significant role for respiration in the carbon budget in this region. The proportion of the total input of particulate organic carbon that is respired by benthic macrofauna estimated in our study in the Upper Bay (18–45%) is similar to the 14 to 40% range estimated for bivalve filter feeders in tidal fresh and oligohaline waters by Cerco & Noel (2010). In the Upper Bay, where the benthic macrofauna respiration is comparable to NPP, if all the NPP were respired solely by benthic macrofauna, net ecosystem production would be zero. However, given the consideration of additional respiration by other organisms (e.g., microbes and pelagic zooplankton) the allochthonous POC from the Susquehanna River must be a critical source of organic carbon driving net heterotrophy in this region. These findings reinforce the earlier conclusion that high

biomass zones in the Upper Bay are sustained by allochthonous organic inputs. The Potomac River Estuary, however, presents a less conclusive case, partly due to the lack of available NPP estimates. In this estuary, where benthic macrofaunal respiration exceeds the estimated POC flux, additional carbon sources, such as autochthonous NPP or tidal wetland outwelling, may be contributing to carbon metabolism. Notably, Herrmann et al. (2015) estimated that the amount of organic carbon exported through wetland outwelling is approximately equal to half of that exported by streamflow in Mid-Atlantic estuaries, highlighting its potential significance in supporting heterotrophic processes in the Potomac.

Benthic macrofaunal respiration plays a smaller role in the rest of the Bay, where autochthonous organic carbon dominates. For both the mainstem and the whole Bay, the estimated primary production far exceeds the average estimated benthic macrofaunal respiration . Kemp et al. (1997) estimated benthic respiration by combining sulfate reduction and sediment oxygen consumption rates, which together account for both microbial and macrofaunal respiration. Their results suggest that benthic respiration is a smaller fraction of NPP in the Mid and Lower Bay, compared to the Upper Bay. This may reflect the relatively modest role of macrofaunal respiration in these lower-biomass regions, despite higher autochthonous production and organic carbon delivery to the sediments. Our estimates of benthic macrofaunal respiration as a fraction of the total input of organic carbon to the mainstem (3–8%) is slightly lower than estimates derived by Hopkinson & Smith (2004) and Rodil et al. (2022). Hopkinson & Smith, (2004) estimated that approximately 24% of total available organic carbon is respired by the benthos, while Rodil et al. (2022) found that benthic macrofauna account for roughly 40% of total benthic respiration. Taken together, these studies suggest that around 10% of the total input

of organic carbon is expected to be respired by benthic macrofauna. Although the Bay-wide fraction is small, macrofaunal respiration may still dominate locally in specific hotspots.

Unlike the extensive research on estuarine benthic respiration, benthic macrofaunal calcification has received relatively little attention. Yet our findings suggest it may play a significant role in the Chesapeake Bay carbon budget. As shown in Table 3, bivalves sampled through the BMP program contribute substantially to calcification, surpassing calcification by present-day Eastern oyster populations but comparable to that of historic populations in the mainstem Bay. The importance of bivalve calcification is further emphasized when considering calcium dynamics. To place bivalve calcification in context, we assumed that all riverine calcium inputs were available for shell production. This is an upper-bound estimate because oceanic calcium greatly exceeds riverine fluxes (Beckwith et al., 2019). While not a full calcium budget, the comparison highlights how large the demand from calcification could be relative to the much smaller riverine supply. Alkalinity fluxes further highlight the biogeochemical significance of calcification. For the whole Bay, our estimated alkalinity consumption from benthic macrofaunal calcification of 2.52 ± 1.13 mol m^{-2} yr^{-1} (6.90 ± 3.10 mmol m^{-2} day^{-1}) accounts for more than half of the Bay-wide alkalinity sink estimated by Waldbusser et al. (2013) at 12 mmol m^{-2} day^{-1}. In the Potomac River Estuary, our estimated alkalinity sink due to benthic calcification (6.31 ± 2.84 mol m^{-2} yr^{-1} or 17.29 ± 7.78 mmol m^{-2} day^{-1}) is comparable to the alkalinity sink of 22 ± 1 mmol m^{-2} day^{-1} estimated by Najjar et al. (2020), who proposed that *C. fluminea* was primarily responsible. Our findings, highlighting contributions from both *R. cuneata* and *C. fluminea*, support their hypothesis and emphasize the substantial role of benthic calcification in modulating alkalinity in estuaries.

Benthic macrofauna may play a major role in CO_2 outgassing, as indicated by our estimated CO_2 fluxes from benthic macrofauna in the Upper Bay and upper tributaries, which exceed typical CO_2 fluxes at the air–sea interface. Our benthic macrofaunal CO_2 generation estimates for the Upper Bay (151 g C m^{-2} yr^{-1}), where bivalve biomass is concentrated, exceed those reported by Chauvaud et al. (2003), who estimated 55 ± 51 g C m^{-2} yr^{-1} of CO_2 production from calcification and respiration by the bivalve *P. amurensis* in northern San Francisco Bay. Our results support their hypothesis that benthic calcifiers can serve as major CO_2 generators in estuaries. Not all of this CO_2 generated would be outgassed. However, the combination of a TA sink and DIC source from the bivalves leads to elevated pCO_2, enhancing the potential for increased CO_2 outgassing (Middelburg et al., 2020). Given the high heterotrophy in the Upper Bay and upper tributaries, as well as the balance between benthic macrofaunal respiration and the total input of organic carbon to the Potomac River Estuary, it is conceivable that benthic macrofauna are major contributors to CO_2 outgassing in these regions.

Although our empirical framework presented here captures the dominant patterns of benthic secondary production, it does not explicitly incorporate seasonal temperature variability. Because we applied summer temperatures associated with biomass, our production estimates likely represent the upper end of expected values. A simple sensitivity analysis comparing summer and winter conditions suggests that production, and by extension calcification and respiration, may be closer to 60% of the values reported here under mean annual cycles. Importantly, this potential bias is encompassed within our uncertainty bounds and therefore does not affect our overall conclusions.

4.2. ***Environmental controls on benthic biomass distribution***

Bivalve species distribution within the Bay is primarily driven by salinity tolerances. Both the GAMs analysis (Table ~~2~~5) and the biomass densities associated with salinity zones (Fig. ~~2~~3) showed that benthic biomass, dominated by bivalves, was much higher at lower salinities. The strong influence of salinity on benthic fauna distribution within estuaries has long been recognized (Cain, 1975; Hopkins et al., 1973). This relationship is illustrated in our study by the preference of the most abundant species, *R. Cuneata*, *L. balthica*, and *C. fluminea*, for less saline water. *R. Cuneata* is widely known to need less saline waters, optimally between 1 and 15 ppt, to survive (Hopkins et al., 1973). *C. fluminea* prefers freshwater environments (Phelps, 1994; Sousa et al., 2008). *L. balthica* has a range of tolerances but abundance declines below 5 ppt (Jansson et al., 2015). In our study, *L. balthica* is more concentrated between 5 and 13 ppt. While salinity determines which species dominate, other factors influence their relative abundances within ~~these~~salinity zones.

Within mesohaline zones, summer hypoxia appears to be driving extremely low benthic biomass. In our GAMs analysis, an association existed between low biomass and extremely low bottom dissolved oxygen values. Among the different salinity zones, low biomass is associated with low dissolved oxygen in the high mesohaline, where we had the lowest biomass densities. Long-term exposure to hypoxia (<2 mg L^{-1} or 62.5 mmol m^{-3}) is often fatal to benthic ~~fauna~~macrofauna (Diaz et al., 1995; Seitz et al., 2006; Seitz et al., 2009) and many benthic communities (approximately 50%) only recover on an annual timescale (Diaz et al., 1995). In other words, regions that suffer frequent hypoxia often see lower levels of benthic biomass even when hypoxic conditions are not occurring. In the Chesapeake Bay, hypoxia is most likely to occur in the deeper, mesohaline regions (Frankel et al., 2022; Zheng & DiGiacomo, 2020), providing evidence that our suppressed values of benthic ~~fauna~~macrofauna at this salinity zone

could be due to mass mortality from hypoxia. This pattern is particularly evident where biomass is extremely low through the Mid Bay and lower Potomac River Estuary, regions typically associated with summer hypoxia (Sturdivant et al., 2013).

Across the Bay, the relatively narrow range of summer bottom water temperatures likely explains why temperature has an insignificant effect on the spatial distribution of benthic biomass. In our GAMs analysis, summer bottom water temperature was not significantly correlated with benthic biomass. Water temperature has been considered an important driver of benthic biomass (Marsh & Tenore, 1990; Seitz et al., 2006; Seitz et al., 2009; Testa et al., 2020), with low temperature specifically creating mass mortality of *R. cuneata* during winter and spring (Tuszer-Kunc et al., 2020). Higher ~~temperatures~~temperature, however, will drive early and larger seasonal hypoxia in the Chesapeake Bay (Hinson et al., 2022; Irby et al., 2018; Ni et al., 2019). So, temperature could still indirectly affect benthic biomass through its effect on dissolved oxygen. Therefore, while temperature many not directly drive spatial patterns of biomass, it could be more relevant to temporal changes in biomass.

Although NO_3^- is a ~~clear~~strong predictor of benthic biomass, the mechanisms ~~driving this association~~ are likely complex~~. NO_3^- is an important limiting nutrient for primary production,~~ and ~~high annually-averaged concentrations indicate an excess of NO_3^-~~ not ~~fully utilized by phytoplankton. Excess NO_3^- from the tributaries flows into the mainstem, fueling a spring phytoplankton bloom (Brush et al., 2020b). The highest primary production zones in the spring are in the mesohaline and fuel hypoxia where the Bay is deeper and stratified (Brush et al., 2020a), possibly explaining why long-term increases in phytoplankton biomass have not been~~necessarily linked ~~with an increase in benthic biomass (Harding & Perry, 1997). In the tidal~~

fresh and oligohaline zones, abundant NO_3^- is present, but high suspended solid loads limit light penetration, consequently inhibiting primary production (Brush et al., 2020b).

Given the complexity of explaining the relationship between NO_3^- and benthic biomass, further insights may come from examining the relationship between inorganic suspended solid loads and POC. A significant portion of suspended solids in the tidal fresh and oligohaline regions is POC, given previous studies have that suggest substantial inputs of POC are respired in the Upper Bay (Kemp et al., 1997; Testa et al., 2020). Canuel & Hardison, (2016) further demonstrated that above the Estuarine Turbidity Maximum (ETM), organic matter is dominated by allochthonous (terrigenous) sources, which could contribute to the high POC content in suspended solids. Further evidence for substantial allochthonous inputs of POC comes from the dissolved oxygen supersaturation ($\Delta[O_2]$) model-derived information (Fig. 4). As explained earlier, $\Delta[O_2]$ was not included as a predictor variable because it was highly correlated with NO_3^- and salinity, the two most influential predictors of the high biomass zones. Under steady-state conditions and ignoring advection and mixing, negative surface $\Delta[O_2]$ indicates net heterotrophy, where oxygen consumption from respiration exceeds oxygen production from photosynthesis. This imbalance leads to undersaturation and uptake from the atmosphere. Conversely, positive $\Delta[O_2]$ indicates net autotrophy, where oxygen production from photosynthesis exceeds oxygen consumption from respiration. The $\Delta[O_2]$ maps (Fig. 4) indicate high levels of heterotrophy year-round throughout the upper reaches of the tributaries and the Upper Bay, corresponding to the tidal fresh and oligohaline zones of the Bay. Autotrophy dominates year-round in the polyhaline Lower Bay. In the lower tributaries and Mid Bay (mesohaline zones), there are seasonal shifts, with heterotrophy in the summer and fall and autotrophy in the spring and winter. High levels of heterotrophy near the freshwater sources of

~~the Bay could indicate substantial inputs of allochthonous organic matter being respired (Kemp et al., 1997).~~

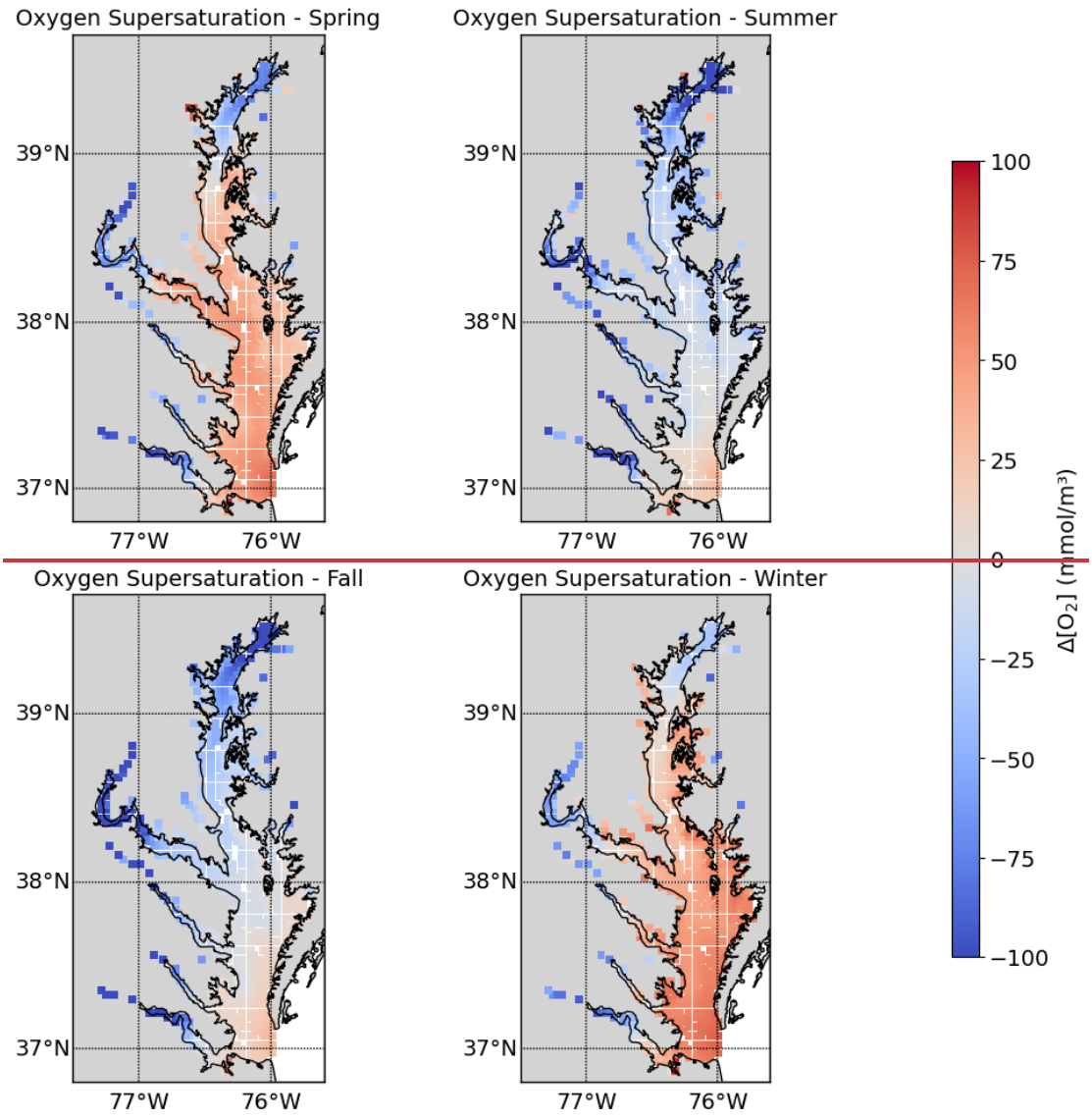

~~Figure 4: Surface oxygen supersaturation for each season in the Bay. Spring (March–April), Summer (July–August), Fall (September–November), and Winter (December–February). Method for calculating oxygen supersaturation is described in the text.~~

~~If the highest NO_3^- concentrations coincide~~autochthonous primary production. In upper estuarine zones, high NO_3^- concentrations are often associated with elevated suspended solid loads ~~at and above the ETM, and if POC is substantially present in~~ , which limit light and may inhibit autotrophy (Brush et al., 2020b). Yet these ~~loads, then annually averaged NO_3^- may act as~~ same areas show strong heterotrophy, suggesting that respiration exceeds local production. Prior studies have shown that POC in upper estuaries contains substantial terrigenous inputs (Canuel & Hardison, 2016), and respiration of this organic matter likely contributes to heterotrophy in these regions (Kemp et al., 1997; Testa et al., 2020). This pattern raises the possibility that NO_3^- may serve as a proxy for allochthonous POC~~. In contrast, below the ETM, NO_3^- is more readily utilized in primary production, and most of the POC is autochthonous. Unfortunately, POC modeled by ROMS-ECB can't be used to support our hypothesis, as model-data evaluation did not meet our robustness threshold (r_s < 0.7). However,~~ delivery. Supporting this, USGS data compiled by Zhang & Blomquist (2018) ~~give long-term averages (1985–2016) of POC input into various tributaries measured at non-tidal gauging stations. Figure 5 compares the concentration of allochthonous input of POC and the average surface nitrate NO_3^- in each tidal region. We calculated the POC concentration using the average load of POC input into the tributary divided by the area of the watershed region. Only the six largest tributaries had POC data reported. The Susquehanna River data was excluded because it discharges directly into the mainstem, making it less comparable to the other river estuaries. There was a substantial linear~~ indicate that tributaries with high NO_3^- also tend have high loads of POC. However, further study is needed to test this hypothesis, and the observed NO_3^-–POC correlation ~~between NO_3^- and POC.~~ should not be interpreted as causal.

Our model explained roughly half of the deviance in biomass, indicating that environmental predictors captured key bottom-up controls. However, our model did not account for top-down factors such as predation, which may also play a significant role in shaping biomass distributions, particularly in an estuary with a densely populated watershed and substantial fishing pressure.

Conclusion

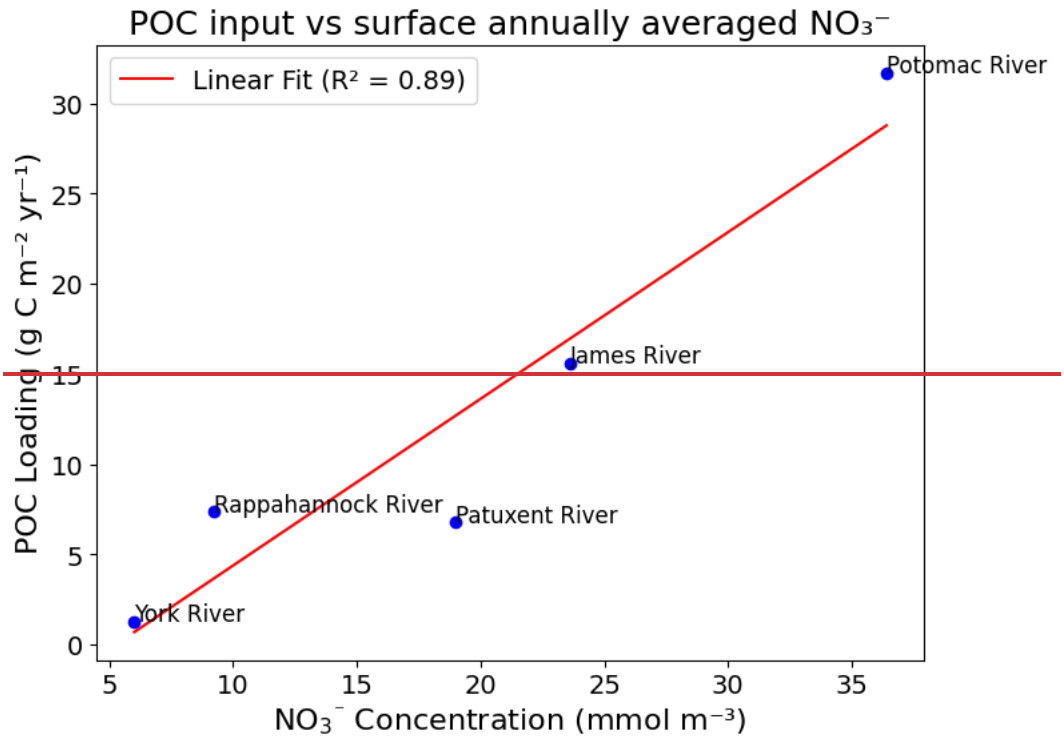

~~Figure 5: Particulate organic carbon (POC) vs surface nitrate (NO_3^-) for five watershed regions. POC fluxes were calculated using load data from USGS compiled by Zhang and Blomquist (2018). The watershed region areas were determined by summing the areas of the Chesapeake Bay Program segments within each watershed. NO_3^- concentrations were obtained from ROMS-ECB output and represent the annually averaged mean concentration in each watershed region.~~

Taken together, these data strongly support the hypothesis that the correlation between surface NO_3^- and benthic biomass is driven by allochthonous POC. This link is further reinforced by our dataset, where regions of high heterotrophy (Fig. 4) align with the highest benthic biomass (Fig. 1). If salinity dictates species distribution by limiting certain taxa to fresher zones and dissolved oxygen reduces benthic biomass in mesohaline zones, then the relative inputs of terrestrial organic matter could be controlling biomass variation in the fresher regions.

4.2. Benthic macrofaunal contributions to estuarine carbon budget

The higher benthic biomass in less saline waters suggests a significant role for respiration in the carbon budget in this region. The proportion of organic carbon respired by benthic macrofauna estimated in our study in the Upper Bay (17 to 50%) is remarkably similar to the 14 to 40% range estimated for bivalve filter feeders in tidal fresh and oligohaline waters by Cerco & Noel (2010). In the Upper Bay, where the benthic macrofauna respiration flux is comparable to the GPP flux, if all the GPP were respired solely by benthic macrofauna, net ecosystem production would be zero. However, given the consideration of additional respiration by other organisms (e.g., microbes and pelagic zooplankton) the allochthonous POC from the Susquehanna River must be a critical source of organic carbon driving net heterotrophy in this region. These findings reinforce the earlier conclusion that high biomass zones in the Upper Bay are sustained by allochthonous organic inputs. The Potomac River, however, presents a less conclusive case, partly due to the lack of available GPP estimates. In the Potomac, where benthic macrofaunal respiration rates exceed the estimated POC flux, additional carbon sources, such as autochthonous GPP or tidal wetland outwelling, may be contributing to carbon metabolism. Herrmann et al., (2015) estimated that wetland outwelling accounts for approximately half of the organic carbon exported by streamflow in Mid-Atlantic estuaries.

~~Benthic macrofaunal respiration plays a smaller role in the rest of the Bay, where autochthonous organic carbon dominates. For both the mainstem and the whole Bay, the estimated primary production far exceeds the average estimated respiration rates calculated from our benthic biomass data. Overall, the autochthonous organic carbon contribution from primary production is about 15 times greater than the allochthonous input from estuaries in the Mid-Atlantic Bight. This ratio is even more pronounced since only a fraction of the total organic carbon (TOC) is particulate (POC) and can be respired by the benthos (Kemp et al., 1997). Kemp et al., (1997) calculated benthic respiration from sulfate reduction and sediment oxygen consumption rates. Their estimates could highlight the relatively modest role of benthic macrofaunal respiration for the entire mainstem, given the lower biomass values in the Mid and Lower Bay, where autochthonous primary production and overall organic carbon flux to the sediments are higher. Their calculation may have underestimated benthic respiration rates, as our respiration rates estimates for benthic macrofaunal respiration are higher than their calculations. Our estimates of benthic macrofaunal respiration in the mainstem (1.8–5.0%) is significantly lower than estimates derived from the combined findings of Hopkinson & Smith, (2004) and Rodil et al., (2022). Hopkinson & Smith, (2004) estimated that approximately 24% of organic carbon is respired by the benthos, while Rodil et al., (2022) found that benthic macrofauna account for roughly 40% of total benthic respiration. Taken together, these studies suggest that around 10% of available organic carbon is expected to be respired by benthic macrofauna, more than double our findings. Although our estimates indicate that benthic macrofaunal respiration accounts for a relatively small fraction of total organic carbon metabolism at the scale of the entire Bay, this does not preclude the existence of localized hotspots where it plays a dominant role.~~

Unlike the extensive research on estuarine benthic respiration, little attention has been given to calcification, yet our findings suggest that benthic macrofaunal calcification could be important to the carbon budget. The relative importance of bivalve calcification in the Bay is illustrated in Table 4. Eastern oysters (*Crassostrea virginica*) have received significant attention due to their ecological and economic importance, but their populations in the Chesapeake Bay used to be at least two orders of magnitude higher than its present levels (Fulford et al., 2007; Newell, 1988). The bivalves sampled in the BMP program contribute substantially more to estuarine carbon cycling than present-day Eastern populations. Evaluating the role of bivalve calcification in utilizing calcium further underscores its biogeochemical significance. Our estimations assume that all calcium input is used in calcification; however, since calcium contributions from the ocean and groundwater may far exceed riverine inputs, this comparison does not represent a complete calcium budget but rather provides a useful context for understanding the scale of bivalve calcification.

Benthic macrofauna may play a major role in CO_2 outgassing, as indicated by our estimated high carbon fluxes in the Upper Bay and upper tributaries relative to air-sea gas exchange. Furthermore, our total CO_2 generation estimates for the Upper Bay (205±70 g C m^{-2} yr^{-1}), where bivalve biomass is concentrated, exceed those reported by Chauvaud et al., (2003), who estimated CO_2 production from calcification and respiration at 55±51 g C m^{-2} yr^{-1} for the bivalve *P. amurensis* in Northern San Francisco Bay. This further supports their hypothesis that benthic calcifiers can serve as major CO_2 generators in estuaries. Given the high heterotrophy in the Upper Bay and upper tributaries, as well as the balance between benthic macrofaunal respiration and organic carbon inputs in the Potomac River, it is conceivable that benthic macrofauna are major contributors to CO_2 outgassing in these regions.

Conclusion

This study examines how water chemistry and sediment composition influence the spatial distribution of benthic biomass and to assess the role macrofaunal respiration and calcification plays in estuarine carbon budgets. We found that benthic macrofauna, especially bivalves, were concentrated in the upper portions of the tributaries and mainstem Bay. High biomass zones generally had low salinity, high surface NO_3^-, moderate dissolved oxygen, and low depth. NO_3^- could behave as a proxy for POC, with high biomass being driven by allochthonous POC in the tidal fresh and oligohaline zones, areas with lower autochthonous primary production and high heterotrophy. Calcification from benthic macrofauna biomass could be a significant sink of calcium in the Bay, and the calcification rates from bivalves collected in the BMP program far exceeds Eastern oyster calcification rates. CO_2 generated from calcification and respiration could substantially contribute to outgassing in the tidal fresh and oligohaline zones. These findings highlight the significant role of benthic macrofauna in estuarine biogeochemical cycling, particularly in Chesapeake Bay.

Estuarine numerical models have historically focused on microbiota while overlooking the role of macrobiota in biogeochemical transformations (Ehrnsten et al., 2020; Ganju et al., 2016). However, our study demonstrates that benthic macrofauna can significantly influence carbon dynamics within the Chesapeake Bay and should be more consistently incorporated into numerical models. Additionally, we show that the spatial distribution of benthic macrofauna is highly predictable based on environmental variables already included in models, reducing the need for high-resolution benthic biomass data. Our findings provide a strong foundation for integrating benthic macrofauna into numerical models, highlight both the feasibility and necessity of doing so.

~~Several limitations in our study must also be acknowledged. One key limitation is the need for better empirical equations relating biomass to metabolic processes, particularly calcification. Our estimates relied heavily on Chauvaud et al., (2003), who assumes a direct proportionality between secondary production rates and calcification rates, but this relationship requires further validation across different estuarine systems. However, we attempted to account for this uncertainty by incorporating a range of estimates in our analysis. Additionally, our study was constrained by the interactions between highly correlated variables. As a result, we did not use our calculated values for Ω_{arag}, despite its potential importance for bivalves. The saturation state of aragonite could strongly influence calcification rates, but due to its correlation with other environmental variables, its independent effect was difficult to parse. Furthermore, while our model explained a little over half of the deviance in biomass from predictor variables, this predictive capability could be improved. In our study we emphasized bottom-up controls. Top-down controls such as predation could also play a significant role in biomass distributions.~~

~~Future research should focus on refining metabolic estimates and further investigating the factors driving temporal changes in biomass. Climate change, along with ongoing management efforts aimed at reducing nutrient loading, is expected to alter key water quality parameters. Understanding how these shifts will impact benthic biomass distribution and metabolism is critical for predicting their broader impacts on ecosystem functioning and biogeochemical cycling.~~

~~Overall, our findings emphasize the predictability of benthic biomass distributions within estuaries and their importance to estuarine carbon budgets, underscoring their need for further integration into numerical models.~~

This study quantifies estuarine-scale benthic macrofaunal biomass and associated carbon fluxes, including secondary production, respiration, and calcification, across the Chesapeake Bay. The results demonstrate that benthic macrofauna play a substantial and spatially structured role in estuarine carbon cycling, particularly in upper estuarine zones where biomass is highest. In these regions, benthic macrofauna respiration is a significant fraction of total available organic carbon inputs, up to 45%, while calcification accounts for a large portion of the observed alkalinity sink. These contributions vary across the salinity gradient, shaped by both environmental drivers and taxonomic composition.

Patterns observed in this study suggest that benthic biomass and its associated carbon fluxes are influenced by gradients in salinity, oxygen, and organic matter inputs. The dominance of bivalves in low-salinity zones has particularly strong biogeochemical implications due to the role of bivalves in secondary production and calcification. Notably, NO_3^- emerged as a strong predictor of benthic biomass, not necessarily due to enhanced autotrophic production, but potentially reflecting allochthonous organic matter inputs that drive heterotrophic metabolism. The significant contributions of benthic communities to alkalinity consumption and DIC release highlight their potential to alter estuarine carbon chemistry in ways that depend on both biological composition and environmental conditions.

To build on these results, future work should examine how benthic biomass and associated carbon fluxes vary over time in response to both natural variability and anthropogenic change. Predicting future responses is especially challenging due to the high-frequency variability in estuarine systems, which can obscure long-term signals. Understanding how POC inputs, particularly allochthonous sources, change seasonally and interannually will be critical, as will clarifying the extent to which NO_3^- serves as a proxy for those inputs. Long-term monitoring

and modeling efforts that link changes in watershed nutrient loading, land use, and climate with benthic community dynamics will be essential for forecasting ecosystem responses and for developing more accurate, responsive biogeochemical models.

Appendix A

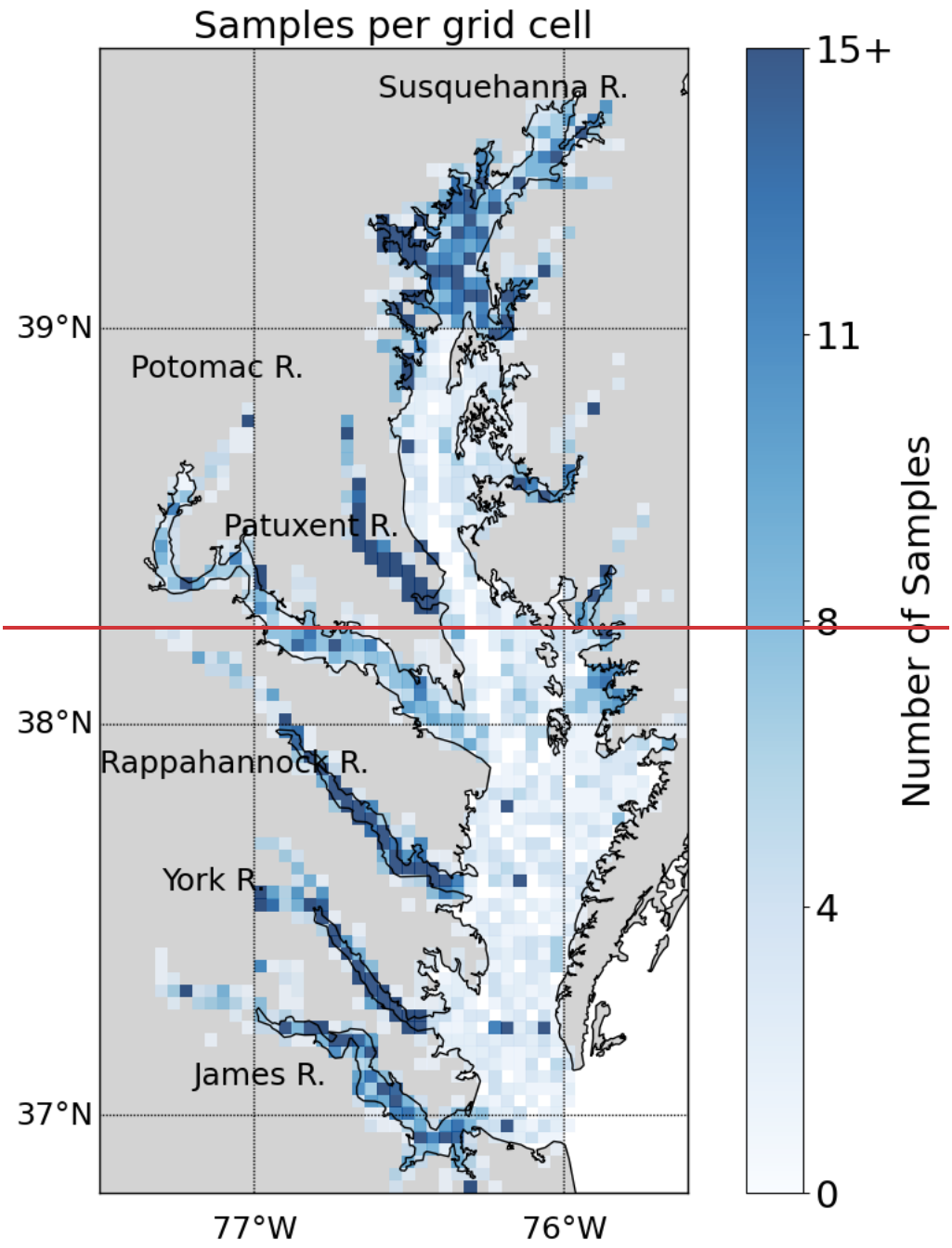

Biomass Sampling Density

This appendix shows the spatial distribution of sampling effort for the BMP from 1995 to 2022. Fig. A1 illustrates the number of samples collected in each grid cell, highlighting areas of higher and lower sampling density across the Chesapeake Bay and its tributaries.

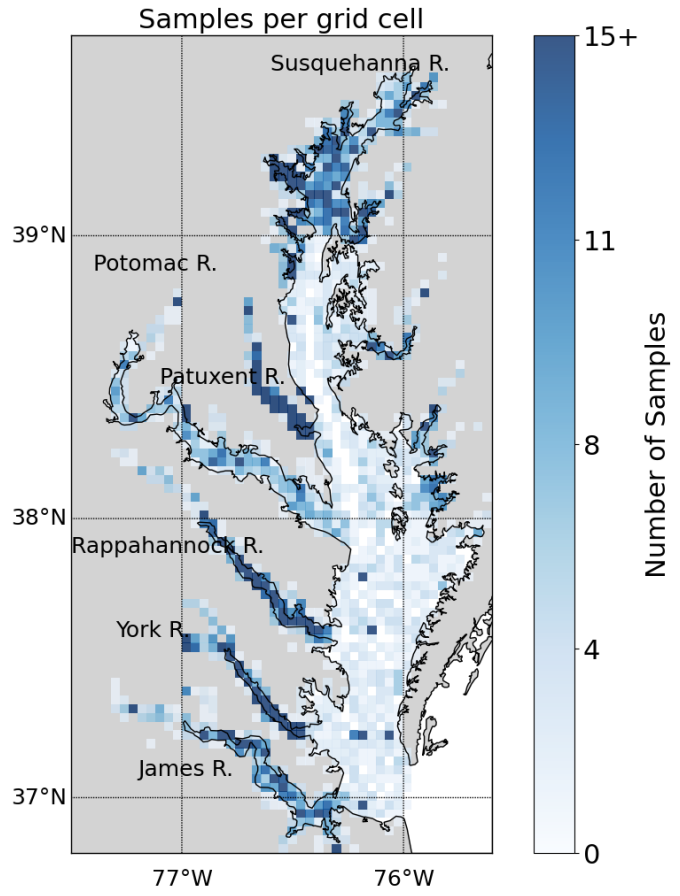

Figure A1: Number of benthic samples collected in each grid cell in the summer (July 15 to September 30) from 1995 to 2022 from the Chesapeake Bay Benthic Monitoring Program. The grids are approximately square, measuring 3.5 km by 3.5 km. Each grid cell contains a time-average of each measurement collected in the cell

Appendix B

Carbon flux uncertainties

This appendix explains the methodology for propagating uncertainty in the benthic macrofaunal carbon flux estimates. It outlines the parameter ranges used, the calculations for uncertainty bounds, and the assumptions underlying these estimates. These details support the uncertainty ranges shown in figures and tables in the Results section. Uncertainty estimates were propagated through empirical equations using standard error propagation techniques (Taylor,

2022) assuming uncorrelated inputs and approximating relative errors when only a range of values was available.

Uncertainty for carbon-based biomass (B_c) is derived from the two different r_c values:

$$\frac{\Delta B_c}{B_c} = \frac{\Delta r_c}{r_c} \quad \text{(B1)}$$

where Δr_c = 0.03 g C g^{-1}, half the range of possible r_c values.

The uncertainty for the first approach for estimating secondary production (S_1) is derived from B_c and α:

$$\frac{\Delta S_1}{S} = \sqrt{\left(\frac{\Delta \alpha}{\alpha}\right)^2 + \left(\frac{\Delta B_c}{B_c}\right)^2} \quad \text{(B2)}$$

$\Delta \alpha$ is half the range of possible α values and equals 1.695 yr^{-1}.

Uncertainty in secondary production (S) arises from the multiple equations used:

$$\frac{\Delta S}{S} = \sqrt{w\left(\frac{\Delta S_1}{S_1}\right)^2 + 2w\varepsilon} \quad \text{(B3)}$$

where each model is equally weighted (w = 1/3). Only Model 1 (Equation 6) includes an explicit source of uncertainty, while Models 2 and 3 (Equations 8 and 9) do not. Therefore a small error term ε = 0.001 was assumed for those two models.

Calcification (C) uncertainty is derived from r_s and S:

$$\frac{\Delta C}{C} = \sqrt{\left(\frac{\Delta r_s}{r_s}\right)^2 + \left(\frac{\Delta S}{S}\right)^2} \quad \text{(B4)}$$

where r_s has one value for *C. fluminea* and one for *P. amurensis*. $\Delta r_s = 2.5$ g $CaCO_3$ (g C)$^{-1}$ and is half the range of possible r_s values.

The uncertainty in respiration (R) is derived solely from S:

$$\Delta R = 2.33\Delta S \quad \text{(B5)}$$

The uncertainties in the fluxes of alkalinity and DIC (F_{TA} and F_{DIC}) are also derived from C and R:

$$\Delta F_{TA} = \frac{-2\Delta C}{M_{CaCO_3}} \quad \text{(B6)}$$

$$\Delta F_{DIC} = \sqrt{\left(\frac{\Delta R}{M_C}\right)^2 + \left(\frac{\Delta C}{M_{CaCO_3}}\right)^2} \quad \text{(B7)}$$

where M_{CaCO_3} and M_C are the molar masses of $CaCO_3$ and C, respectively.

Finally, we propagate the error in the flux of carbon dioxide (F_{CO_2}) from the errors in F_{TA} and F_{DIC}:

$$\Delta F_{CO_2} = \sqrt{\left(\frac{[CO_2]\zeta_{TA}\,\Delta F_{TA}}{[TA]}\right)^2 + \left(\frac{[CO_2]\,\zeta_{DIC}\Delta F_{DIC}}{[DIC]}\right)^2} \quad \text{(B8)}$$

We do not consider errors in the buffer factors, $[CO_2]$, [DIC], and [TA] in ROMS.

Appendix C

Secondary production model comparison

This appendix details the comparison of secondary production estimates from the three approaches described in Section 2.3.1. Seasonal and spatial variations are shown to illustrate the influence of temperature and other parameters on production estimates. These comparisons provide context for interpreting model differences presented in the main text.

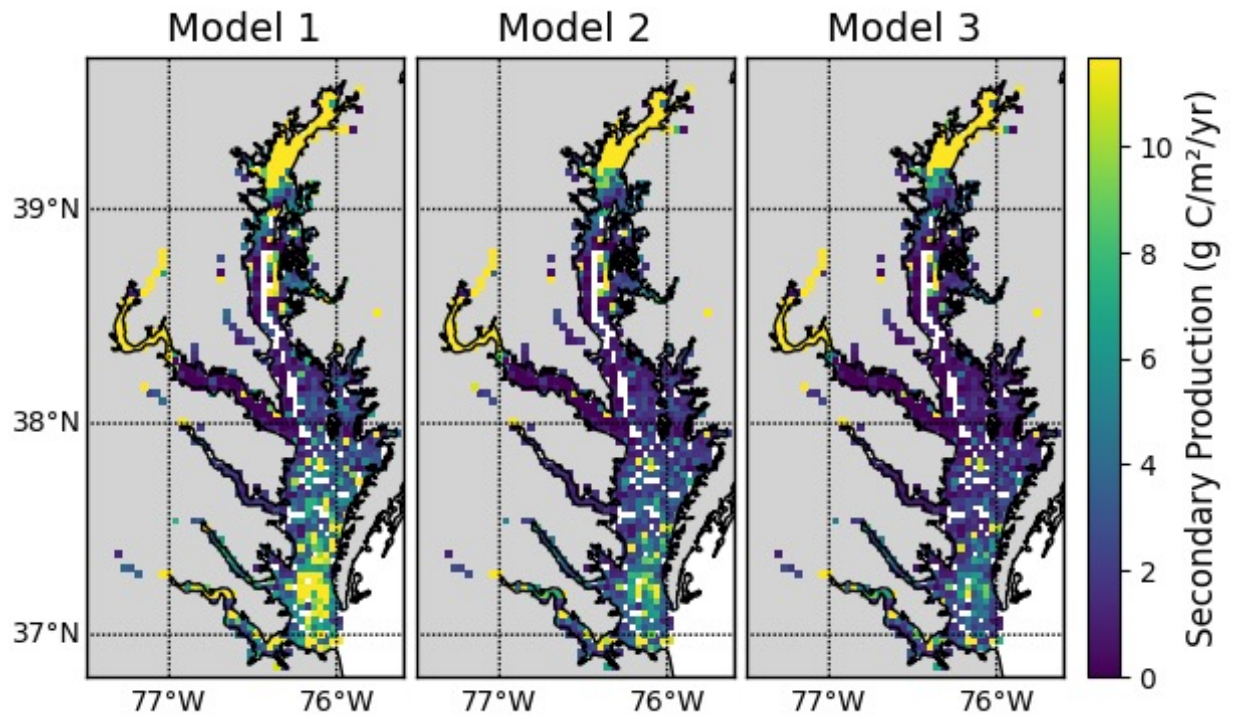

Figure C1: Long-term average secondary production across the Chesapeake Bay for each of the three secondary production models.

The models have similar spatial patterns (Fig. C1), which are similar to the pattern of benthic biomass (Fig. 2). Secondary production is generally higher in Model 1 than in Models 2 and 3, which can be seen most clearly in the means, which are 17.92, 8.31, and 7.59 g C m^{-2} yr^{-1} in Models 1, 2, and 3, respectively.

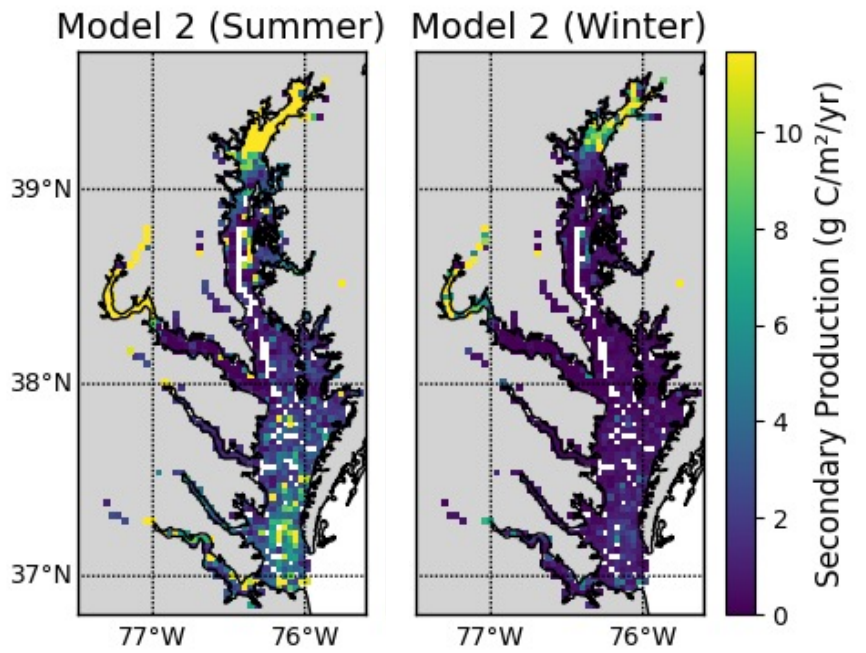

Figure C2: Seasonal sensitivity of Model 2 to bottom temperature inputs.

Fig. C2 and C3 compare secondary production between summer and winter scenarios. The summer scenario uses summer bottom water temperatures measured concurrently with biomass samples, while the winter scenario assumes a temperature of 1 °C. Fig. C2 shows the results for Model 2, which has a mean secondary production of 8.31 g C m^{-2} yr^{-1} in summer and 1.89 g C m^{-2} yr^{-1} in winter. Fig. C3 shows the results for Model 3, which has a mean secondary production of 7.59 g C m^{-2} yr^{-1} in summer and 1.44 g C m^{-2} yr^{-1} in winter. For both models, production in summer is about 5 times that of winter, as expected from the rough estimates in the Methods section. Assuming spring and fall are halfway between winter and summer, and weighting the seasons equally, the annually averaged secondary production rate would be about 60% of the summer rate.

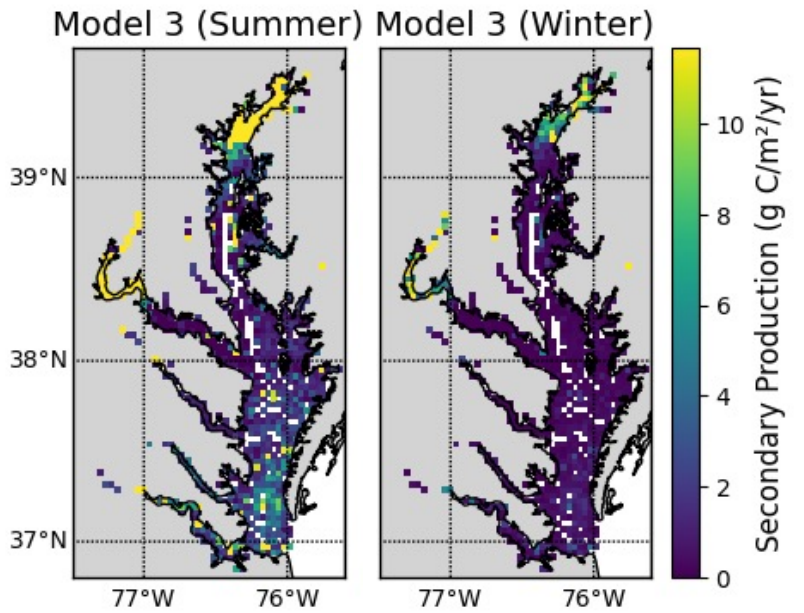

Figure C3: Seasonal sensitivity of Model 3 to bottom temperature inputs.

Appendix D

Species biomass distribution

This appendix expands on the biomass distribution results in Section 3.1 by showing detailed spatial patterns for individual species and taxonomic classes. Fig. D1 complements the summary figures in the main text, highlighting species-specific habitat associations.

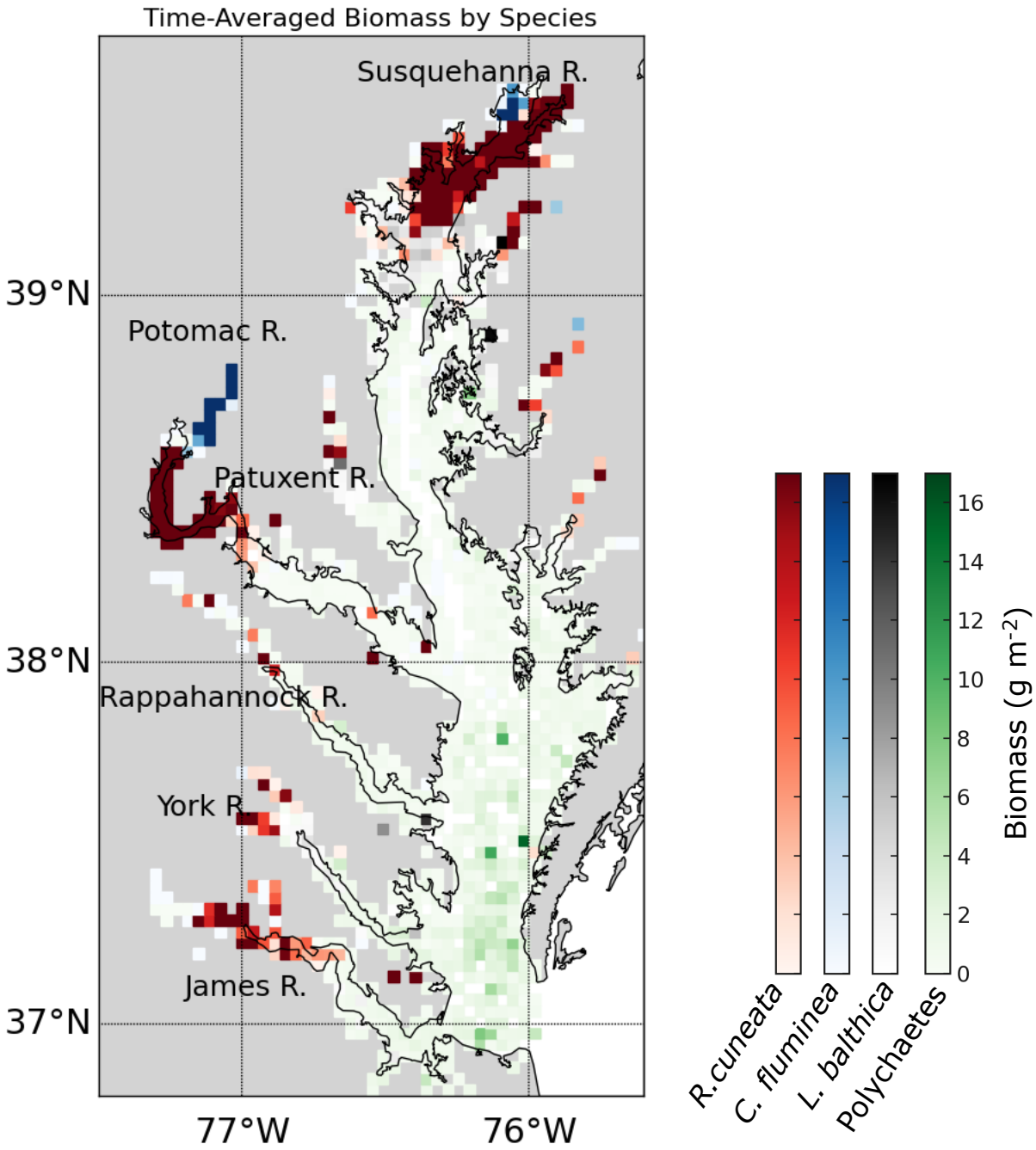

Figure D1: Average summer biomass density from 1995 to 2022 from the Maryland and Virginia Benthic Monitoring Program. ~~The grids are approximately square, measuring 3.5 km by 3.5 km. Each grid cell contains a time-average of each measurement collected in the cell~~

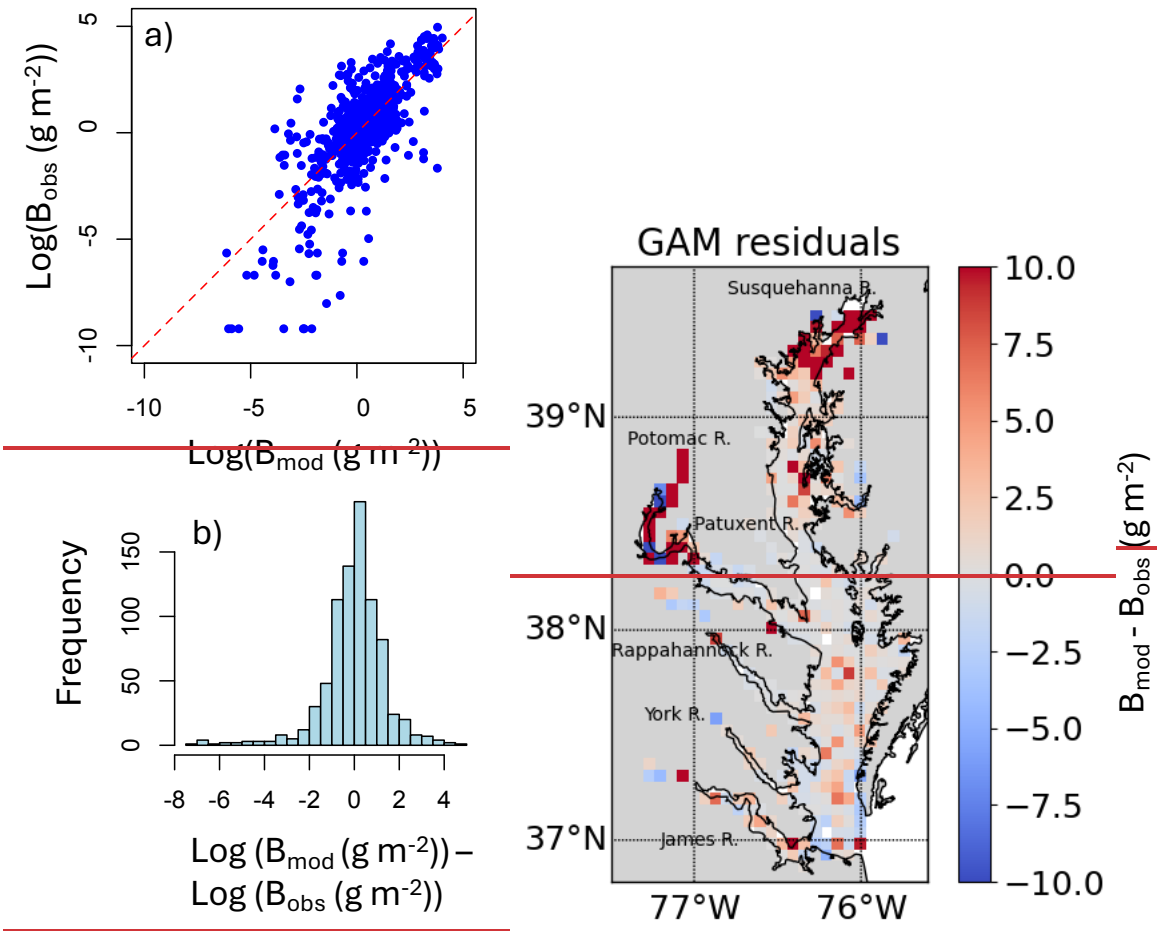

~~Figure A2~~Each color corresponds to a specific bivalve species (*M. balthica, C. fluminea, or R. cuneata*) or polychaetes. The color shown on the map is the species with the highest time-averaged biomass in that grid cell.

Appendix E

Carbon flux-related parameters

To illustrate estuarine variability in carbonate system drivers, we summarized a suite of flux and water column properties across tidal salinity zones of the Chesapeake Bay (Fig. E1). The patterns highlight strong gradients from tidal fresh through polyhaline regions. Notably $[CO_2]$ is elevated in tidal fresh waters, underscoring the combined influence of salinity, TA, and the TA:DIC ratio on estuarine carbonate chemistry.

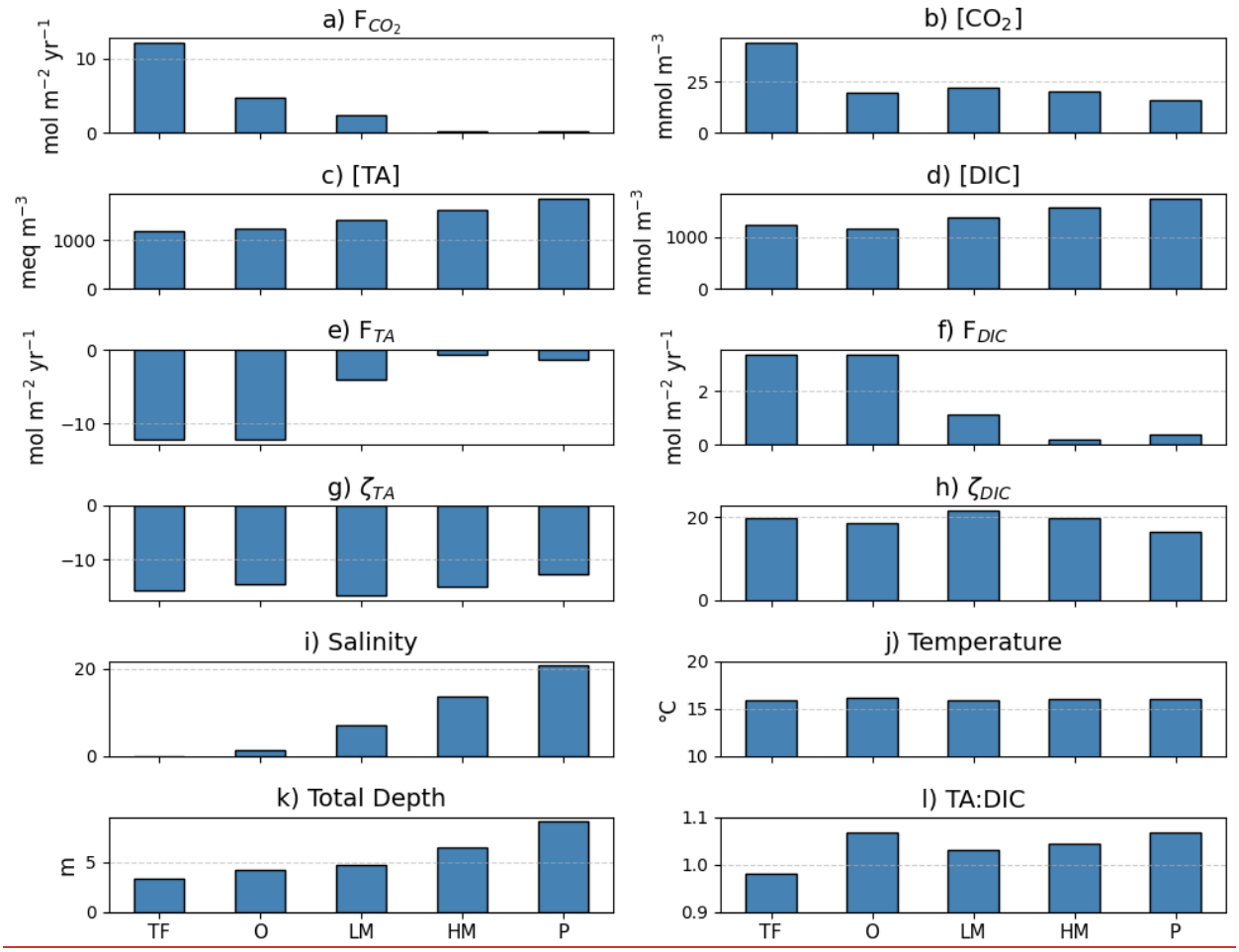

Figure E1: Carbon flux-related parameters averaged within salinity zones of Chesapeake Bay. [CO_2] was calculated using PyCO2SYS; temperature, salinity, total depth, [TA] and [DIC] were obtained from ROMS model output. F_{TA} and F_{DIC} were calculated following Equations 13–14, ζ_{TA} and ζ_{DIC} from Equations 16–17, and F_{CO_2} from Equation 15.

Appendix F

GAMs evaluation

This appendix presents diagnostic plots and statistics for the generalized additive models described in Section 2.5. Residual maps, histograms, and fitted-vs-observed plots (Fig. F1) are included to evaluate model performance and identify patterns in prediction errors.

A good model would have points on a modeled vs. observed scatterplot fall close to a 1:1 line and have the departures from that line (residuals) be close to normally distributed. Although GAMs can handle non-normal distributions of the response variable (Guisan et al., 2002), we found the best model fit by applying a natural logarithmic transformation to the biomass. A small constant (0.0001 g m^{-2}) was added to the biomass values before applying the natural logarithmic transformation to account for zeros in the data. The resulting biomass was normally distributed after applying the natural logarithm function, so the GAM was fitted with a Gaussian distribution with an identity link function.

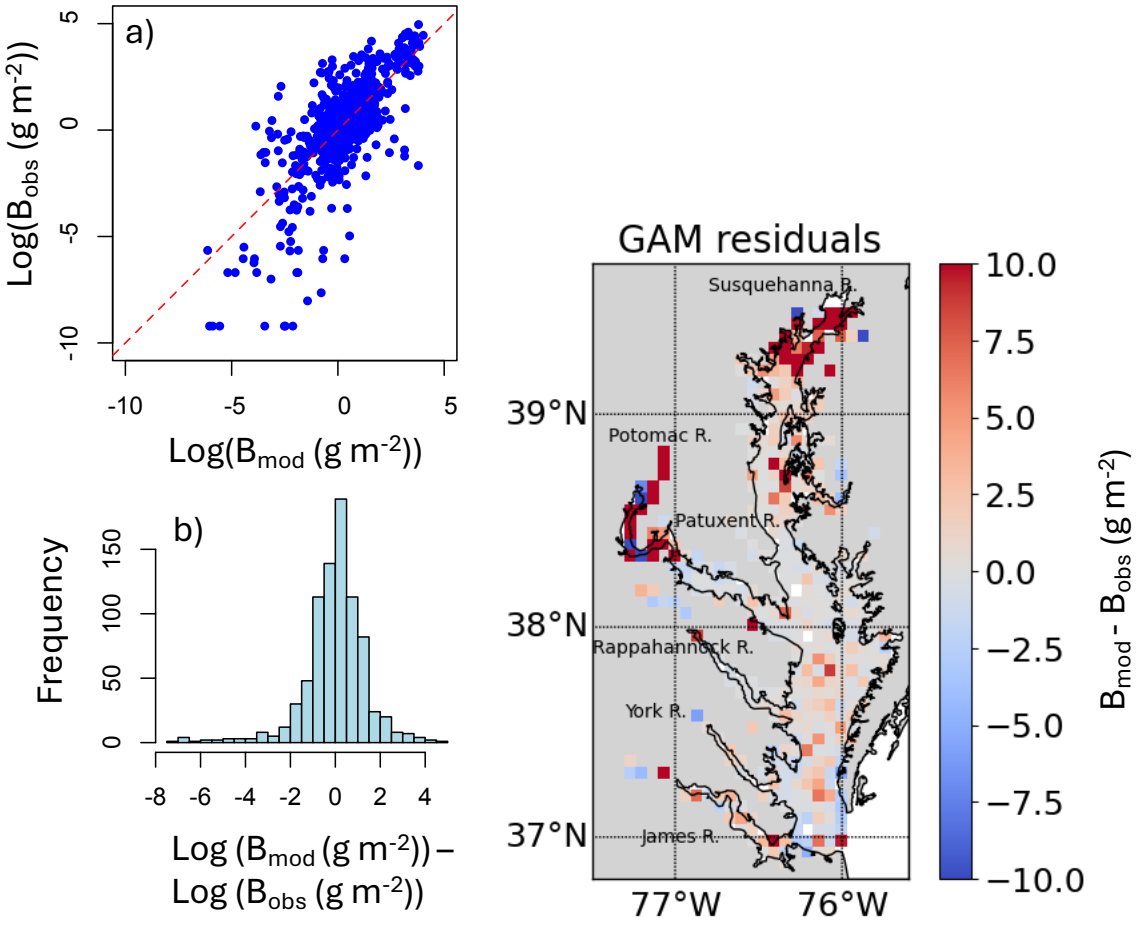

Figure F1: Evaluation of the total biomass GAM, which includes ~~DO~~O_2, salinity, total depth, ~~,~~ ~~and~~ NO_3~~,~~, sand fraction, and water temperature as predictor variables. "Log" refers to the natural logarithm. (a) Modeled vs. observed values. (b) Histogram of biomass residuals (modeled minus observed values, $B_{mod} - B_{obs}$). ~~-~~(c) Spatial distribution of the residuals.

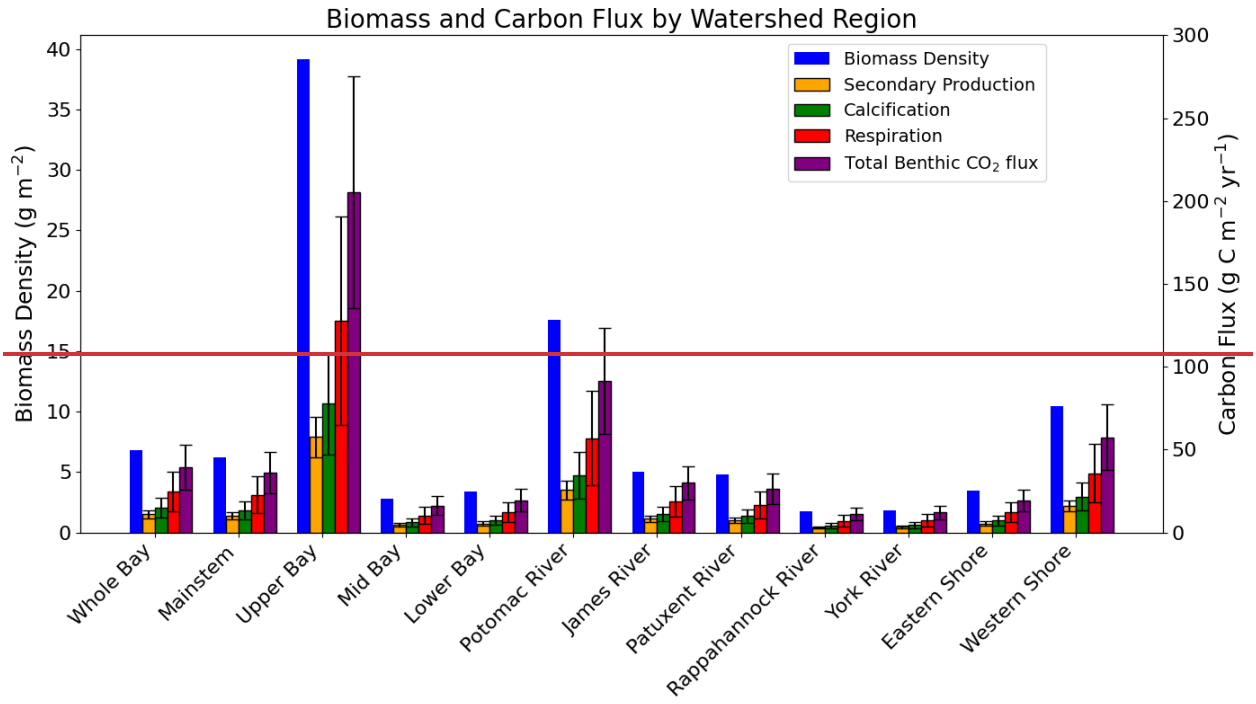

~~Figure A3: Biomass density and carbon fluxes for each watershed region in the Bay. The carbon fluxes are the mean value with associated total uncertainty range, as described in the text.~~

Data Availability

All data used in this study are publicly available and have been described in the Methods section. Water quality data were obtained from the *Chesapeake Bay Water Quality Monitoring Program* (https://datahub.chesapeakebay.net/WaterQuality), and benthic data were sourced from the *Chesapeake Bay Long-Term Benthic Monitoring Program* (https://www.baybenthos.versar.com/data.htm). Model output used in this study is publicly available at https://www.seanoe.org/data/00882/99441/.

Author Contribution

SA led the research, conducted data analysis, interpreted results, and wrote the initial and subsequent drafts of the manuscript.

RN conceptualized the project, defined overarching research goals, secured financial support, and contributed substantially to manuscript drafts through critical reviews, commentary, and revisions.

ER provided significant insights from her expertise on the physiological responses of marine invertebrates to environmental variables, influencing the scope and direction of the study. She also substantially contributed to manuscript revisions through critical reviews and commentary.

RW contributed significant expertise on benthic biomass distribution in Chesapeake Bay and generalized additive modeling techniques, shaping the analytical framework of the study. He provided critical feedback and revisions during manuscript preparation.

MF provided ongoing feedback throughout the research process, particularly regarding the integration of modeling information and interpretation of results, and contributed critical commentary on multiple presentations of the work.

PS consistently provided feedback and contributed modeling expertise, assisting with data interpretation and manuscript revisions through critical reviews and commentary.

SD developed the original empirical models linking benthic macrofaunal biomass to carbon fluxes, laying foundational methodological contributions to the study.

Competing Interests

The authors declare that they have no conflict of interest.

Acknowledgements

We thank Maria Herrmann, Jill Arriola, and Alexa Labossiere for their valuable discussions and feedback that contributed to this manuscript. We also acknowledge Riley Westman and Edward Stets for providing riverine calcium input data from the USGS. Additionally, we used AI tools, including Grammarly and ChatGPT, to assist with grammar and clarity in sentence editing.

Financial Support

This work is supported by the National Science Foundation (NSF) Chemical and Biological Oceanography Program under Grant ~~No~~Nos. **OCE-2148949** (Penn State), OCE-2148950 (VIMS), and OCE-2148952 (UMCES), and by the U.S. Department of Energy (DOE) as part of the Integrated Coastal Modeling (ICoM) project.

References

Akoglu, H. (2018). User's guide to correlation coefficients. *Turkish Journal of Emergency Medicine*, *18*(3), 91–93. https://doi.org/10.1016/j.tjem.2018.08.001

~~Alden, R. W., Dauer, D. M., Ranasinghe, J. A., Scott, L. C., & Llansó, R. J. (2002). Statistical verification of the Chesapeake Bay benthic index of biotic integrity. *Environmetrics: The Official Journal of the International Environmetrics Society*, *13*(5–6), 473–498. https://doi.org/10.1002/env.548~~

Beckwith, S. T., Byrne, R. H., & Hallock, P. (2019). Riverine calcium end-members improve coastal saturation state calculations and reveal regionally variable calcification potential. *Frontiers in Marine Science*, *6*(APR). https://doi.org/10.3389/fmars.2019.00169

Birchenough, S. N. R., Reiss, H., Degraer, S., Mieszkowska, N., Borja, Á., Buhl-Mortensen, L., Braeckman, U., Craeymeersch, J., De Mesel, I., Kerckhof, F., Kröncke, I., Parra, S., Rabaut, M., Schröder, A., Van Colen, C., Van Hoey, G., Vincx, M., & Wätjen, K. (2015). Climate change and marine benthos: ~~a~~A review of existing research and future directions in the North Atlantic. *Wiley Interdisciplinary Reviews: Climate Change*, *6*(2), 203–223. https://doi.org/10.1002/wcc.330

Borja, A., Dauer, D. M., Díaz, R., Llansó, R. J., Muxika, I., Rodríguez, J. G., & Schaffner, L. (2008). Assessing estuarine benthic quality conditions in Chesapeake Bay: ~~a~~A comparison of three indices. *Ecological Indicators*, *8*(4), 395–403. https://doi.org/10.1016/j.ecolind.2007.05.003

Brey, T. (1990). Confidence limits for secondary production estimates: ~~application~~Application of the bootstrap to the increment summation method~~*~~. *Marine Biology*, *106*, 503–508.

~~Brush, M. J., Giani, M., Totti, C., Testa, J. M., Faganeli, J., Ogrinc, N., Michael Kemp, W., & Umani, S. F. (2020). Eutrophication, harmful algae, oxygen depletion, and acidification. In T. C. Malone, A. Malej, & J. Faganeli (Eds.), *Coastal ecosystems in transition: A comparative analysis of the Northern Adriatic and Chesapeake Bay* (pp. 75–104). Wiley. https://doi.org/10.1002/9781119543626.ch5~~

Brush, M. J., Mozetič, P., Francé, J., Aubry, F. B., Djakovac, T., Faganeli, J., Harris, L. A., & Niesen, M. (2020). Phytoplankton dynamics in a changing environment. In T. C. Malone, A. Malej, & J. Faganeli (Eds.), *Coastal ~~ecosystems~~Ecosystems in ~~transition~~Transition: A ~~comparative analysis~~Comparative Analysis of the Northern Adriatic and Chesapeake Bay* (pp. 49–74). Wiley. https://doi.org/10.1002/9781119543626.ch4

Cain, T. D. (1975). Reproduction and recruitment of the brackish water clam, Rangia cuneata in the James River, Virginia. *Fishery Bulletin*, *73*(2), 412. https://scholarworks.wm.edu/vimsarticles/2139

Canuel, E. A., & Hardison, A. K. (2016). Sources, ages, and alteration of organic matter in estuaries. *Annual Review of Marine Science*, *8*, 409–434. https://doi.org/10.1146/annurev-marine-122414-034058

Cerco, C. F., & Noel, M. R. (2010). Monitoring, modeling, and management impacts of bivalve filter feeders in the oligohaline and tidal fresh regions of the Chesapeake Bay system. *Ecological Modelling*, *221*(7), 1054–1064. https://doi.org/10.1016/j.ecolmodel.2009.07.024

Chauvaud, L., Thompson, J. K., Cloern, J. E., & Thouzeau, G. (2003). Clams as CO2 generators: The Potamocorbula amurensis example in San Francisco Bay. *Limnology and Oceanography*, *48*(6), 2086–2092. https://doi.org/10.4319/lo.2003.48.6.2086

Chen, C. T. A., Huang, T. H., Chen, Y. C., Bai, Y., He, X., & Kang, Y. (2013). Air–sea exchanges of CO2 in the world's coastal seas. *Biogeosciences*, *10*(10), 6509–6544. https://doi.org/10.5194/bg-10-6509-2013

Chesapeake Bay Program. (n.d.). *CBP Water Quality Database (1984-present)*.

Chesapeake Bay Program analytical segmentation scheme: Revisions, decisions and rationales, 1983–2003. (2004).

Dauer, D. M. (1993). Biological criteria, environmental health and estuarine macrobenthic community structure. *Marine Pollution Bulletin*, *26*(5), 249–257. https://doi.org//10.1016/0025-326X(93)90063-P

Dauer, D. M., & Alden III, R. W. (1995). Long-term trends in the macrobenthos and water quality of the lower Chesapeake Bay (1985-1991). *Marine Pollution Bulletin*, *30*(12), 840–850.

Dauer, D. M., & Lane, M. F. (2010). *Quality ~~assurance/quality control plan~~Assurance/Quality Control Plan: Benthic ~~biological monitoring program~~Biological Monitoring Program of the Lower Chesapeake Bay (July 1, 2010 to June 30, 2011)*.

Dauer, D. M., Ranasinghe, J. A., & Weisberg, S. B. (2000). Relationships between benthic community condition, water quality, sediment quality, nutrient loads, and land use patterns in Chesapeake Bay. *Estuaries*, *23*(1), 80–96.

Diaz, R. J., & Rosenberg, R. (2008). Spreading dead zones and consequences for marine ecosystems. *Science*, 926–929. https://www.science.org~~J., & Schaffner, L. C. (1990). *Perspectives on the Chesapeake Bay, 1990* (M. Haire & E. C. Krome, Eds.).~~

Diaz, R. J., & Schaffner, L. C. (1990). The functional role of estuarine benthos. In M. Haire & E. C. ~~.,~~Krome (Eds.), *Perspectives on the Chesapeake Bay* (pp. 25–56). Chesapeake Research Consortium.

Diaz, R., & Rosenberg, R~~., D Ansell R N Gibson, C. A., Barnes, M., & Diaz, R. J.~~ (1995). Marine benthic hypoxia: ~~a~~A review of its ecological effects and the behavioural responses of benthic macrofauna. *Oceanography and Marine Biology. An Annual Review*, *33*, 245–303. https://www.researchgate.net/publication/236628341

Dolbeth, M., Cusson, M., Sousa, R., & Pardal, M. A. (2012). Secondary production as a tool for better understanding of aquatic ecosystems. *Canadian Journal of Fisheries and Aquatic Sciences*, *69*(7), 1230–1253. https://doi.org/10.1139/F2012-050

Dormann, C. F., Elith, J., Bacher, S., Buchmann, C., Carl, G., Carré, G., García Marquéz, J. R., Gruber, B., Lafourcade, B., Leitão, P. J., Münkemüller, T., McClean, C., Osborne, P. E., Reineking, B., Schröder, B., Skidmore, A. K., Zurell, D., & Lautenbach, S. (2013). Collinearity: ~~a~~A review of methods to deal with it and a simulation study evaluating their performance. *Ecography*, *36*(1), 27–46.

Drexler, M., & Ainsworth, C. H. (2013). Generalized ~~Additive Models Used~~additive models used to ~~Predict Species Abundance~~predict species abundance in the Gulf of Mexico: An ~~Ecosystem Modeling Tool~~ecosystem modeling tool. *PLoS ONE*, *8*(5). https://doi.org/10.1371/journal.pone.0064458

Edgar, G. J. (1990). The use of the size structure of benthic macrofaunal communities to estimate faunal biomass and secondary production. *Journal of Experimental Marine Biology and Ecology*, *137*(3), 195–214.

Egleston, E. S., Sabine, C. L., ~~Ehrnsten, E., Norkko, A., Müller-Karulis, B., Gustafsson, E., & Gustafsson, B. G. (2020). The meagre future of benthic fauna in a coastal sea – Benthic responses to recovery from eutrophication in a changing climate. *Global Change Biology*, *26*(4), 2235–2250. https://doi.org/10.1111/gcb.15014~~

& Morel, F. M. M. (2010). Revelle revisited: Buffer factors that quantify the response of ocean chemistry to changes in DIC and alkalinity. *Global Biogeochemical Cycles*, *24*(1). https://doi.org/10.1029/2008GB003407

Ehrnsten, E., Norkko, A., Timmermann, K., & Gustafsson, B. G. (2019). Benthic-pelagic coupling in coastal seas – Modelling macrofaunal biomass and carbon processing in response to organic matter supply. *Journal of Marine Systems*, *196*, 36–47. https://doi.org/10.1016/j.jmarsys.2019.04.003

Eleftheriou, A., & Moore, D. C. (2013). Macofauna techniques. *Methods for the Study of Marine Benthos*, 175–251.

Frankel, L. T., Friedrichs, M. A. M., St-Laurent, P., Bever, A. J., Lipcius, R. N., Bhatt, G., & Shenk, G. W. (2022). Nitrogen reductions have decreased hypoxia in the Chesapeake Bay: Evidence from empirical and numerical modeling. *Science of the Total Environment*, *814*. https://doi.org/10.1016/j.scitotenv.2021.152722

~~Fujii, T., & Raffaelli, D. (2008). Sea-level rise, expected environmental changes, and responses of intertidal benthic macrofauna in the Humber estuary, UK. *Marine Ecology Progress Series*, *371*, 23–35. https://doi.org/10.3354/meps07652~~

Frankignoulle, M., Abril, G., Borges, A., Bourge, I., Canon, C., Delille, B., Libert, E., & Théate, J.-M. (1998). Carbon dioxide emission from European estuaries. *Science*, *282*(5388), 434–436. https://www.science.org

Fulford, R. S., Breitburg, D. L., Newell, R. I. E., Kemp, W. M., & Luckenbach, M. (2007). Effects of oyster population restoration strategies on phytoplankton biomass in Chesapeake Bay: a flexible modeling approach. *Marine Ecology Progress Series*, *336*, 43–1.

Galimany, E., Lunt, J., Freeman, C. J., Houk, J., Sauvage, T., Santos, L., Lunt, J., Kolmakova, M., Mossop, M., Domingos, A., Phlips, E. J., & Paul, V. J. (2020). Bivalve feeding responses to microalgal bloom species in the Indian River Lagoon: the potential for top-down control. *Estuaries and Coasts*, *43*(6), 1519–1532. https://doi.org/10.1007/s12237-020-00746-9

~~Ganju, N. K., Brush, M. J., Rashleigh, B., Aretxabaleta, A. L., del Barrio, P., Grear, J. S., Harris, L. A., Lake, S. J., McCardell, G., O'Donnell, J., Ralston, D. K., Signell, R. P., Testa, J. M., & Vaudrey, J. M. P. (2016). Progress and challenges in coupled hydrodynamic-ecological estuarine modeling. *Estuaries and Coasts*, *39*(2), 311–332. https://doi.org/10.1007/s12237-015-0011-y~~

Garcia, H. E., & Gordon, L. I. (1992). Oxygen solubility in seawater: Better fitting equations. *Limnology and Oceanography*, *37*(6), 1307–1312. https://doi.org/10.4319/lo.1992.37.6.1307

Glud, R. N. (2008). Oxygen dynamics of marine sediments. *Marine Biology Research*, *4*(4), 243–289. https://doi.org/10.1080/17451000801888726

Grant, J., & Thorpe, B. (1991). Effects of suspended sediment on growth, respiration, and excretion of the soft-shell clam (Mya arenaria). *Canadian Journal of Fisheries and Aquatic Sciences*, *48*(7).

Grebmeier, J. M., Bluhm, B. A., Cooper, L. W., Denisenko, S. G., Iken, K., Kędra, M., & Serratos, C. (2015). Time-series benthic community composition and biomass and associated environmental characteristics in the Chukchi Sea during the RUSALCA 2004-2012 Program. *Oceanography*, *28*(3), 116–133. https://doi.org/10.2307/24861905

Green, M. A., Waldbusser, G. G., Reilly, S. L., Emerson, K., & O'Donnell, S. (2009). Death by dissolution: Sediment saturation state as a mortality factor for juvenile bivalves. *Limnology and Oceanography*, *54*(4), 1037–1047. https://doi.org/10.4319/lo.2009.54.4.1037

Grüss, A., Drexler, M., & Ainsworth, C. H. (2014). Using delta generalized additive models to produce distribution maps for spatially explicit ecosystem models. *Fisheries Research*, *159*, 11–24. https://doi.org/10.1016/j.fishres.2014.05.005

Guisan, A., Edwards, T. C., & Hastie, T. (2002). Generalized linear and generalized additive models in studies of species distributions: setting the scene. *Ecological Modelling*, *157*(2–3), 89. www.elsevier.com/locate/ecolmodel

Hagy, J. D. (2002). *Eutrophication, hypoxia and trophic transfer efficiency in Chesapeake Bay* [Doctoral dissertation, University of Maryland, College Park]. https://www.researchgate.net/publication/237005296

Harding, L. W., Mallonee, M. E., & Perry, E. S. ~~& Perry, E. S. (1997). Long-term increase of phytoplankton biomass in Chesapeake Bay, 1950-1994. *Marine Ecology Progress Series*, *157*, 39–52.~~(2002). Toward a predictive understanding of primary productivity in a temperate, partially stratified estuary. *Estuarine, Coastal and Shelf Science*, *55*(3), 437–463. https://doi.org/10.1006/ecss.2001.0917

Hartwell, S. I., Wright, D. A., Takacs, R., & Hocutt, C. H. (1991). Relative respiration and feeding rates of oyster and brackish water clam in variously contaminated waters. *Marine Pollution Bulletin*, *22*(4), 191–197.

Hastie, T., & Tibshirani, R. (1987). Generalized additive models: ~~some~~Some applications. *Journal of the American Statistical Association*, *82*(398).

Hauke, J., & Kossowski, T. (2011). Comparison of values of Pearson's and Spearman's correlation coefficients on the same sets of data. *Quaestiones Geographicae*, *30*(2), 87–93. https://doi.org/10.2478/v10117-011-0021-1

Herrmann, M., Najjar, R. G., Da, F., Friedman, J. R., Friedrichs, M. A. M., Goldberger, S., Menendez, A., Shadwick, E. H., Stets, E. G., & St-Laurent, P. (2020). Challenges in quantifying air-water carbon dioxide flux using estuarine water quality data: Case study for Chesapeake Bay. *Journal of Geophysical Research: Oceans*, *125*(7). https://doi.org/10.1029/2019JC015610

Herrmann, M., Najjar, R. G., Kemp, W. M., Alexander, R. B., Boyer, E. W., Cai, W. J., Griffith, P. C., Kroeger, K. D., McCallister, S. L., & Smith, R. A. (2015). Net ecosystem production and organic carbon balance of U.S. East Coast estuaries: A synthesis approach. *Global Biogeochemical Cycles*, *29*(1), 96–111. https://doi.org/10.1002/2013GB004736

Hinson, K. E., Friedrichs, M. A. M., St-Laurent, P., Da, F., & Najjar, R. G. (2022). Extent and causes of Chesapeake Bay warming. *Journal of the American Water Resources Association*, *58*(6), 805–825. https://doi.org/10.1111/1752-1688.12916

Hirsch, R. M., Moyer, D. L., & Archfield, S. A. (2010). Weighted regressions on time, discharge, and season (WRTDS), with an application to Chesapeake Bay river inputs. *Journal of the American Water Resources Association*, *46*(5), 857–880. https://doi.org/10.1111/j.1752-1688.2010.00482.x

Holland, A. F., Shaughnessy, A. T., & Hiegel, M. H. (1987). Long-~~*Term Variation*~~term variation in ~~*Mesohaline*~~mesohaline Chesapeake ~~*Macrobenthos*~~Bay macrobenthos: Spatial and ~~*Temporal Patterns Bay*~~ ~~(Vol.~~temporal patterns. *Estuaries*, *10*~~, Issue~~ ~~(3).~~), 227–245.

Hopkins, S. H., Anderson, J. W., & Horvath, K. (1973). *The brackish water* ~~*calm*~~*clam Rangia cuneata as an indicator of ecological effects of salinity changes in coastal waters*.

Hopkinson, C. S., & Smith, E. M. (2004). Estuarine respiration: ~~an~~An overview of benthic, pelagic, and whole system respiration. *Respiration in Aquatic Ecoystems*, 122–146.

Humphreys, M. P., Lewis, E. R., Sharp, J. D., & Pierrot, D. (2022). PyCO2SYS v1.8: Marine carbonate system calculations in Python. *Geoscientific Model Development*, *15*(1), 15–43. https://doi.org/10.5194/gmd-15-15-2022

Irby, I. D., Friedrichs, M. A. M., Da, F., & Hinson, K. E. (2018). The competing impacts of climate change and nutrient reductions on dissolved oxygen in Chesapeake Bay. *Biogeosciences*, *15*(9), 2649–2668. https://doi.org/10.5194/bg-15-2649-2018

Jakubowska, M., & Normant-Saremba, M. (2015). The effect of CO2-induced seawater acidification on the behaviour and metabolic rate of the Baltic clam Macoma balthica. *Annales Zoologici Fennici*, *52*(5–6), 353–367. https://doi.org/10.5735/086.052.0509

Jansson, A., Norkko, J., Dupont, S., & Norkko, A. (2015). Growth and survival in a changing environment: Combined effects of moderate hypoxia and low pH on juvenile bivalve Macoma balthica. *Journal of Sea Research*, *102*, 41–47. https://doi.org/10.1016/j.seares.2015.04.006

Jansson, A., Norkko, J., & Norkko, A. (2013). Effects of reduced pH on Macoma balthica larvae from a system with naturally fluctuating pH-dynamics. *PLoS One*, *8*(6). https://doi.org/10.1371/journal.pone.0068198

Kemp, W. M., Boynton, W. R., Adolf, J. E., Boesch, D. F., Boicourt, W. C., Brush, G., Cornwell, J. C., Fisher, T. R., Glibert, P. M., Hagy, J. D., Harding, L. W., Houde, E. D., Kimmel, D. G., Miller, W. D., Newell, R. I. E., Roman, M. R., Smith, E. M., & Stevenson, J. C. (2005). Eutrophication of Chesapeake Bay: ~~historical~~Historical trends and ecological interactions. *Marine Ecology Progress Series*, *303*, 1–29. www.int-res.com

Kemp, W. M., Smith, E. M., Marvin-DiPasquale, M., & Boynton, W. R. (1997). Organic carbon balance and net ecosystem metabolism in Chesapeake Bay. *Marine Ecology Progress Series*, *150*, 229–248.

Kroeker, K. J., Kordas, R. L., Crim, R., Hendriks, I. E., Ramajo, L., Singh, G. S., Duarte, C. M., & Gattuso, J. P. (2013). Impacts of ocean acidification on marine organisms: quantifying sensitivities and interaction with warming. *Global Change Biology*, *19*(6), 1884–1896. https://doi.org/10.1111/gcb.12179

Levin, L. A., Ekau, W., Gooday, A. J., Jorissen, F., Middelburg, J. J., Naqvi, S. W. A., Neira, C., Rabalais, N. N., & Zhang, J. (2009). Effects of natural and human-induced hypoxia on coastal benthos. In *Biogeosciences* (Vol. 6). www.biogeosciences.net/6/2063/2009/

Little, S., Wood, P. J., & Elliott, M. (2017). Quantifying salinity-induced changes on estuarine benthic fauna: The potential implications of climate change. *Estuarine, Coastal and Shelf Science*, *198*, 610–625. https://doi.org/10.1016/j.ecss.2016.07.020

Llansó, R. J. (2002). *Methods for calculating the Chesapeake Bay benthic index of biotic integrity*. http://www.baybenthos.versar.com

Llansó, R. J., & Scott, L. (2011). *Chesapeake Bay water quality monitoring program: Long-term benthic monitoring and assessment component, quality assurance project plan, 2011–2012*.

Llansó, R. J., & Zaveta, D. (2017). *Chesapeake Bay water quality monitoring program: Long-term benthic monitoring and assessment component level 1 comprehensive report, July 1984 – December 2016 (Volume 1)*.

Marsh, A. G., & Tenore, K. R. (1990). The role of nutrition in regulating the population dynamics of opportunistic, surface deposit feeders in a mesohaline community. *Limnology and Oceanography*, *35*(3), 710–724. https://doi.org/10.4319/lo.1990.35.3.0710

Meysman, F. J. R., Middelburg, J. J., & Heip, C. H. R. (2006). Bioturbation: A fresh look at Darwin's last idea. *Trends in Ecology and Evolution*, *21*(12), 688–695. https://doi.org/10.1016/j.tree.2006.08.002

Middelburg, J. J. (2018). Reviews and syntheses: To the bottom of carbon processing at the seafloor. In *Biogeosciences* (Vol. 15, Issue 2, pp. 413–427). Copernicus GmbH. https://doi.org/10.5194/bg-15-413-2018

Middelburg, J. J., Soetaert, K., & Hagens, M. (2020). Ocean alkalinity, buffering and biogeochemical processes. *Reviews of Geophysics*, *58*(3). https://doi.org/10.1029/2019RG000681

Mo, C., & Neilson, B. (1994). Standardization of oyster soft tissue dry weight measurements. *Water Research*, *28*(1), 243–246.

Murphy, R. R., Kemp, W. M., & Ball, W. P. (2011). Long-term trends in Chesapeake Bay seasonal hypoxia, stratification, and nutrient loading. *Estuaries and Coasts*, *34*(6), 1293–1309. https://doi.org/10.1007/s12237-011-9413-7

Murphy, R. R., Perlman, E., Ball, W. P., & Curriero, F. C. (2015). Water-distance-based kriging in Chesapeake Bay. *Journal of Hydrologic Engineering*, *20*(9). https://doi.org/10.1061/(asce)he.1943-5584.0001135

Najjar, R. G., Herrmann, M., Alexander, R., Boyer, E. W., Burdige, D. J., Butman, D., Cai, W. J., Canuel, E. A., Chen, R. F., Friedrichs, M. A. M., Feagin, R. A., Griffith, P. C., Hinson, A. L., Holmquist, J. R., Hu, X., Kemp, W. M., Kroeger, K. D., Mannino, A., McCallister, S. L., … Zimmerman, R. C. (2018). Carbon budget of tidal wetlands, estuaries, and shelf waters of Eastern North America. *Global Biogeochemical Cycles*, *32*(3), 389–416. https://doi.org/10.1002/2017GB005790

Najjar, R. G., Herrmann, M., Cintrón Del Valle, S. M., Friedman, J. R., Friedrichs, M. A. M., Harris, L. A., Shadwick, E. H., Stets, E. G., & Woodland, R. J. (2020). Alkalinity in tidal tributaries of the Chesapeake Bay. *Journal of Geophysical Research: Oceans*, *125*(1). https://doi.org/10.1029/2019JC015597

Nakamura, Y., & Kerciku, F. (2000). Effects of filter-feeding bivalves on the distribution of water quality and nutrient cycling in a eutrophic coastal lagoon. *Journal of Marine Systems*, *26*, 209–221. www.elsevier.nlrlocaterjmarsys

Newell, R. I. E. (1988). Ecological changes in Chesapeake Bay: are they the result of overharvesting the American oyster, Crassostrea virginica. *Understanding the Estuary: Advances in Chesapeake Bay Reserach*, *129*, 536–546.

Newell, R. I. E., & Ott, J. A. (2011). Macrobenthic communities and eutrophication. *Ecosystems at the Land-Sea Margin: Drainage Basin to Coastal Sea*, *55*, 265–293. https://doi.org/10.1029/ce055p0265

Ni, W., Li, M., Ross, A. C., & Najjar, R. G. (2019). Large projected decline in dissolved oxygen in a eutrophic estuary due to climate change. *Journal of Geophysical Research: Oceans*, *124*(11), 8271–8289. https://doi.org/10.1029/2019JC015274

Olson, M. (2012). *Guide to using Chesapeake Bay Program water quality monitoring data*.

Pearson, T. H., & Rosenberg, R. (1978). Macrobenthic succession in relation to organic enrichment and pollution of the marine environment. *Oceanography and Marine Biology: An Annual Review*, *16*, 229–311.

Phelps H.L. (1994). The Asiatic ~~*Clam*~~clam (Corbicula fluminea) ~~*Invasion*~~invasion and ~~*System-Level Ecological Change*~~system-level ecological change in the Potomac River ~~*Estuary Near* (Vol.~~estuary near Washington, DC. *Estuaries*, *17*~~, Issue (3).~~), 614–621.

Redfield, A. C. (1963). The influence of organisms on the composition of seawater. *The Sea*, 26–77.

Rodil, I. F., Lohrer, A. M., Attard, K. M., Thrush, S. F., & Norkko, A. (2022). Positive contribution of macrofaunal biodiversity to secondary production and seagrass carbon metabolism. *Ecology*, *103*(4). https://doi.org/10.1002/ecy.3648

Rosenberg, R. (1995). Benthic marine fauna structured by hydrodynamic processes and food availibility. *Netherlands Journal of Sea Research*, *34*(4), 303–317.

Rousi, H., Korpinen, S., & Bonsdorff, E. (2019). Brackish-water benthic fauna under fluctuating environmental conditions: the role of eutrophication, hypoxia, and global change. *Frontiers in Marine Science*, *6*(JUL), 464. https://doi.org/10.3389/fmars.2019.00464

Schratzberger, M., & Ingels, J. (2018). Meiofauna matters: the roles of meiofauna in benthic ecosystems. *Journal of Experimental Marine Biology and Ecology*, *502*, 12–25. https://doi.org/10.1016/j.jembe.2017.01.007

Schwinghamer, P., Hargrave, B., Peer, D., & Hawkins, C. M. (1986). Partitioning of production and respiration among size groups of organisms in an intertidal benthic community. *Marine Ecology Progress Series*, *31*(2), 131–142.

Seitz, R. D., Dauer, D. M., Llansó, R. J., & Long, W. C. (2009). Broad-scale effects of hypoxia on benthic community structure in Chesapeake Bay, USA. *Journal of Experimental Marine Biology and Ecology*, *381*(SUPPL.). https://doi.org/10.1016/j.jembe.2009.07.004

Seitz, R., Lipcius, R. N., Olmstead, N. H., Seebo, M. S., & Lambert, D. M. (2006). Influence of shallow-water habitats and shoreline development on abundance, biomass, and diversity of benthic prey and predators in Chesapeake Bay. *Marine Ecology Progress Series*, *326*, 11–27.

Shchepetkin, A. F., & McWilliams, J. C. (2005). The regional oceanic modeling system (ROMS): A split-explicit, free-surface, topography-following-coordinate oceanic

model. *Ocean Modelling*, *9*(4), 347–404. https://doi.org/10.1016/j.ocemod.2004.08.002

Simon N. Wood. (2017). *Generalized Additive Models* (2nd ed.).

Smith, M., Paperno, R., Flaherty-Walia, K., & Markwith, S. (2023). Species Distributions in a Changing Estuary: Predictions Under Future Climate Change, Sea-Level Rise, and Watershed Restoration. *Estuaries and Coasts*, *46*(6). https://doi.org/10.1007/s12237-023-01219-5

Snelgrove, P. V. R. (1997). The importance of marine sediment biodiversity in ecosystem processes. *Ambio*, *26*(8), 578–583. https://doi.org/https://www.jstor.org/stable/4314672

Snelgrove, P. V. R. (1999). Snelgrove, P. V. (1999). Getting to the bottom of marine biodiversity: sedimentary habitats: ocean bottoms are the most widespread habitat on earth and support high biodiversity and key ecosystem services. *BioScience*, *42*(2), 129–138. www.jstor.org

Snelgrove, P. V. R., Soetaert, K., Solan, M., Thrush, S., Wei, C. L., Danovaro, R., Fulweiler, R. W., Kitazato, H., Ingole, B., Norkko, A., Parkes, R. J., & Volkenborn, N. (2018). Global carbon cycling on a heterogeneous seafloor. *Trends in Ecology & Evolution*, *33*(2), 96–105. https://doi.org/10.1016/j.tree.2017.11.004

Sousa, R., Antunes, C., & Guilhermino, L. (2008). Ecology of the invasive Asian clam Corbicula fluminea (Müller, 1774) in aquatic ecosystems: ~~an~~An overview. In *Annales de Limnologie-International Journal of Limnology* (Vol. 44, Issue 2, pp. 85–94). https://doi.org/10.1051/limn:2008017

St-Laurent, P., & Friedrichs, M. A. M. (2024a). An atlas for physical and biogeochemical conditions in the Chesapeake Bay. *SEANOE*.

St-Laurent, P., & Friedrichs, M. A. M. (2024b). On the sensitivity of coastal hypoxia to its external physical forcings. *Journal of Advances in Modeling Earth Systems*, *16*(1). https://doi.org/10.1029/2023MS003845

Sturdivant, S. K., Seitz, R. D., & Diaz, R. J. (2013). Effects of seasonal hypoxia on macrobenthic production and function in the Rappahannock River, Virginia, USA. *Marine Ecology Progress Series*, *490*, 53–68. https://doi.org/10.3354/meps10470

Symonds, M. R. E., & Moussalli, A. (2011). A brief guide to model selection, multimodel inference and model averaging in behavioural ecology using Akaike's information criterion. *Behavioral Ecology and Sociobiology*, *65*(1), 13–21. https://doi.org/10.1007/s00265-010-1037-6

Taylor, J. R. (2022). *An introduction to error analysis: the study of uncertainties in physical measurements*. MIT Press.

Testa, J. M., Faganeli, J., Giani, M., Brush, M. J., De Vittor, C., Boynton, W. R., Covelli, S., Woodland, R. J., Kovač, N., & Michael Kemp, W. (2020a). Advances in our understanding of ~~Pelagic-Benthic Coupling. In T. C. Malone, A. Malej, & J. Faganeli (Eds.), *Coastal Ecosystems in Transition: A Comparative Analysis of the Northern Adriatic and Chesapeake Bay* (pp. 147–175). Wiley. https://doi.org/10.1002/9781119543626.ch8~~

~~Testa, J. M., Faganeli, J., Giani, M., Brush, M. J., De Vittor, C., Boynton, W. R., Covelli, S., Woodland, R. J., Kovač, N., & Michael Kemp, W. (2020b). Advances in our understanding of~~ pelagic-benthic coupling. In T. C. Malone, A. Malej, & J. Faganeli (Eds.), *Coastal Ecosystems in Transition: A Comparative Analysis of the Northern Adriatic and Chesapeake Bay* (pp. 147–175). wiley. https://doi.org/10.1002/9781119543626.ch8

Testa, J. M., Faganeli, J., Giani, M., Brush, M. J., De Vittor, C., Boynton, W. R., Covelli, S., Woodland, R. J., Kovač, N., & Michael Kemp, W. (2020b). Advances in our understanding of Pelagic-Benthic Coupling. In T. C. Malone, A. Malej, & J. Faganeli (Eds.), *Coastal Ecosystems in Transition: A Comparative Analysis of the Northern Adriatic and Chesapeake Bay* (pp. 147–175). Wiley. https://doi.org/10.1002/9781119543626.ch8

Thomsen, J., Haynert, K., Wegner, K. M., & Melzner, F. (2015). Impact of seawater carbonate chemistry on the calcification of marine bivalves. *Biogeosciences*, *12*(14), 4209–4220. https://doi.org/10.5194/bg-12-4209-2015

Tumbiolo, M. L., & Downing, J. A. (1994). An empirical model for the prediction of secondary production in marine benthic invertebrate populations. *Marine Ecology Progress Series*, *114*(1), 165–174.

Tuszer-Kunc, J., Normant-Saremba, M., & Rychter, A. (2020). The combination of low salinity and low temperature can limit the colonisation success of the non-native bivalve Rangia cuneata in brackish Baltic waters. *Journal of Experimental Marine Biology and Ecology*, *524*. https://doi.org/10.1016/j.jembe.2019.151228

Vaquer-Sunyer, R., & Duarte, C. M. (2008). Thresholds of hypoxia for marine biodiversity. *Proceeds of the National Academy of Sciences*, *105*(40), 15452–15457. www.pnas.org/cgi/content/full/

Waldbusser, G. G., Hales, B., Langdon, C. J., Haley, B. A., Schrader, P., Brunner, E. L., Gray, M. W., Miller, C. A., & Gimenez, I. (2015). Saturation-state sensitivity of marine bivalve larvae to ocean acidification. *Nature Climate Change*, *5*(3), 273–280. https://doi.org/10.1038/nclimate2479

Waldbusser, G. G., Powell, E. N., & Mann, R. (2013). Ecosystem effects of shell aggregations and cycling in coastal waters: an example of Chesapeake Bay oyster reefs. *Ecology*, *94*(4), 895–903. https://doi.org/10.1890/12-1179.1

Ware, J. R., Smith, S. V, & Reaka-Kudla, M. L. (1992). Coral reefs: Sources or sinks of atmospheric CO2? *Coral Reefs*, *11*(3), 127–130.

Weisberg, S., Ranasingiie, A., Schaffner Robert J Diaz, L. C., Dauer, D. M., & Frithsen, F. B. (1997). An estuarine benthic index of biotic integrity (B-IBI) for Chesapeake Bay. *Estuaries*, *20*(1), 149–158.

Wilson, J. G., & Fleeger, J. W. (2023). Estuarine ~~*Ecology* (~~benthos. In B. C. Crump, J. M. Testa, & K. H. Dunton~~,~~ (Eds~~.~~.), *Estuarine Ecology* (3rd ed~~.~~)., pp. 253–273). Wiley.

Wolf-Gladrow, D. A., Zeebe, R. E., Klaas, C., Körtzinger, A., & Dickson, A. G. (2007). Total alkalinity: The explicit conservative expression and its application to biogeochemical processes. *Marine Chemistry*, *106*(1-2 SPEC. ISS.), 287–300. https://doi.org/10.1016/j.marchem.2007.01.006

Wood, S. N. (2011). Fast stable restricted maximum likelihood and marginal likelihood estimation of semiparametric generalized linear models. *Journal of the Royal Statistical Society Series B: Statistical Methodlogy*, *73*(1), 3–36. https://academic.oup.com/jrsssb/article/73/1/3/7034726

Woodland, R. J., Buchheister, A., Latour, R. J., Lozano, C., Houde, E., Sweetman, C. J., Fabrizio, M. C., & Tuckey, T. D. (2021). Environmental drivers of forage fishes and benthic invertebrates at multiple spatial scales in a large temperate estuary. *Estuaries and Coasts*, *44*(4), 921–938. https://doi.org/10.1007/s12237-020-00835-9

Woodland, R. J., & Testa, J. M. (2020). Response of ~~Benthic Biodiversity~~benthic biodiversity to ~~Climate-Sensitive Regional~~climate-sensitive regional and ~~Local Conditions~~local conditions in a ~~Complex Estuarine System~~complex estuarine system. In V. Lyubchich, Y. R. Gel, K. H. Kilbourne, T. J. Miller, N. K. Newlands, & A. B. Smith (Eds.), *Evaluating Climate Change IMpacts* (Vol. 1, pp. 87–22). CRC Press.

Zhang, Q., & Blomquist, J. D. (2018). Watershed export of fine sediment, organic carbon, and chlorophyll-a to Chesapeake Bay: Spatial and temporal patterns in 1984–2016. *Science of the Total Environment*, *619–620*, 1066–1078. https://doi.org/10.1016/j.scitotenv.2017.10.279

Zhang, Q., Fisher, T. R., Trentacoste, E. M., Buchanan, C., Gustafson, A. B., Karrh, R., Murphy, R. R., Keisman, J., Wu, C., Tian, R., Testa, J. M., & Tango, P. J. (2021). Nutrient limitation of phytoplankton in Chesapeake Bay: Development of an empirical approach for water-quality management. *Water Research*, *188*. https://doi.org/10.1016/j.watres.2020.116407

Zheng, G., & DiGiacomo, P. M. (2020). Linkages between phytoplankton and bottom oxygen in the Chesapeake Bay. *Journal of Geophysical Research: Oceans*, *125*(2). https://doi.org/10.1029/2019JC015650